Supplementary material to EMEP Status Report 1/2011
Date: July 2011

METEOROLOGISK INSTITUTT
Norwegian Meteorological Institute

EMEP/MSC-W model performance for acidifying and eutrophying components and photo-oxidants in 2009

EMEP/MSC-W: Michael Gauss, Anna Carlin Benedictow, Hilde Fagerli, and Birthe Marie Steensen

EMEP/CCC: Anne-Gunn Hjellbrekke

Supplementary material to EMEP Status Report 1/2011

Contents

CHAPTER 1

Acidifying and eutrophying components: evaluation and combined maps

H. Fagerli, M. Gauss, A. C. Benedictow, B. M. Steensen and A.-G. Hjellbrekke

In this chapter the EMEP/MSC-W model is evaluated with respect to acidifying and eutrophying components. Model results for 2009 are validated against measurements from the EMEP network for 2009. The agreement between model results and observations depends on a combination of several elements; the quality and representativeness of the measurement sites, the adequacy of emissions and the model performance. Therefore, the following discussion on model *underestimation* and *overestimation* only implies that the calculated values are lower or higher than the observations and does not necessarily refer to model deficiency.

1.1 Evaluation

Evaluations of the EMEP/MSC-W model performance for acidifying and eutrophying components have been presented in numerous EMEP reports (e.g. Berge and Hjellbrekke 2010, Nyíri and Hjellbrekke 2009, Fagerli and Hjellbrekke 2008, Fagerli and Aas 2008a, Fagerli 2007, Fagerli and Aas 2007, Fagerli 2005, 2004, Fagerli et al. 2003). It has been shown that the EMEP model performance is rather homogeneous over the years (Fagerli et al. 2003), but depends on geographical coverage and quality of the measurement data. The EMEP model has also been validated for nitrogen compounds in Simpson et al. (2006a) and for dry and wet depositions of sulphur, and for wet deposition of nitrogen in Simpson et al. (2006b) with measurements outside

Component	N_{stat}	Obs.	Mod.	Bias (%)	RMSE	Corr.	IOA
NO_2 (μg(N) m^{-3})	42	1.70	1.75	3	0.96	0.74	0.86
SO_2 (μg(S) m^{-3})	48	0.42	0.66	58	0.67	0.39	0.53
SO_4^{2-} (μg(S) m^{-3})	53	0.58	0.33	-43	0.33	0.74	0.68
NH_3 (μg(N) m^{-3})	11	0.92	0.82	-10	0.56	0.29	0.56
NH_4^+ (μg(N) m^{-3})	27	0.85	0.51	-40	0.47	0.66	0.63
NH_3+NH_4^+ (μg(N) m^{-3})	35	1.51	1.24	-18	0.60	0.85	0.90
HNO_3 (μg(N) m^{-3})	14	0.16	0.10	-35	0.18	0.48	0.55
NO_3^-+HNO_3 (μg(N) m^{-3})	45	0.61	0.42	-31	0.47	0.64	0.57
NO_3^- (μg(N) m^{-3})	24	0.45	0.32	-27	0.28	0.85	0.77
SO_4^{2-} wd (μg(S)m^{-2})	61	14375	15017	4	140	0.67	0.81
SO_4^{2-} cp (μg(S)l^{-1})	61	0.29	0.30	1	0.13	0.80	0.89
NH_4^+ wd (μg(N)m^{-2})	61	16960	16822	-1	171	0.64	0.79
NH_4^+ cp (μg(N)l^{-1})	61	0.34	0.33	-3	0.20	0.52	0.70
NO_3^- wd (μg(N)l^{-1})	62	14693	12666	-14	135	0.71	0.79
NO_3^- cp (μg(N)l^{-1})	62	0.29	0.24	-15	0.14	0.66	0.76
precip. mm	62	56367	59153	5	313	0.71	0.83

Table 1.1: Comparison of model results and observations for 2009. Annual averages over all EMEP sites with measurements. N_{stat}= number of stations, wd=wet deposition, cp= concentration in precipitation, Corr. = spatial correlation coefficient, RMSE = root mean square error, IOA = index of agreement.

the EMEP network. Calculated trends of total nitrate (HNO_3 and NO_3^-) and ammonia + ammonium in air and precipitation have been evaluated in Fagerli and Aas (2008b) and have shown in general good correspondence to observations.

This year we present results from EMEP/MSC-W model version v.2011-06, slightly different from last years model (EMEP MSC-W & CCC 2009). Changes in the model are described in Simpson (2011). As last year the meteorological input data are based on data from the ECMWF-IFS model.

The scatter-plots are based on yearly averages for 2009. The lines on the scatter-plots display deviations in the scatter of 30% ('30% line') and 50% ('50% line') relative bias, respectively. Relative bias is defined here as $\frac{Mod-Obs}{0.5\,(Mod+Obs)} \times 100\%$, where 'Mod' refers to yearly averaged modelled concentrations, while 'Obs' refers to yearly averaged measured concentrations.

Table 1.1 shows for each component the number of stations where measurements were available and data coverage criteria was satisfied (N_{stat}), measured yearly average over all stations (Obs), modelled yearly average over all stations (Mod), bias ($\frac{Mod-Obs}{Obs} \times 100\%$), correlation between observation and model for station yearly averages (Corr), root mean square error, Rmse ($\sqrt{\frac{1}{n}\sum_{i=1}^{n}(m_i - o_i)^2}$ where m_i and o_i are modelled and measured concentration in monitoring station *i*), and index of agreement,

IOA ($1 - \frac{\sum_{i=1}^{N_{stat}}(m_i - o_i)^2}{\sum_{i=1}^{N_{stat}}(|m_i - Obs| + |o_i - Obs|)^2}$). IOA was introduced for the first time last year to give a more robust evaluation of the model result. IOA varies from 0 (theoretical minimum) to 1 (perfect agreement between observed and predicted values) and gives the degree to which model predictions are error free.

1.1.1 Sulphur dioxide in air

In 2009 the modelled yearly averages for most acidifying and eutrophying components are lower than the observations. An exception is SO_2, for which modelled air concentrations are on average 58% higher than measured ones. This is a higher overestimation than last year (48%), probably due to a combination of model changes and a difference with respect to which sites that are included in the comparison (It is not exactly the same sites that reported SO_2 concentrations this year as last year). Specifically, for the first time this year Armenia reported measurements for one site, Amberd. At this site, the model results are a lot higher than the reported measurements. Armenia has not reported emissions to the CLRTAP, thus expert estimates are used for this country. Furthermore, the site is located at around 2000 meter above sea level. Because of the high elevation, for a long-term run, this site will often be above the boundary layer, especially in the winter. With the coarse topography in the regional scale model, this cannot be well captured by the model. Consequently, sulphur dioxide concentrations are overestimated. This applies also for sulfate.

It can be noted (Figure 1.1) that the largest over-prediction for SO_2 is at the stations AM01, SE14, IS02 and RU18. One of these sites (SE14) is situated on the coast of southern Sweden. The overestimation of SO_2 at this site might indicate that the ship emissions included in the EMEP inventory are somewhat too high, or that the model resolution is too low for this area.

For the Russian site, Danki (RU18), high discrepancies between the modelled and observed values have been identified also for other components and in previous years. Danki lies relatively close to Moscow, and this local influence might be the reason of the poor performance for this site.

For the Norwegian site, Zeppelin (NO42), underestimations of all components have been identified. Zeppelin is located on Svalbard and underestimation at this site could reflects the model's difficulties in modelling transport to the Arctic and/or problems in emissions or boundary conditions.

Time series for SO_2 are shown in Figures 1.5–1.9. As it can be seen from the time series, overestimation is generally highest during winter time and autumn. In the model seasonal variation of the emissions is considered based on data provided by the University of Stuttgart, IER, for 1990. However, it is likely that the seasonal variation of emissions has changed over time. Nowadays a larger part of emissions is released during the summer time with increasing use of air condition, and more importantly, the growth of telecommunications and computer hardware use.

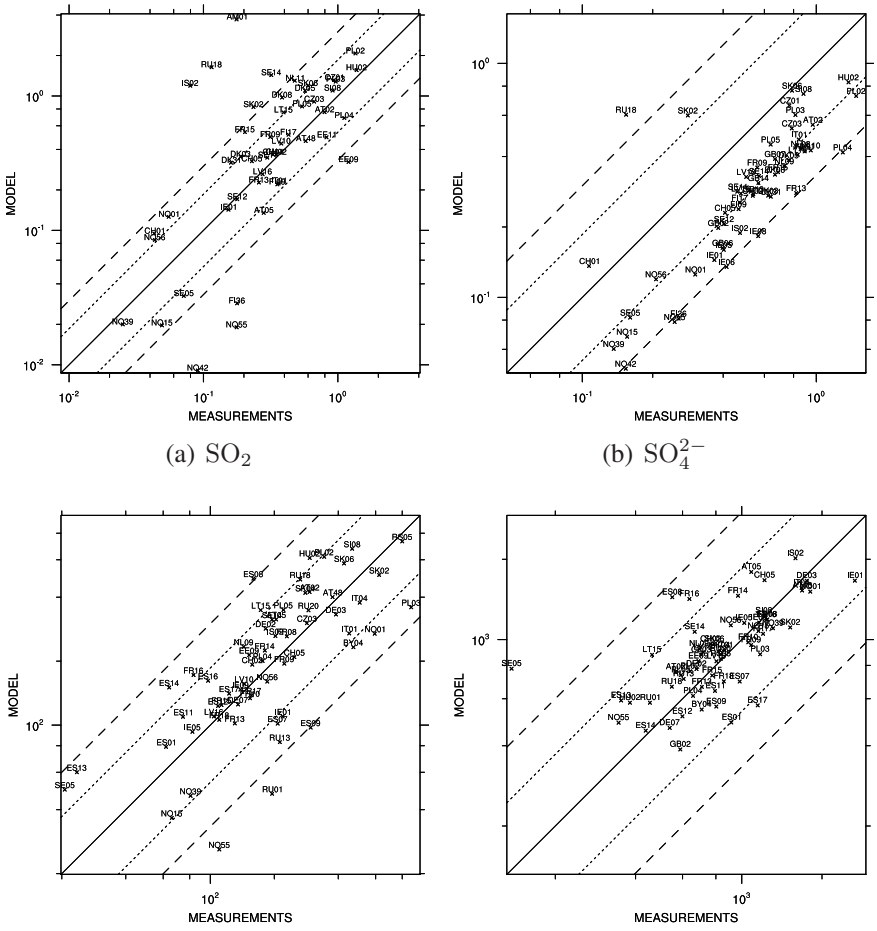

(a) SO_2 (b) SO_4^{2-}

(c) SO_4^{2-} wet dep. (d) Precipitation

Figure 1.1: Scatter-plots of modelled versus observed concentrations of sulphur dioxide and sulfate in air [μg(S) m^{-3}], wet deposition of sulphur [μg(S)m^{-2}] and precipitation [mm].

1.1.2 Sulfate in air

A scatter-plot for modelled versus measured sulfate concentrations in air for 2009 is presented in Figure 1.1. For 2009 the modelled concentrations of sulfate in air are 43% underestimated. This is in the same range as in last year (underestimated by 42%). The observations used for the comparison to EMEP model results are non-corrected sulfate measurements. In Figure 1.2 we show EMEP model results compared to corrected sulfate (only 28 sites) and results where 7 % modelled sea salt (sea salt is assumed to consist of approximately 7 % sulfate) has been added to modelled sulfate and compared to non-corrected sulfate. The modelled and measured sulfate levels are in somewhat better agreement when sea salt sulfate is taken into account (e.g. -34 % in the comparison where sea salt sulfate is added to chemically produced sulfate).

Nevertheless, the underestimation is higher than in previous years (before 2007),

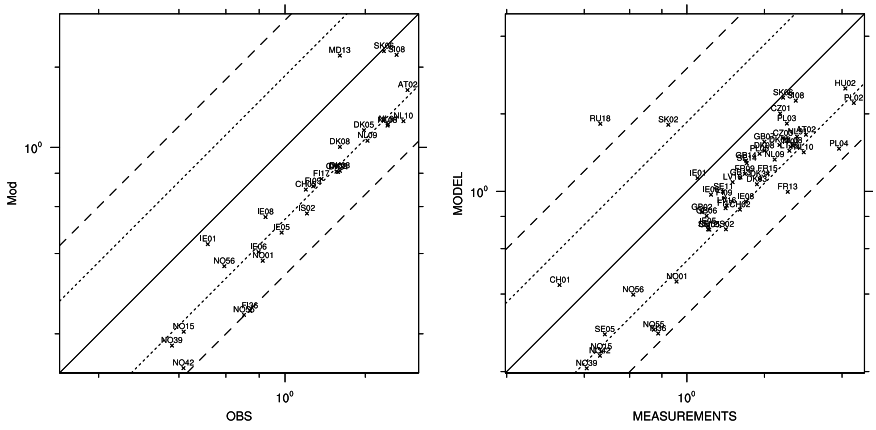

(a) SO_4^{2-}, sea salt corrected (b) SO_4^{2-}, not sea salt corrected

Figure 1.2: Scatter-plots of modelled versus observed sulfate concentrations [μg(S) m^{-3}]. The first plot show a comparison of model results to sea salt corrected sulfate measurements, the second show EMEP model results of sulfate plus 7 % sea salt in comparison to non-corrected measurement data.

which is probably caused by a combination of the change of the meteorological driver from PARLAM-PS to ECMWF-IFS, a change in model version and a changing atmosphere.

For several sites SO_4^{2-} is underestimated while there is an overestimation of SO_2, while for other sites the model under-predicts both SO_4^{2-} and SO_2, with a higher underestimation for sulfate. This might indicate that there is too little oxidation of SO_2 to sulfate in the model. The bulk production of SO_4^{2-} results from the oxidation of SO_2 to sulphuric acid in liquid clouds, primarily by H_2O_2 and O_3. Of these two, H_2O_2 is by far the most important oxidant for low pH values.

However, SO_2 emissions have decreased significanly even the last 5 years (e.g. almost 40% in EU from 2005 to 2009), whilst the changes in NH_3 and NO_x emissions have been significantly smaller. The oxidation rate for the SO_2 + O_3 aqueous reaction grows with increasing pH, and this pathway therefore becomes increasingly important. In the standard runs, the pH is kept constant, whilst preliminary results (not shown) indicates better results for sulfate (and SO_2) when pH is allowed to change in accordance with the changing atmosphere.

Time series for sulfate in air are shown in Figures 1.10–1.15.

1.1.3 Ammonia and ammonium aerosol in air

For 2009, as for the previous years, there is a rather limited number of sites (35 in 2009) that report measurements for NH_3+NH_4^+ (NH_x). In order to evaluate the model performance for NH_x properly, ammonia and ammonium should be studied separately. However, the number of measurements for 2009 where the gaseous and particle phase

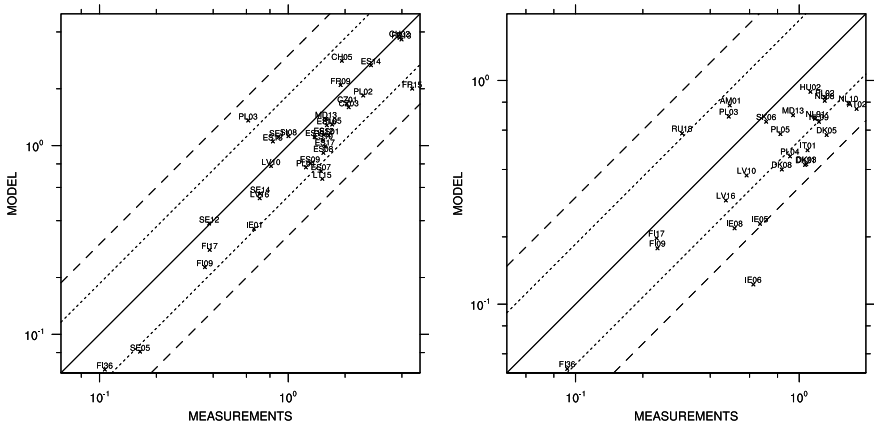

(a) NH_3+NH_4^+ (b) NH_4^+

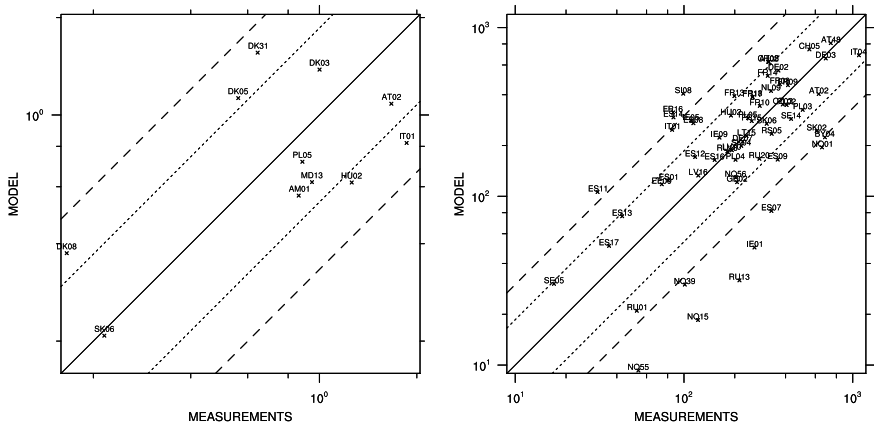

(c) NH_3 (d) NH_4^+ wet dep.

Figure 1.3: Scatter-plots of modelled versus observed concentrations of total ammonium+ammonia, aerosol ammonium and ammonia in air [μg(N) m^{-3}] and wet deposition of reduced nitrogen [μg(N)m^{-2}].

are analyzed both separately and at the same time is rather limited.

The individual concentrations of ammonia and ammonium are biased when using the common filter-pack method due to the volatile nature of ammonium nitrate. Separation of these gases and particles by a simple aerosol filter is unreliable, and to obtain better quality data it is necessary to use denuders. However, this is a much more demanding method and several sites in the EMEP network are still using the filter-pack method and report the individual concentrations of ammonia and ammonium based on this.

Scatter-plots for modelled versus measured concentrations for ammonia, aerosol ammonium and total ammonium+ammonia in air in 2009 are presented in Figure 1.3, while time series for NH_3+NH_4^+ are shown in Figures 1.20–1.23.

The modelled yearly average of the concentration of the sum of ammonia and

ammonium in air is underestimated by 16% compared with the monitoring data. The spatial correlation for NH_3+NH_4^+ is among the highest for the modelled acidifying compounds, while NH_3 have a low spatial correlation (r=0.29). Partly this is due to the low number of sites that have reported measurements, and the sites that have reported measuremenst are in areas which have relatively similar NH_3 concentrations/emission.

1.1.4 Nitrate and nitric acid in air

Measurements of airborne nitrate are expected to have a rather large uncertainty due to the very different physical characteristics of the compounds making up total nitrate. Whilst nitric acid is a spatially variable volatile gas with fast dry deposition, particulate nitrate dry deposits only slowly and hence concentrations are more determined by long range transport.

In Figure 1.4 we show scatter-plots for total nitrate, particulate nitrate and nitric acid in air. Time series for total nitrate in air are shown in Figures 1.16–1.19.

Normally, the results for nitrate aerosol and nitric acid are somewhat worse than for total nitrate, because the monitoring data quality for these components are in general not as good as for total nitrate. The reason for this is that, similarly to the total ammonia+ammonium (as described in Section 1.1.3), the individual concentrations of nitrate and nitric acid are biased when using the common filter-pack method. This has also been shown in the evaluation of the EMEP model performance for nitrogen compounds using intensive measurement data from two sampling periods, June 2006 and January 2007 (Fagerli and Aas 2008a).

In this year's model results, NO_3^- was underestimated by -27%, HNO_3 was underestimated by - 35% and the sum of NO_3^-+HNO_3 was 31% underestimated. The spatial correlation is best for nitrate aerosol (r = 0.85), somewhat worse for the sum of aerosol and gas (r = 0.64) and the lowest for nitric acid (r = 0.48).

1.1.5 Concentrations in precipitation and wet depositions

The ability of the model to predict concentrations in precipitations and wet depositions is limited by the accuracy of the precipitation fields used in the model. The precipitation field pattern is very patchy (e.g. influenced by local topographic effects), and the regional scale model is unable to resolve this sub grid scale distribution. A typical problem arises with small scale showers. In reality precipitation is high in a small area of a given grid, but a large fraction of the grid should remain dry. Within the model, however, this precipitation is averaged out to cover the whole grid at a lower intensity. Thus, even though average precipitation amounts may be simulated well, the model experiences precipitation more often, but in lower amounts, than occur in reality. On a shorter time scale, e.g on daily basis, this may lead to too high concentrations in precipitation for episodes when it rains only in a small part of the grid square. For a regional scale model it is more sensible to compare the bulk concentrations, i.e the sum of the wet deposited compounds divided by the sum of precipitation.

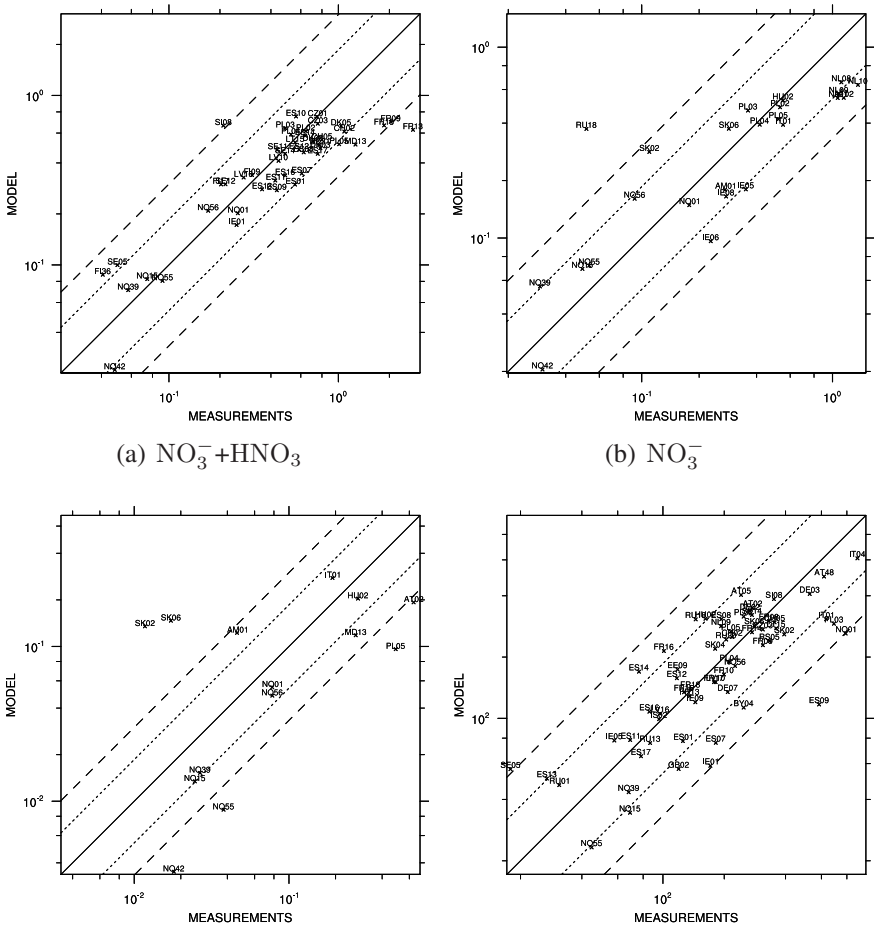

(a) NO_3^-+HNO_3 (b) NO_3^-

(c) HNO_3 (d) NO_3^- wet dep.

Figure 1.4: Scatter-plots of modelled versus observed concentrations of total nitrate, nitrate aerosol, nitric acid [μg(N) m^{-3}] and wet deposition of oxidized nitrogen [μg(N)m^{-2}].

The correlation between model and measurements for concentrations in precipitation and wet depositions will to a large extent depend on the model precipitation field.

Scatter-plot for modelled versus observed precipitation is shown in Figure 1.1(d). In average, the observed and modelled precipitation is very similar (bias=5 %). The spatial correlation coefficient is 0.71.

Model calculations of wet depositions and concentrations in precipitation compare well to the observations ranging from -14% (oxidized nitrogen in wet deposition) to +4% (wet deposition of sulphur). Concentrations in precipitation and wet depositions show similar results.

The highest underestimation is found for oxidized nitrogen both for wet deposition and concentration in precipitation (-15% and -14%, respectively).

Scatter-plots for modelled versus observed wet depositions of sulphur, reduced

nitrogen and oxidized nitrogen are shown in in Figures 1.1(c), 1.3(d) and 1.4(d), respectively.

Time series for sulphur, oxidized nitrogen and reduced nitrogen concentrations in precipitation are shown in Figures 1.24–1.30, Figures 1.31–1.37 and Figures 1.38–1.44, respectively.

1.2 Time series

In this section we present time series plots for a selection of stations supplying data on acidifying and eutrophying components to EMEP CCC in 2009. The plots show daily model results and measurements, where available. Time series are shown also for those measurement sites which were excluded from the scatter-plots. Time series for sulphur dioxide in air are shown in Figures 1.5–1.9, for sulfate in air in Figures 1.10–1.15, for total nitrate in air in Figures 1.16–1.19 and for ammonia+ammonium in air in Figures 1.20–1.23. In addition, time series are shown for sulphur, oxidized nitrogen and reduced nitrogen concentrations in precipitation in Figures 1.24–1.30, Figures 1.31–1.37 and Figures 1.38–1.44, respectively.

Sulphur dioxide in air

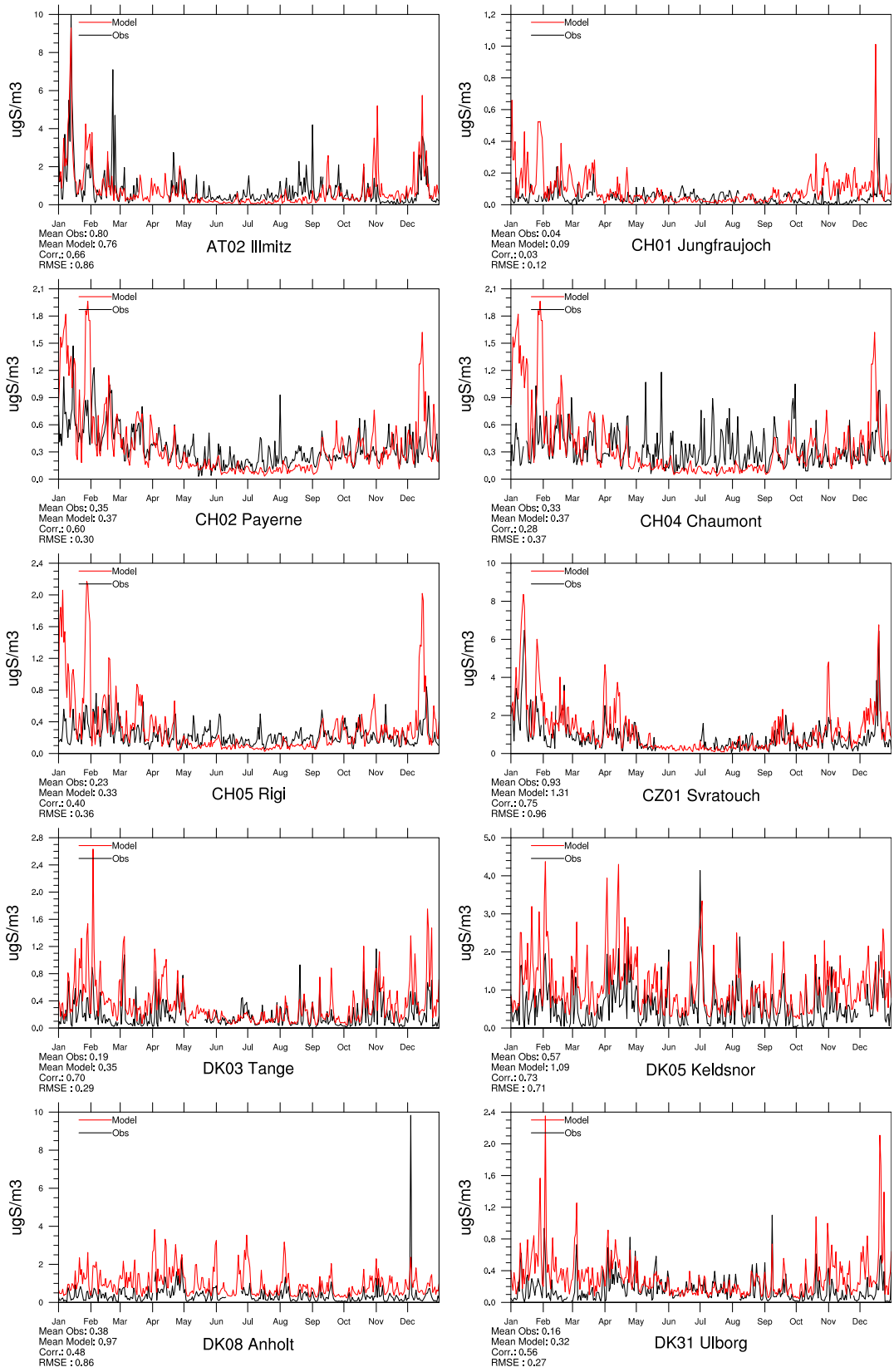

Figure 1.5: Comparison of model results and measurements (daily) for SO_2 in air [ugS] for stations that have measured SO_2 in 2009.

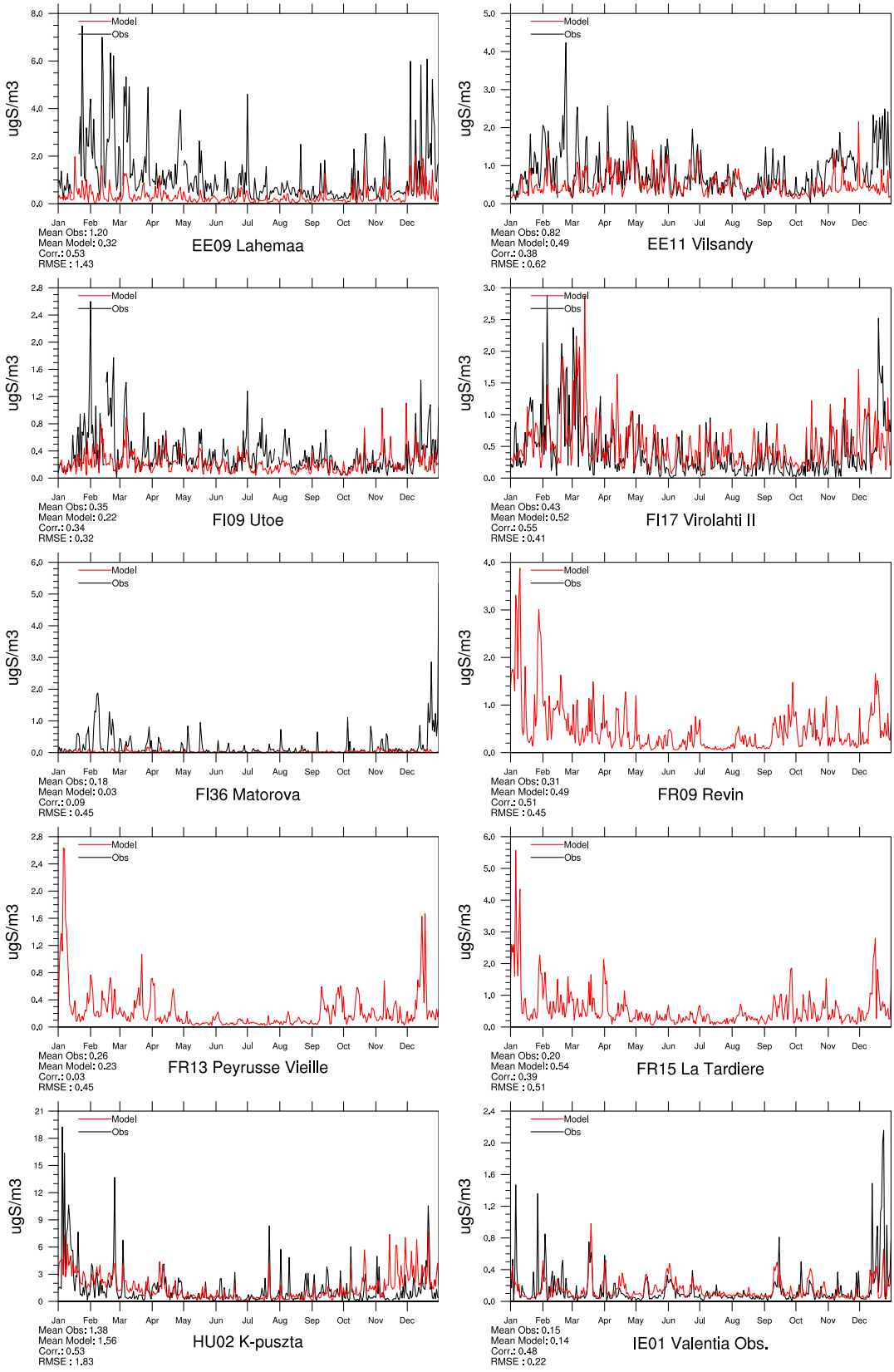

Figure 1.6: Comparison of model results and measurements (daily) for SO_2 in air [ugS] for stations that have measured SO_2 in 2009.

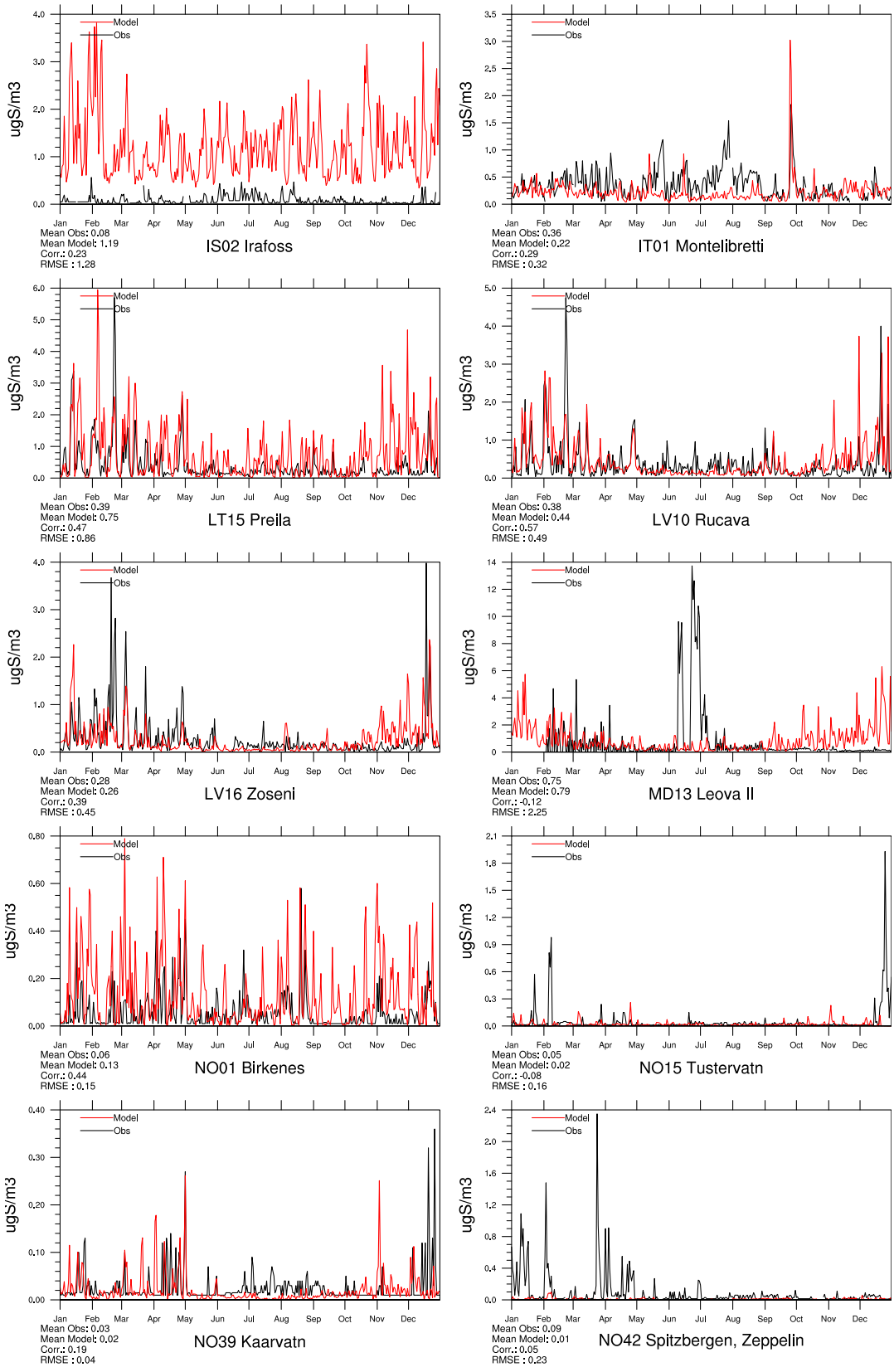

Figure 1.7: Comparison of model results and measurements (daily) for SO_2 in air [ugS] for stations that have measured SO_2 in 2009.

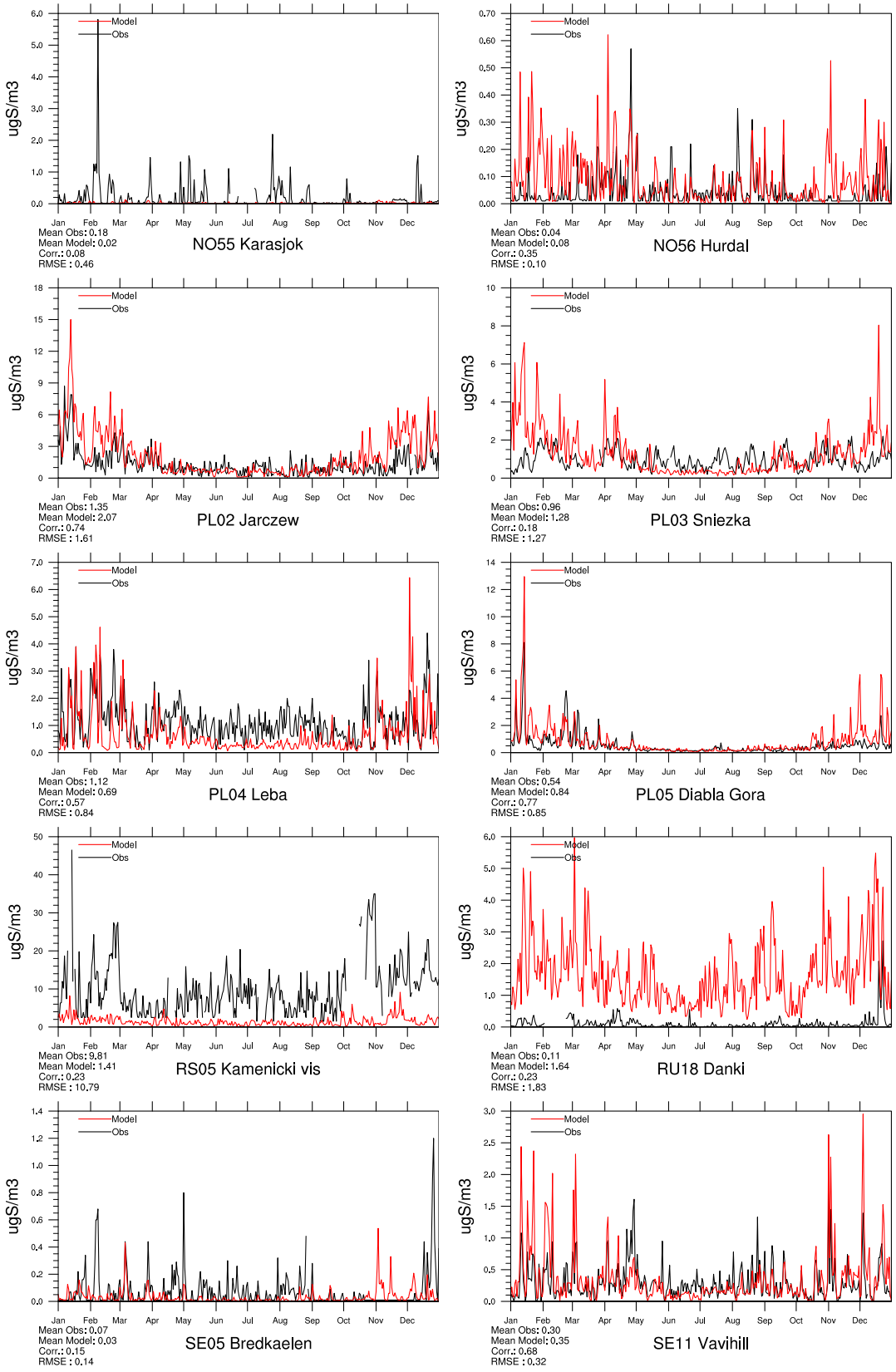

Figure 1.8: Comparison of model results and measurements (daily) for SO_2 in air [ugS] for stations that have measured SO_2 in 2009.

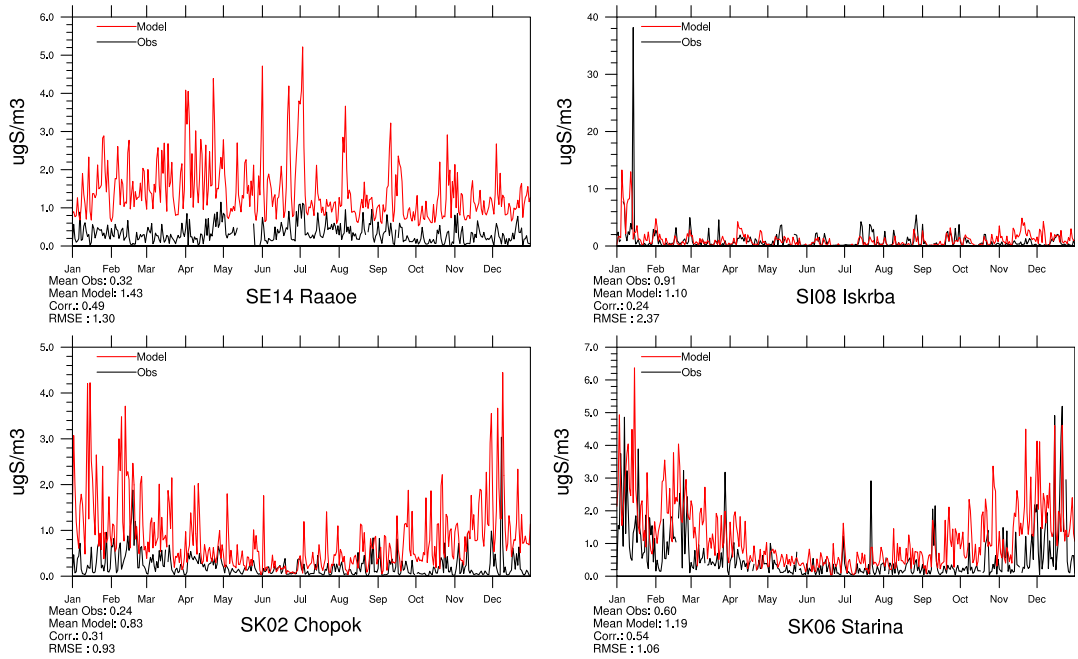

Figure 1.9: Comparison of model results and measurements (daily) for SO_2 in air [ugS] for stations that have measured SO_2 in 2009.

Sulfate in air

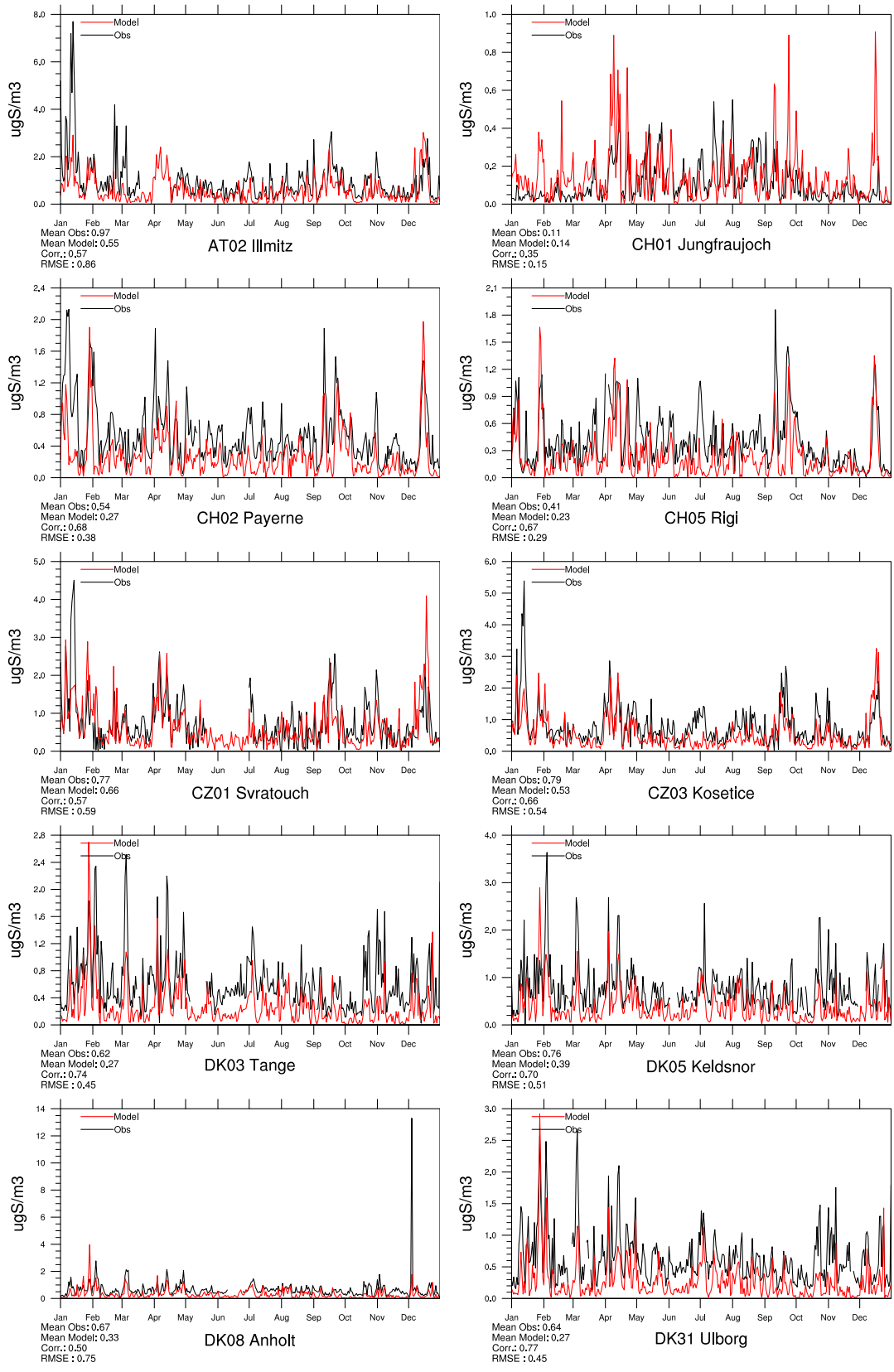

Figure 1.10: Comparison of model results and measurements (daily) for sulfate in air [ugS] for stations that have measured sulfate in 2009.

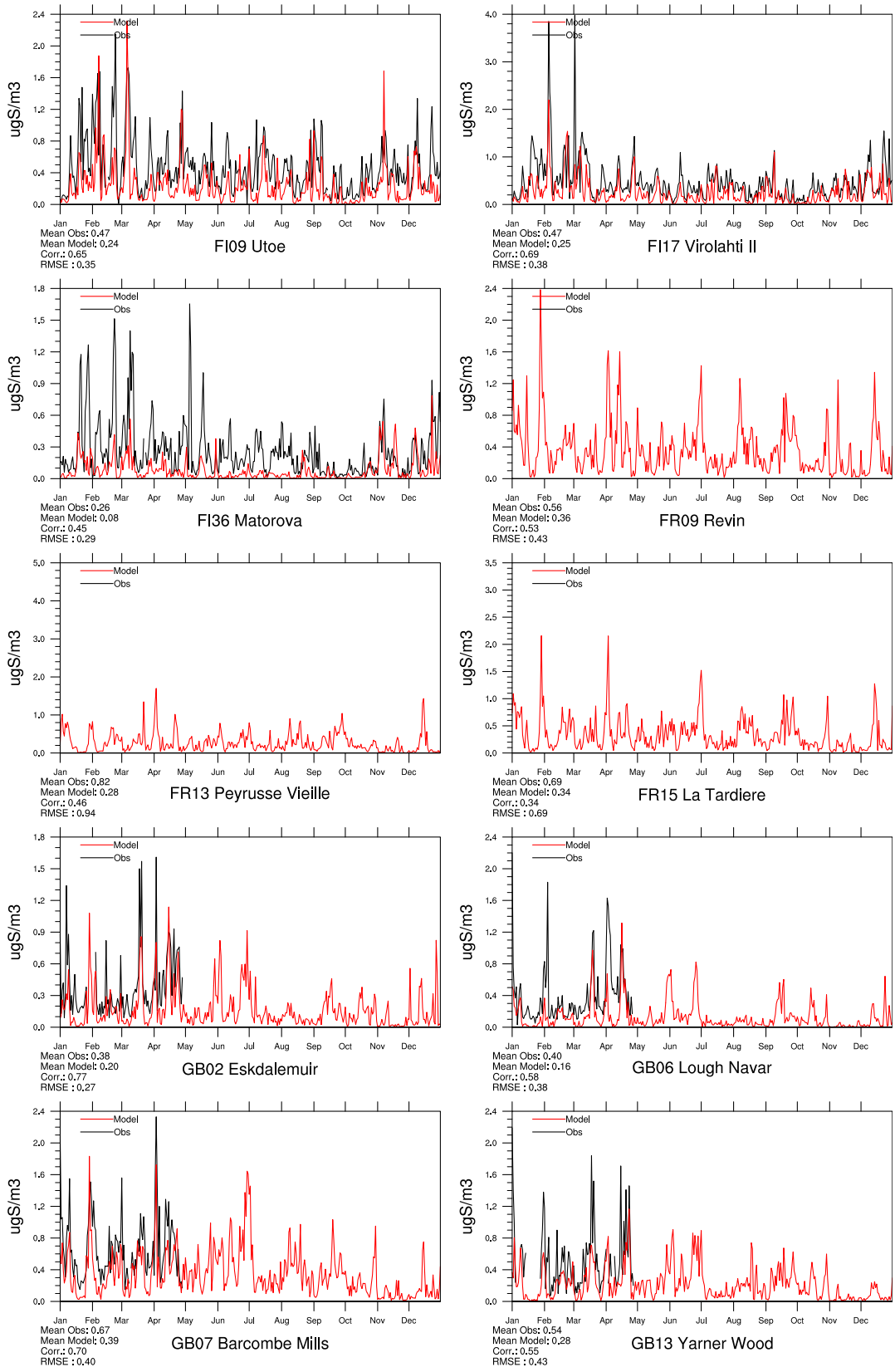

Figure 1.11: Comparison of model results and measurements (daily) for sulfate in air [ugS] for stations that have measured sulfate in 2009.

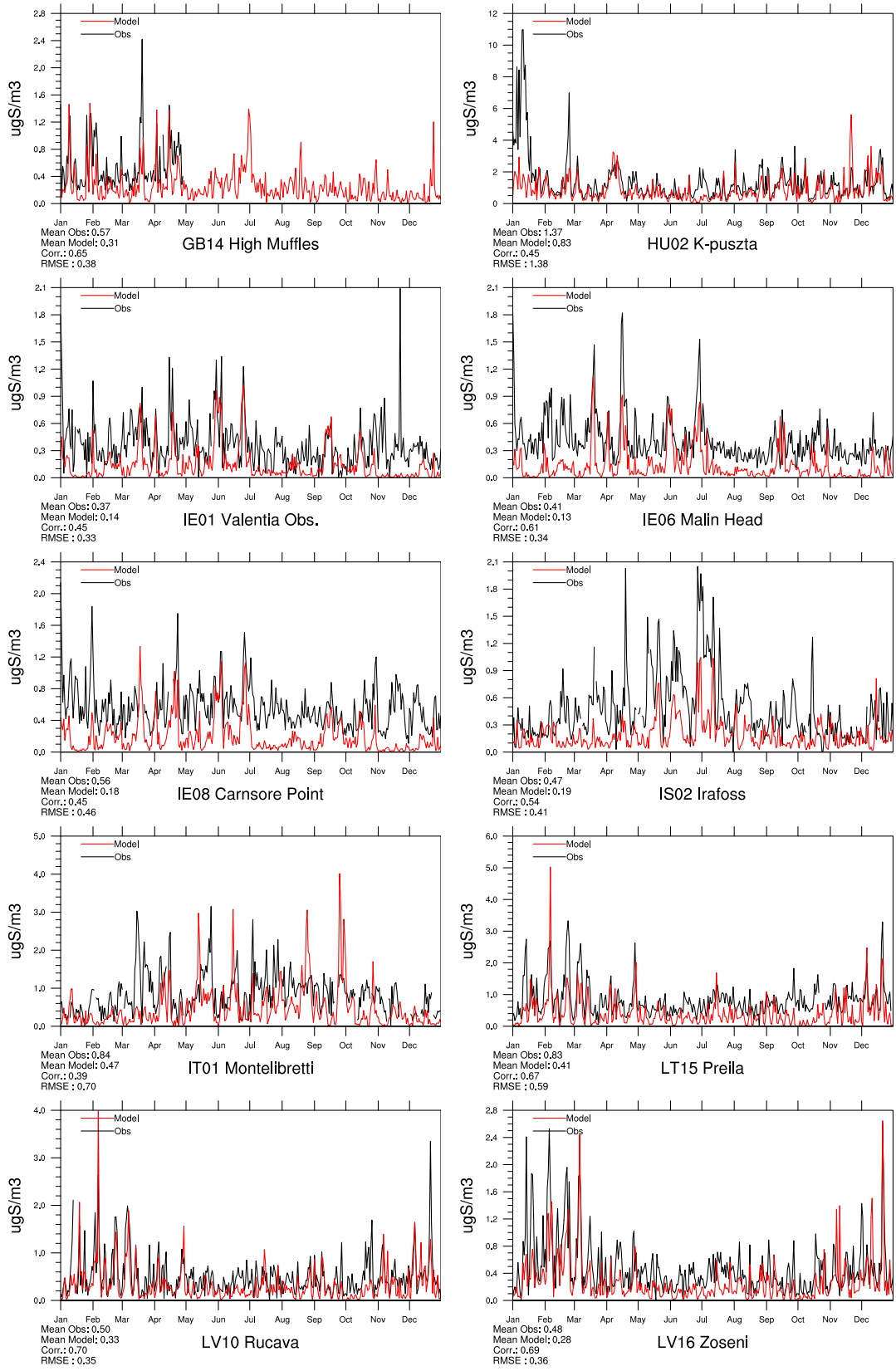

Figure 1.12: Comparison of model results and measurements (daily) for sulfate in air [ugS] for stations that have measured sulfate in 2009.

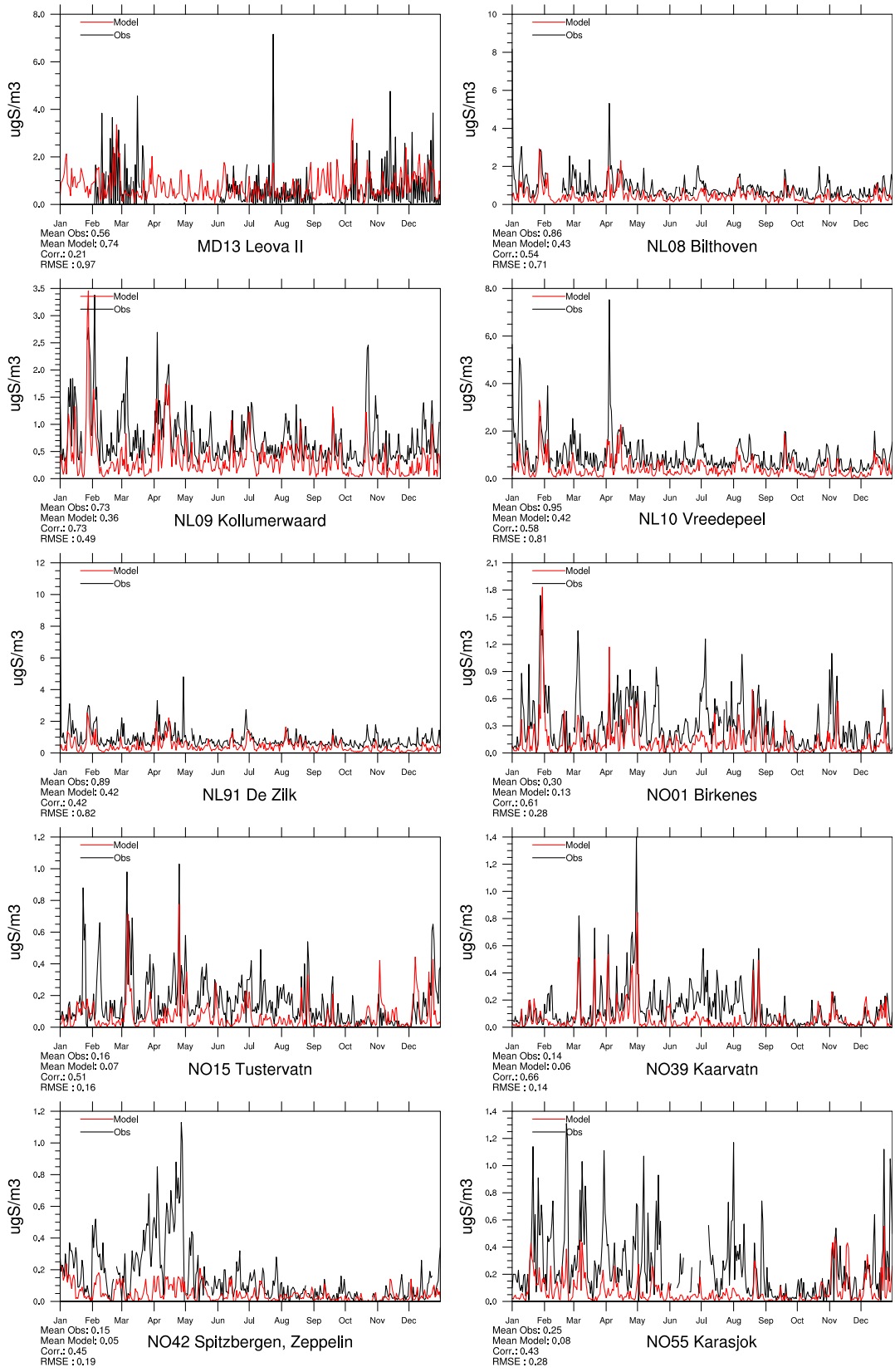

Figure 1.13: Comparison of model results and measurements (daily) for sulfate in air [ugS] for stations that have measured sulfate in 2009.

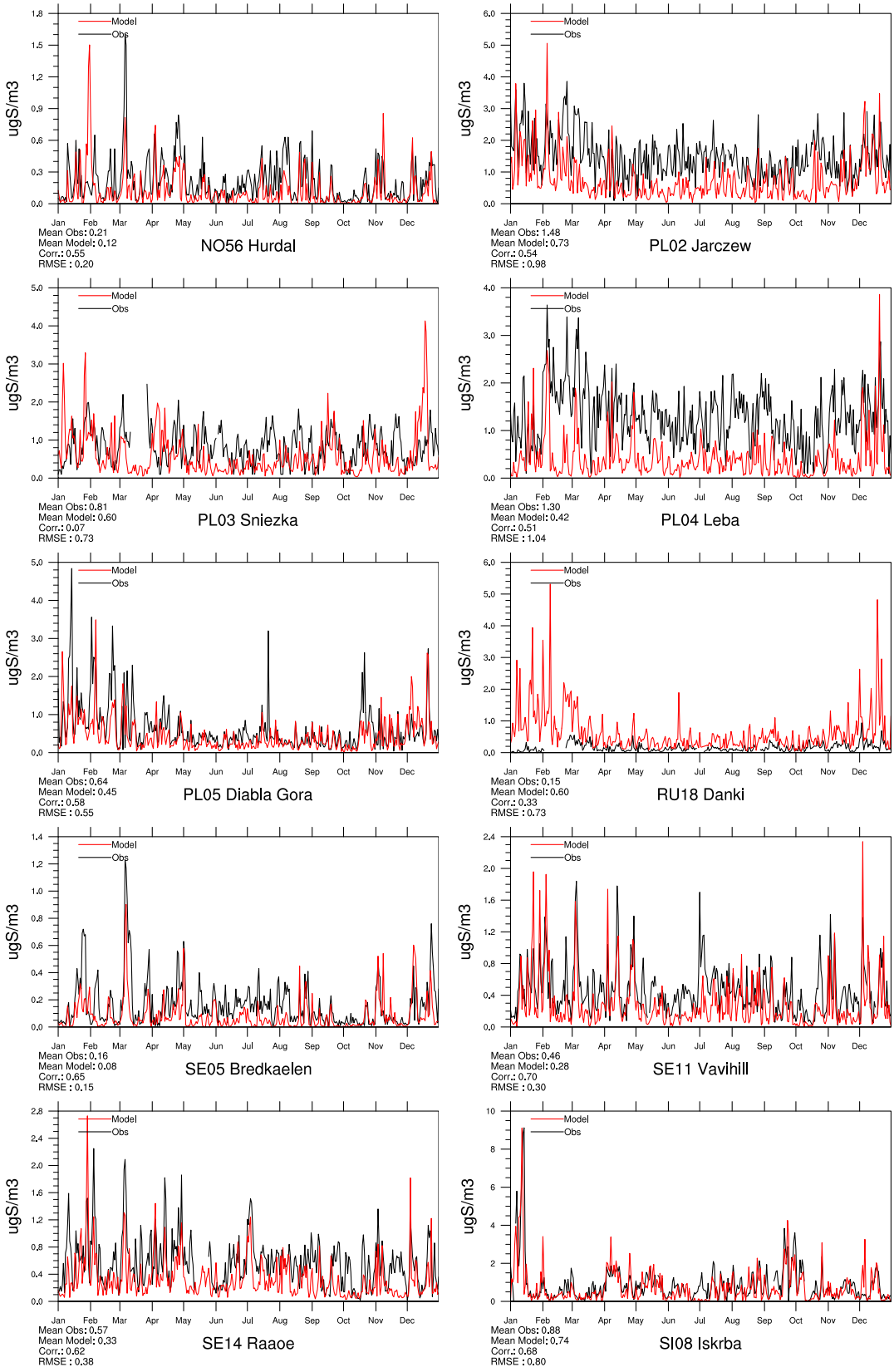

Figure 1.14: Comparison of model results and measurements (daily) for sulfate in air [ugS] for stations that have measured sulfate in 2009.

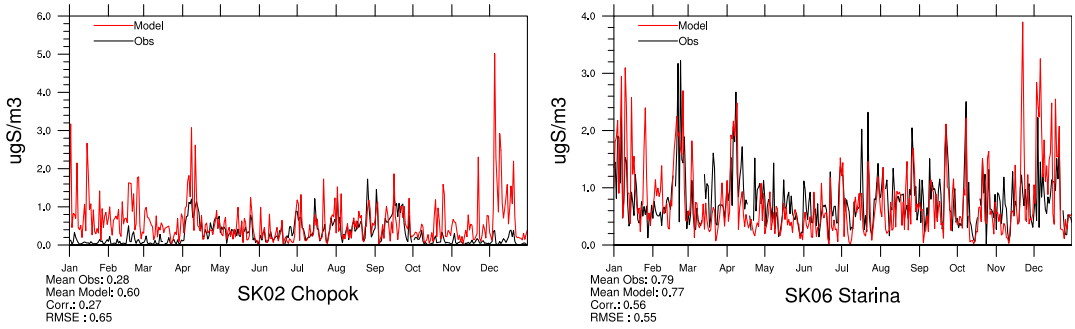

Figure 1.15: Comparison of model results and measurements (daily) for sulfate in air [ugS] for stations that have measured sulfate in 2009.

Total nitrate in air

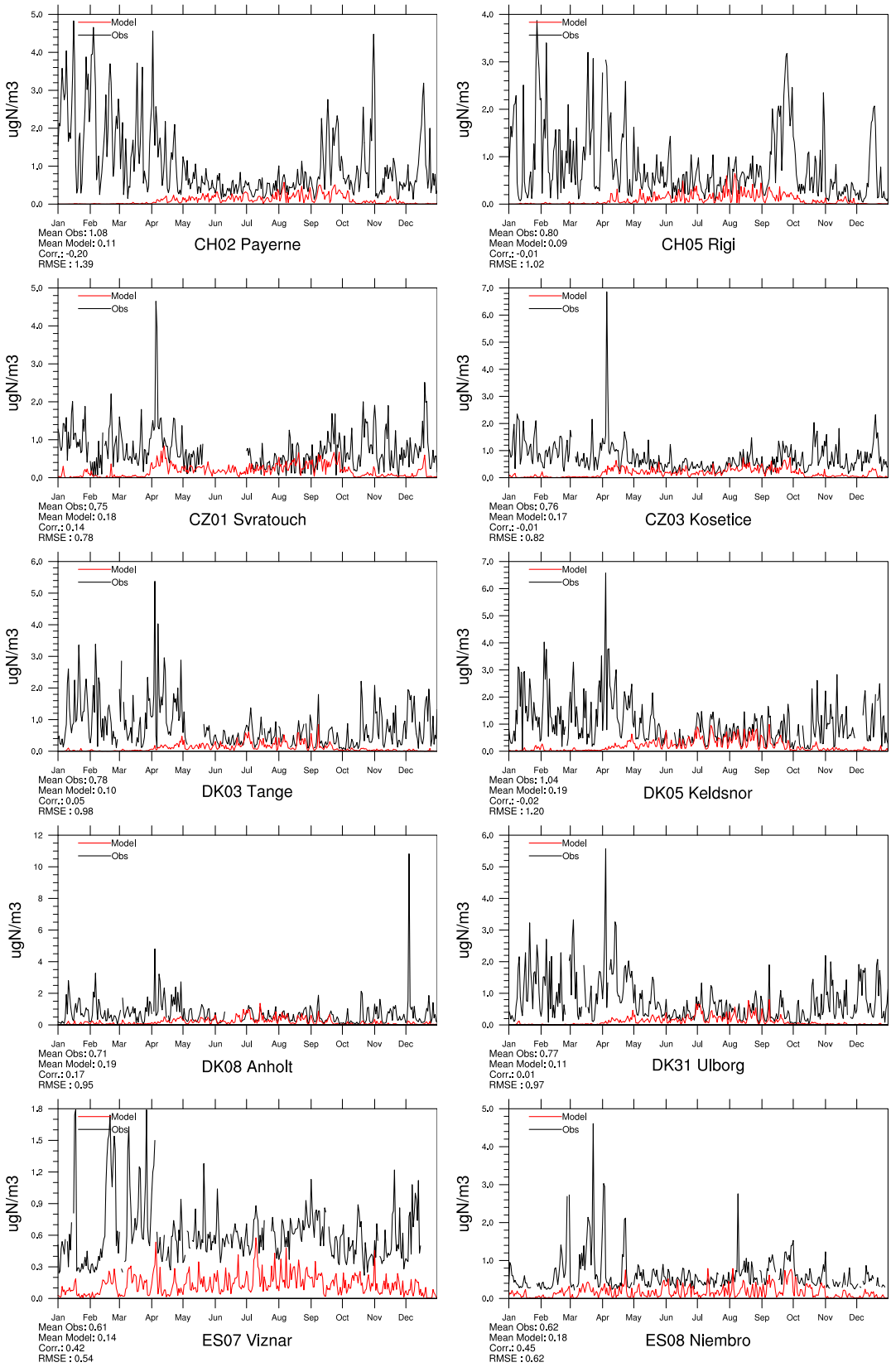

Figure 1.16: Comparison of model results and measurements (daily) total nitrate concentrations [μg(N) m^{-3}] for stations that have measured total nitrate in 2009.

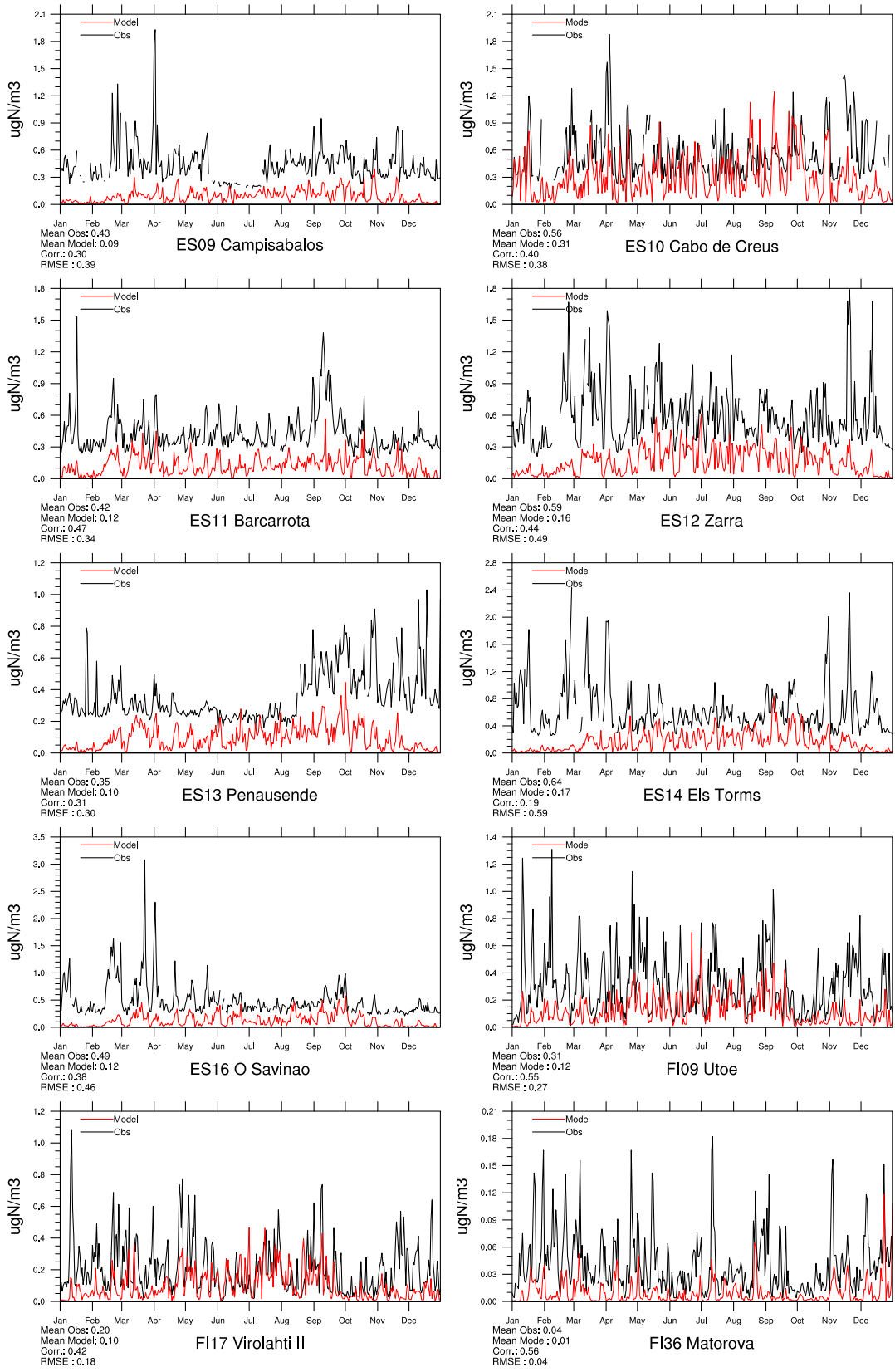

Figure 1.17: Comparison of model results and measurements (daily) total nitrate concentrations [μg(N) m^{-3}] for stations that have measured total nitrate in 2009.

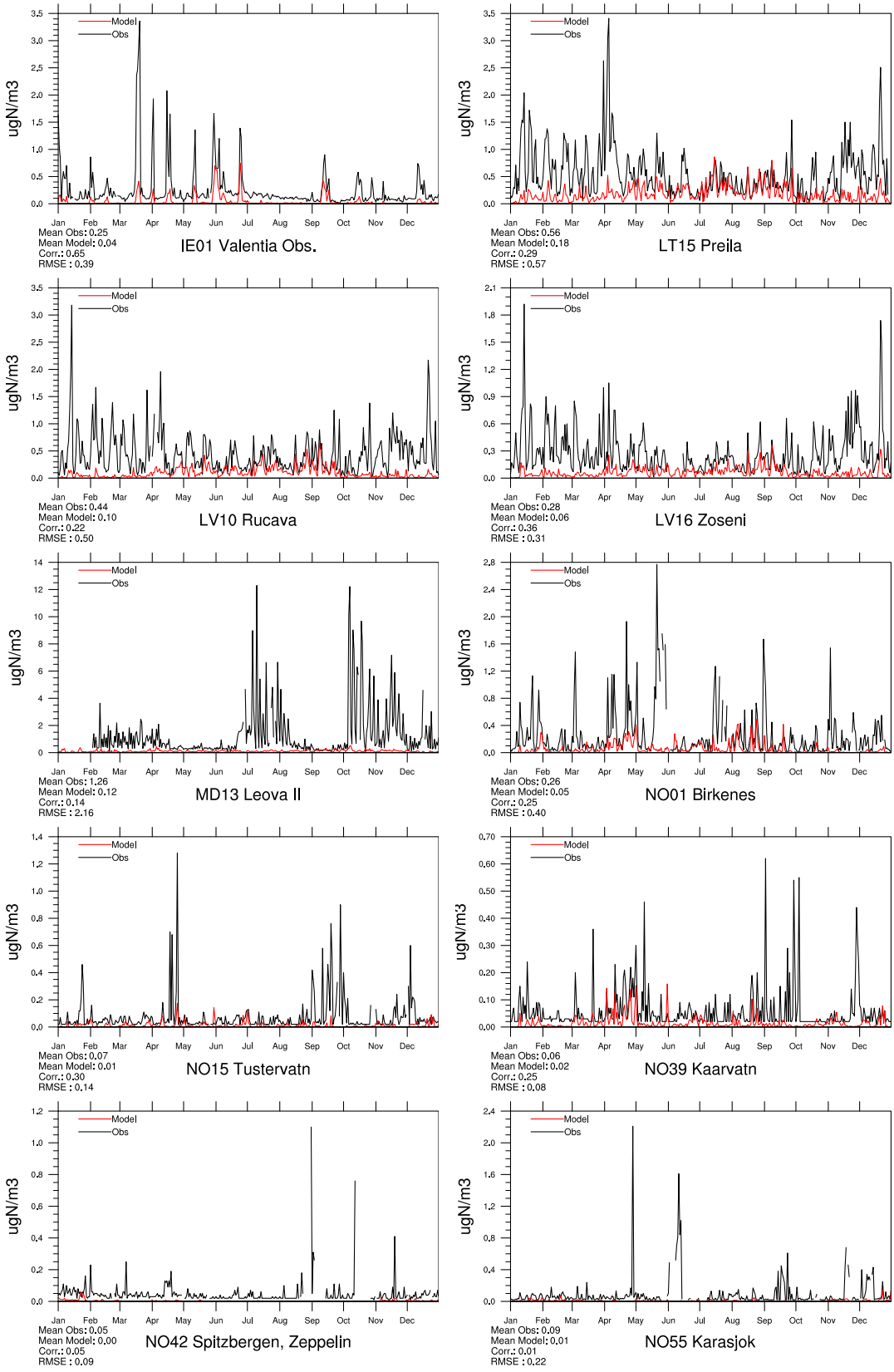

Figure 1.18: Comparison of model results and measurements (daily) total nitrate concentrations [μg(N) m^{-3}] for stations that have measured total nitrate in 2009.

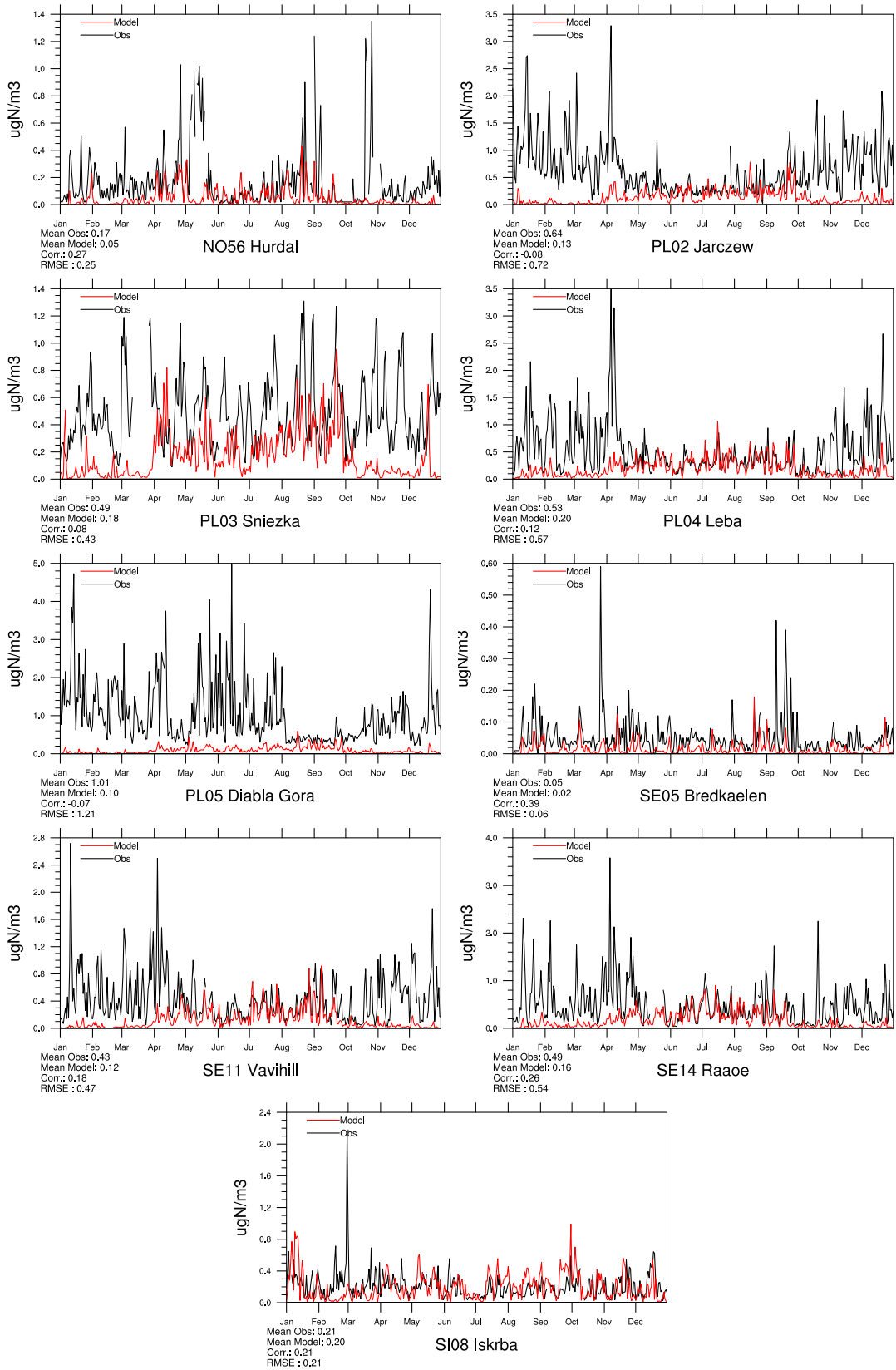

Figure 1.19: Comparison of model results and measurements (daily) total nitrate concentrations [μg(N) m^{-3}] for stations that have measured total nitrate in 2009.

Ammonia+ammonium in air

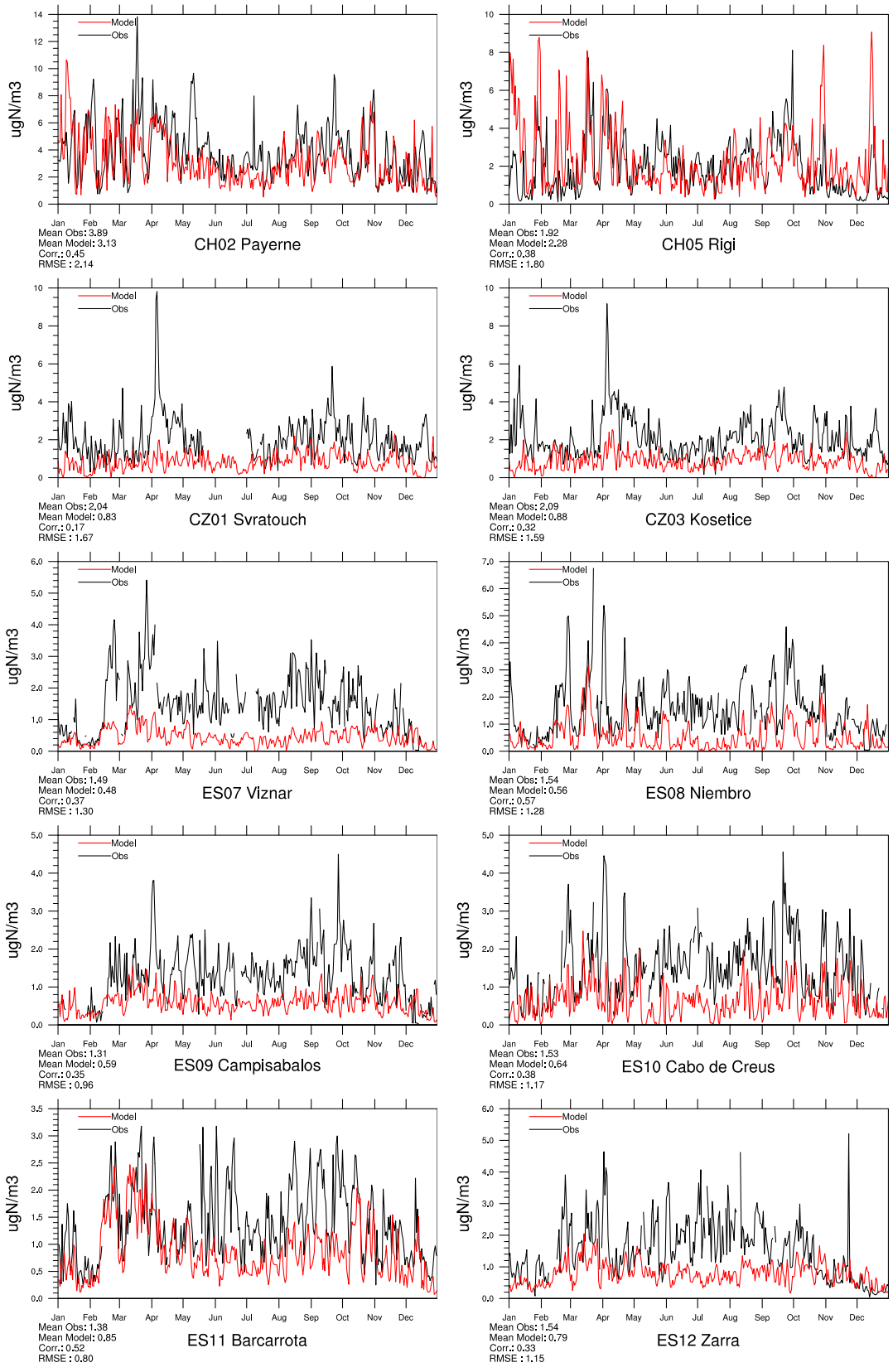

Figure 1.20: Comparison of model results and measurements (daily) total ammonium+ammonia concentrations [μg(N) m^{-3}] for stations that have measured total ammonium+ammonia in 2009.

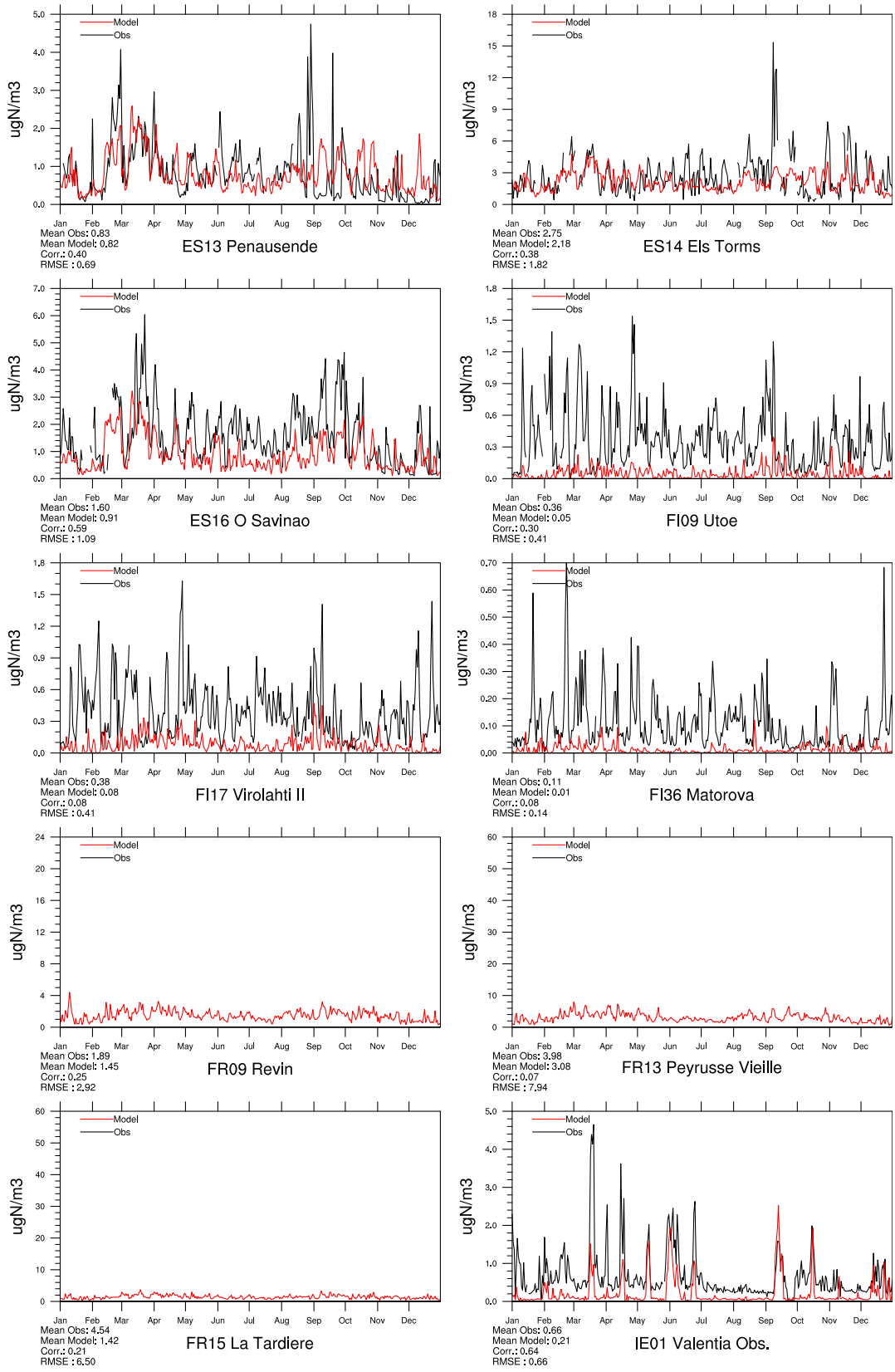

Figure 1.21: Comparison of model results and measurements (daily) total ammonium+ammonia concentrations [μg(N) m^{-3}] for stations that have measured total ammonium+ammonia in 2009.

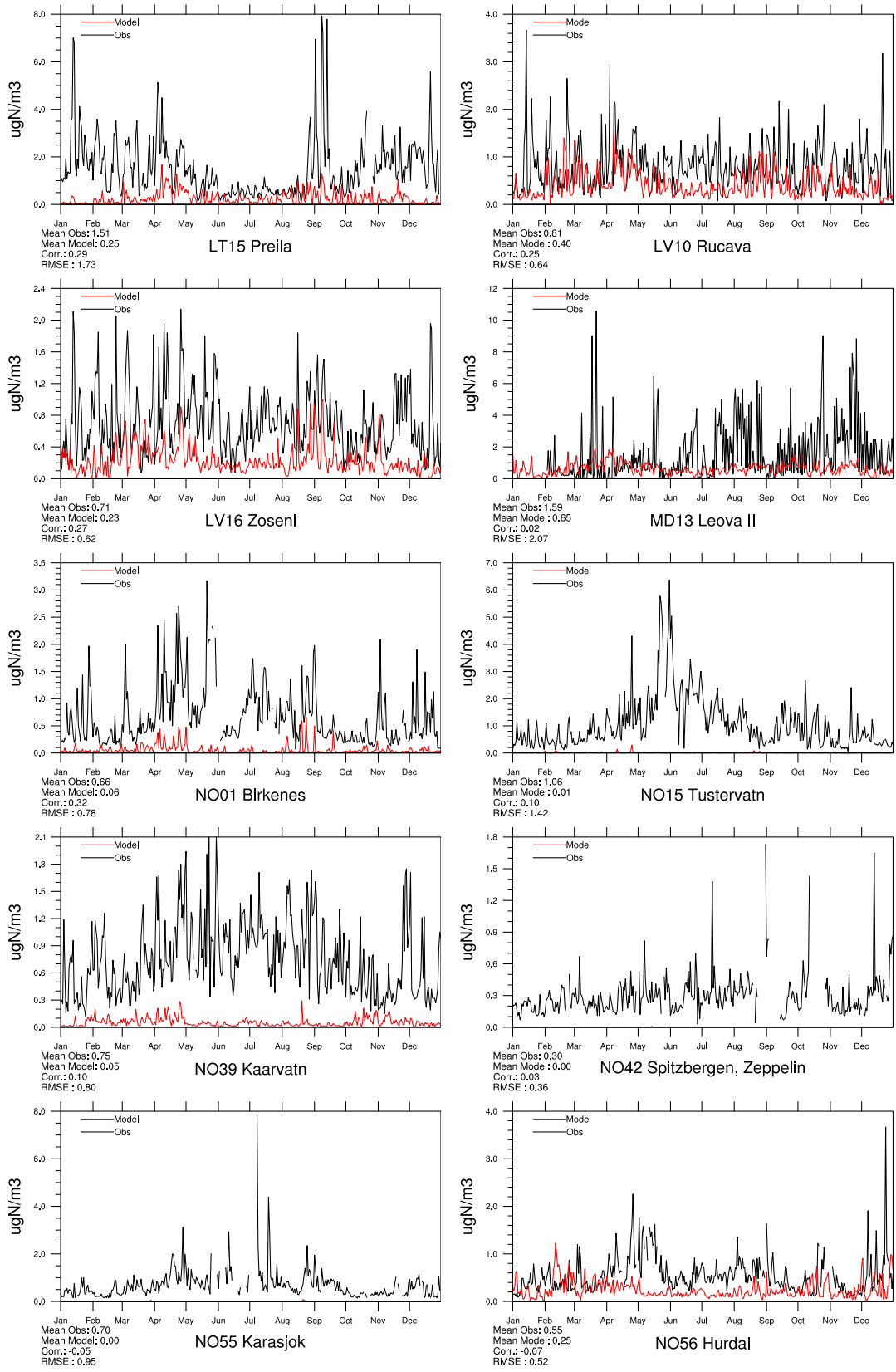

Figure 1.22: Comparison of model results and measurements (daily) total ammonium+ammonia concentrations [μg(N) m^{-3}] for stations that have measured total ammonium+ammonia in 2009.

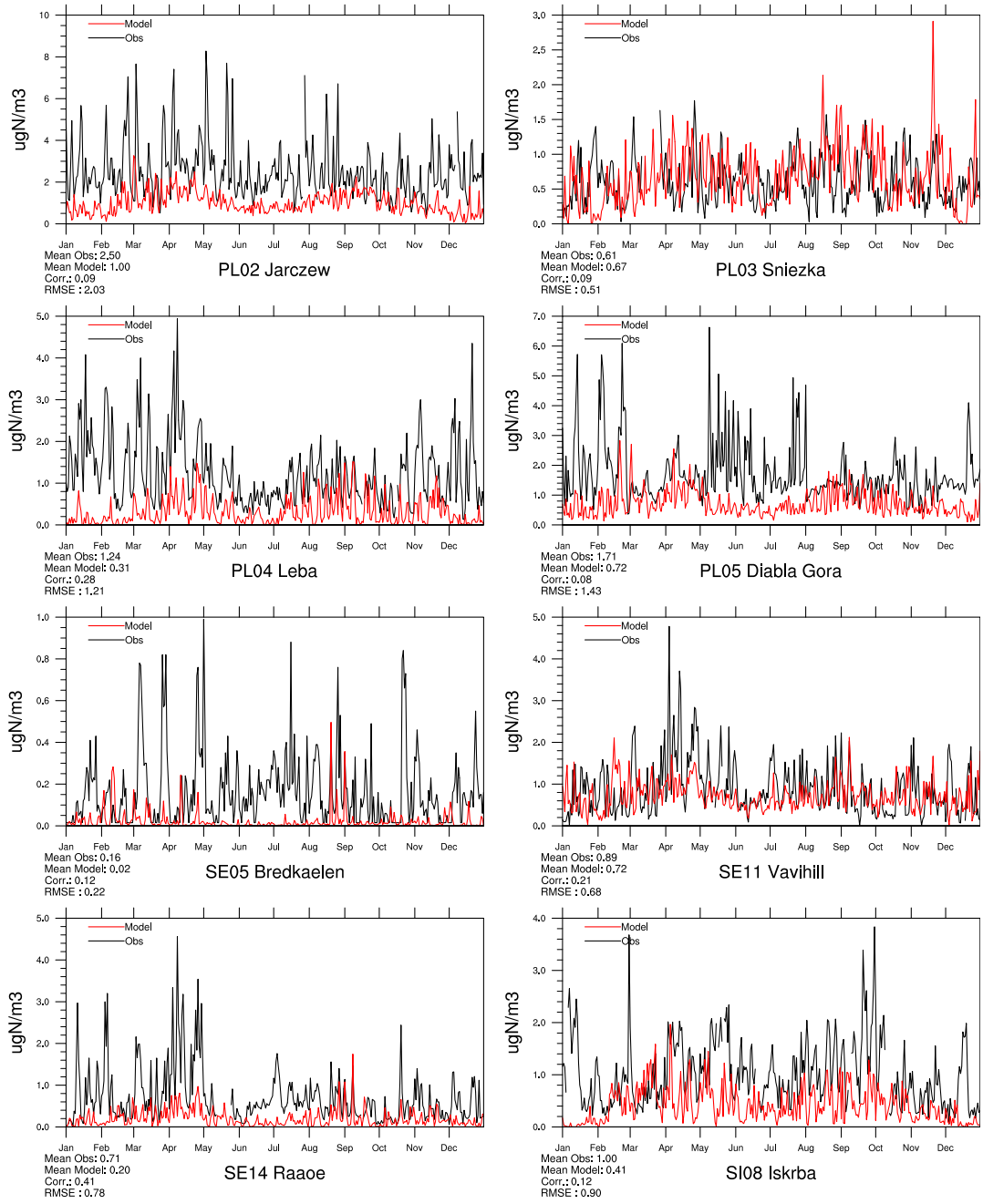

Figure 1.23: Comparison of model results and measurements (daily) total ammonium+ammonia concentrations [μg(N) m^{-3}] for stations that have measured total ammonium+ammo nia in 2009.

Sulphur in precipitation

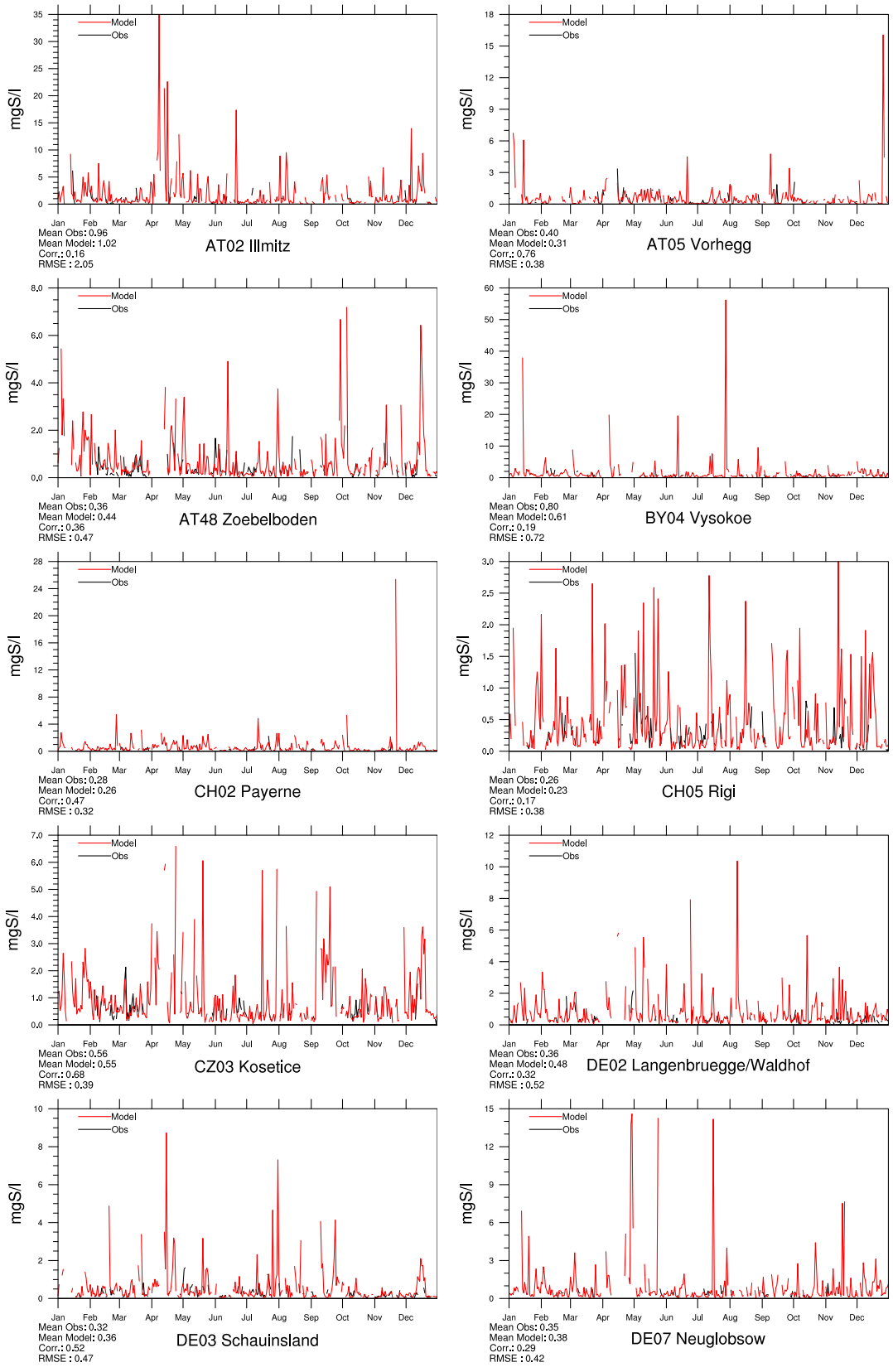

Figure 1.24: Comparison of model results and measurements (daily) for sulphur concentrations in precipitation [μg(S)l^{-1}] in 2009.

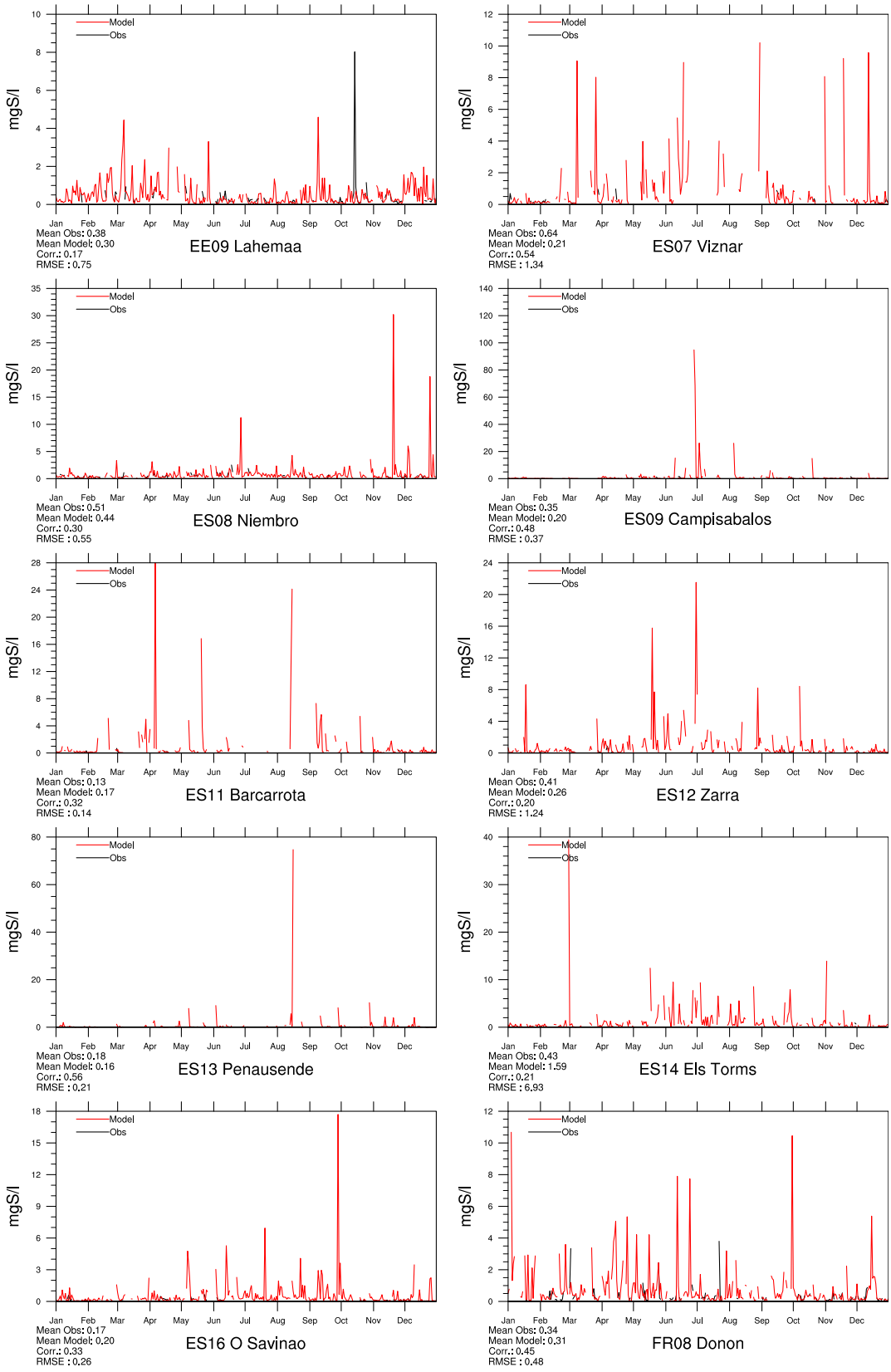

Figure 1.25: Comparison of model results and measurements (daily) for sulphur concentrations in precipitation [μg(S)l^{-1}] in 2009.

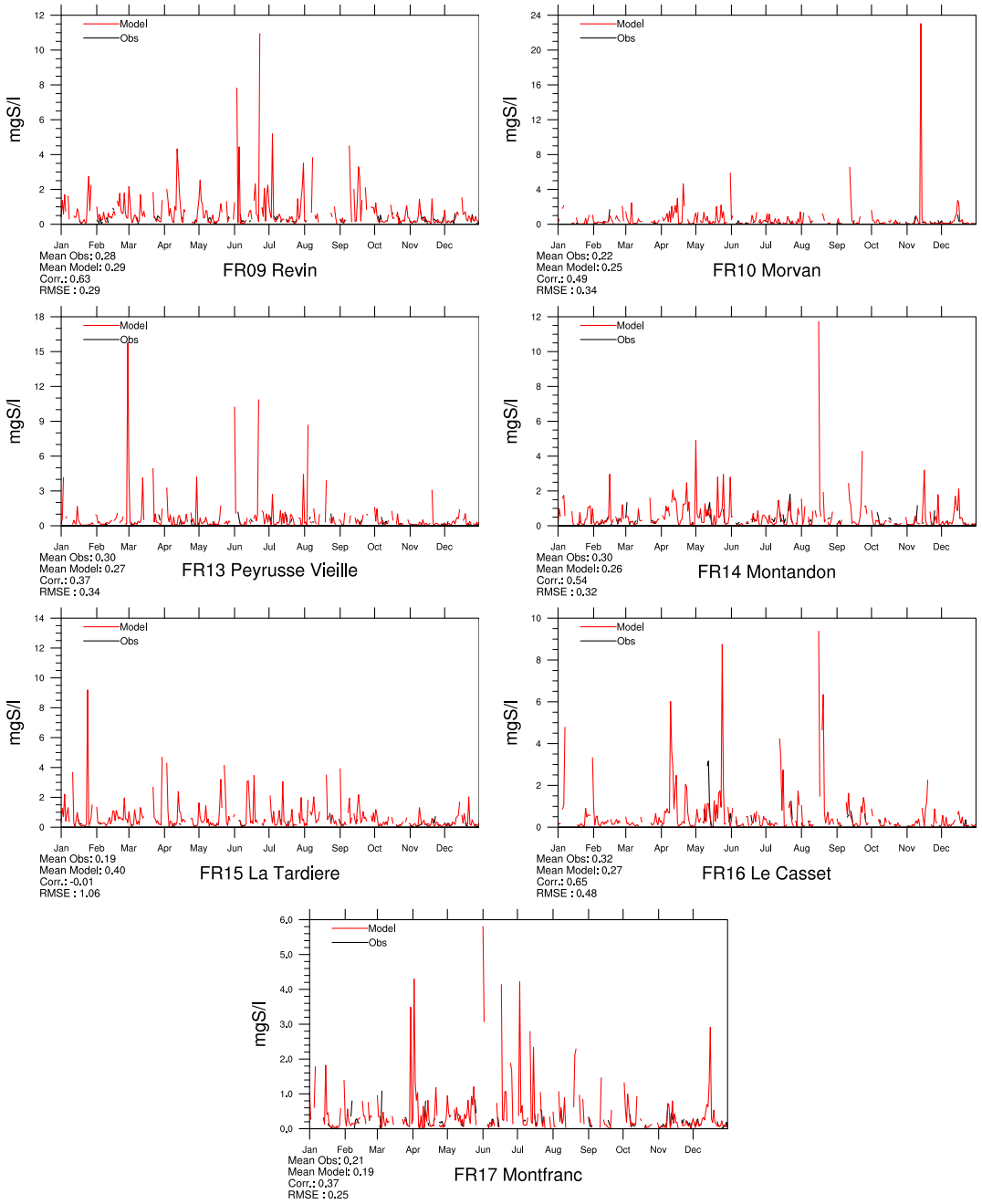

Figure 1.26: Comparison of model results and measurements (daily) for sulphur concentrations in precipitation [μg(S)l^{-1}] in 2009.

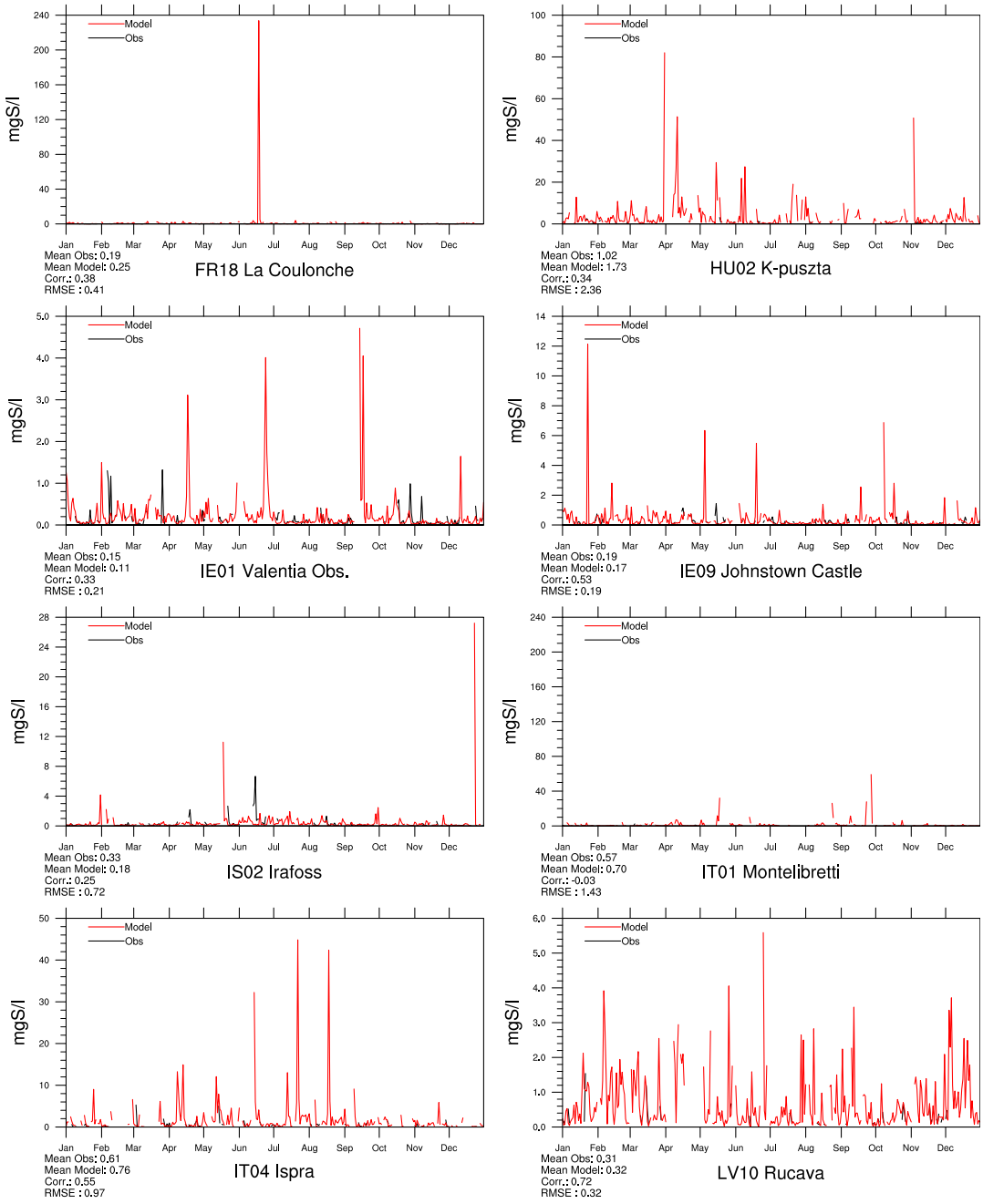

Figure 1.27: Comparison of model results and measurements (daily) for sulphur concentrations in precipitation [μg(S)l^{-1}] in 2009.

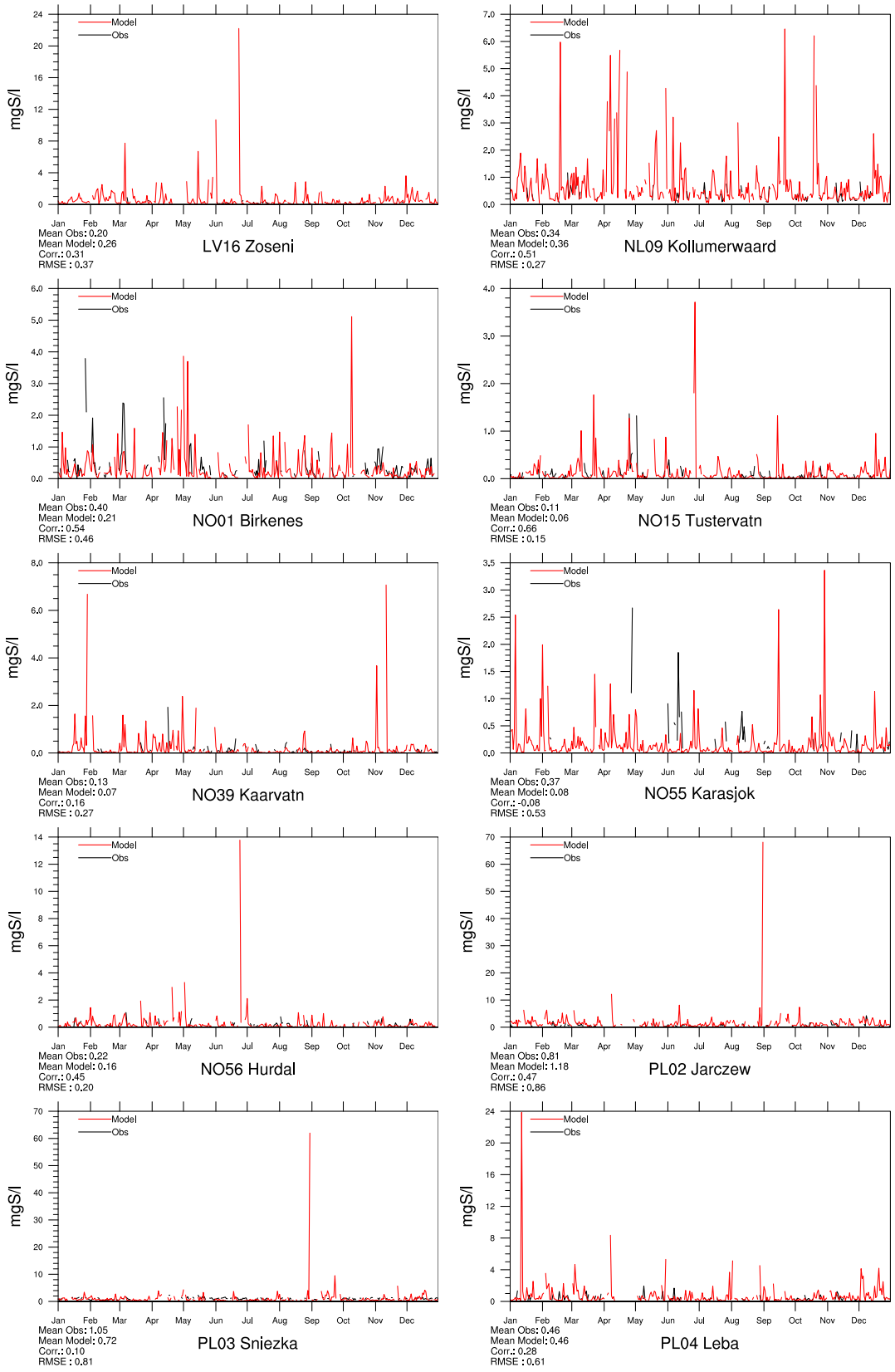

Figure 1.28: Comparison of model results and measurements (daily) for sulphur concentrations in precipitation [μg(S)l^{-1}] in 2009.

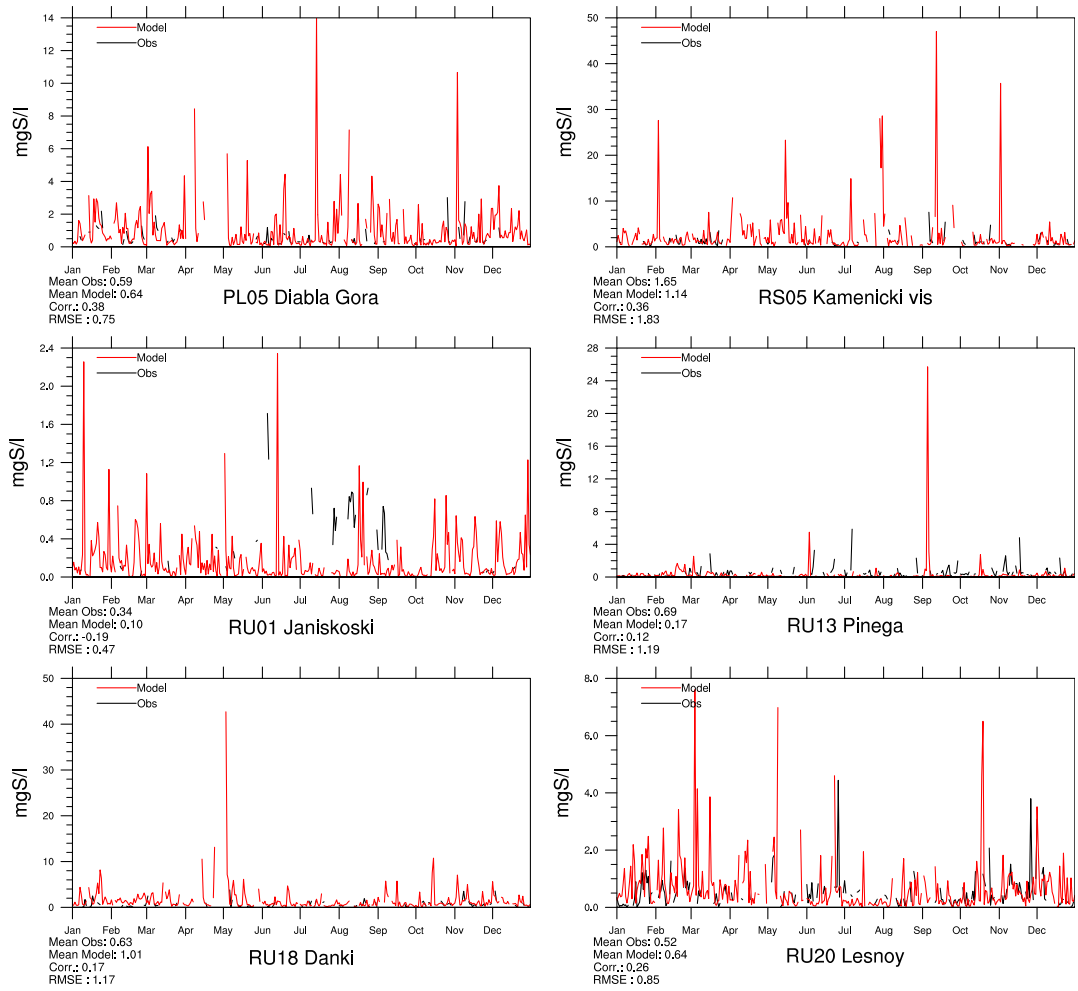

Figure 1.29: Comparison of model results and measurements (daily) for sulphur concentrations in precipitation [μg(S)l^{-1}] in 2009.

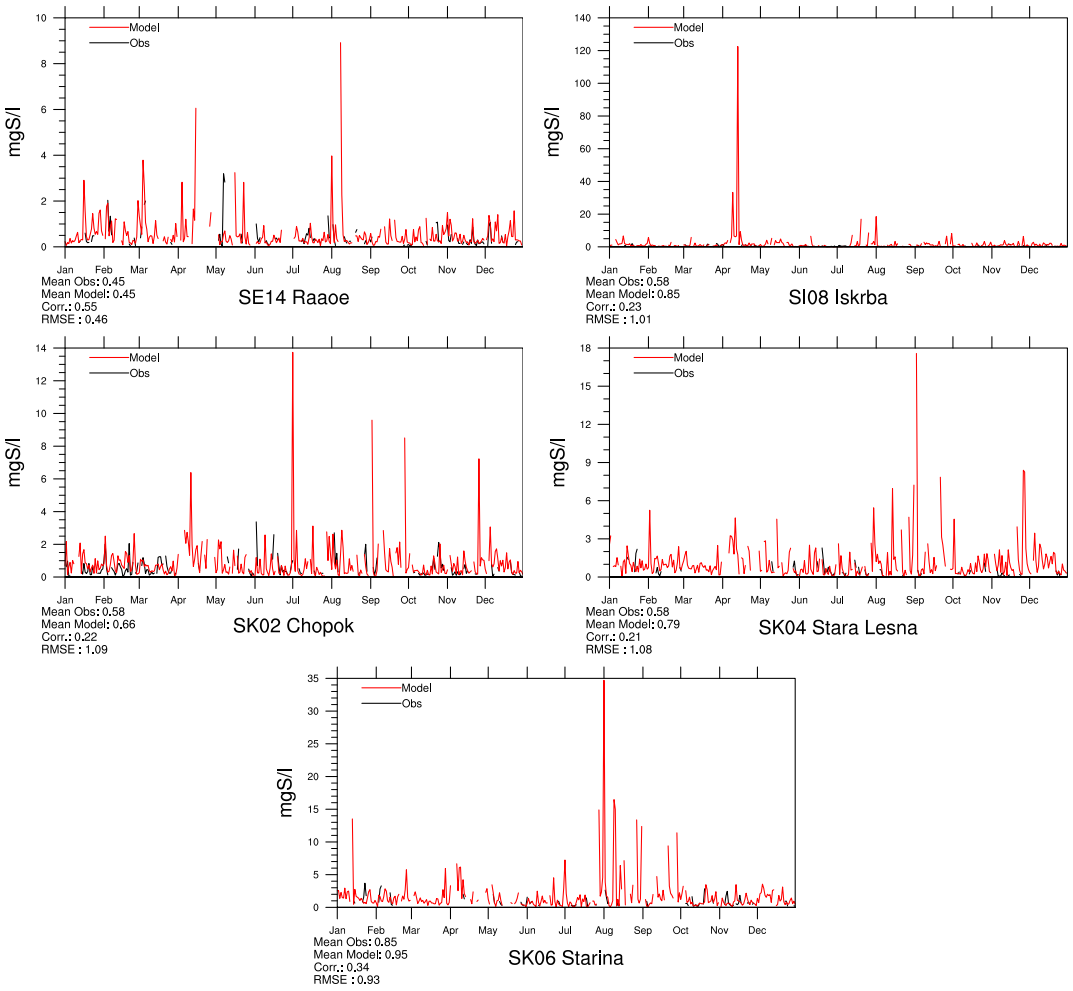

Figure 1.30: Comparison of model results and measurements (daily) for sulphur concentrations in precipitation [μg(S)l^{-1}] in 2009.

Oxidized nitrogen in precipitation

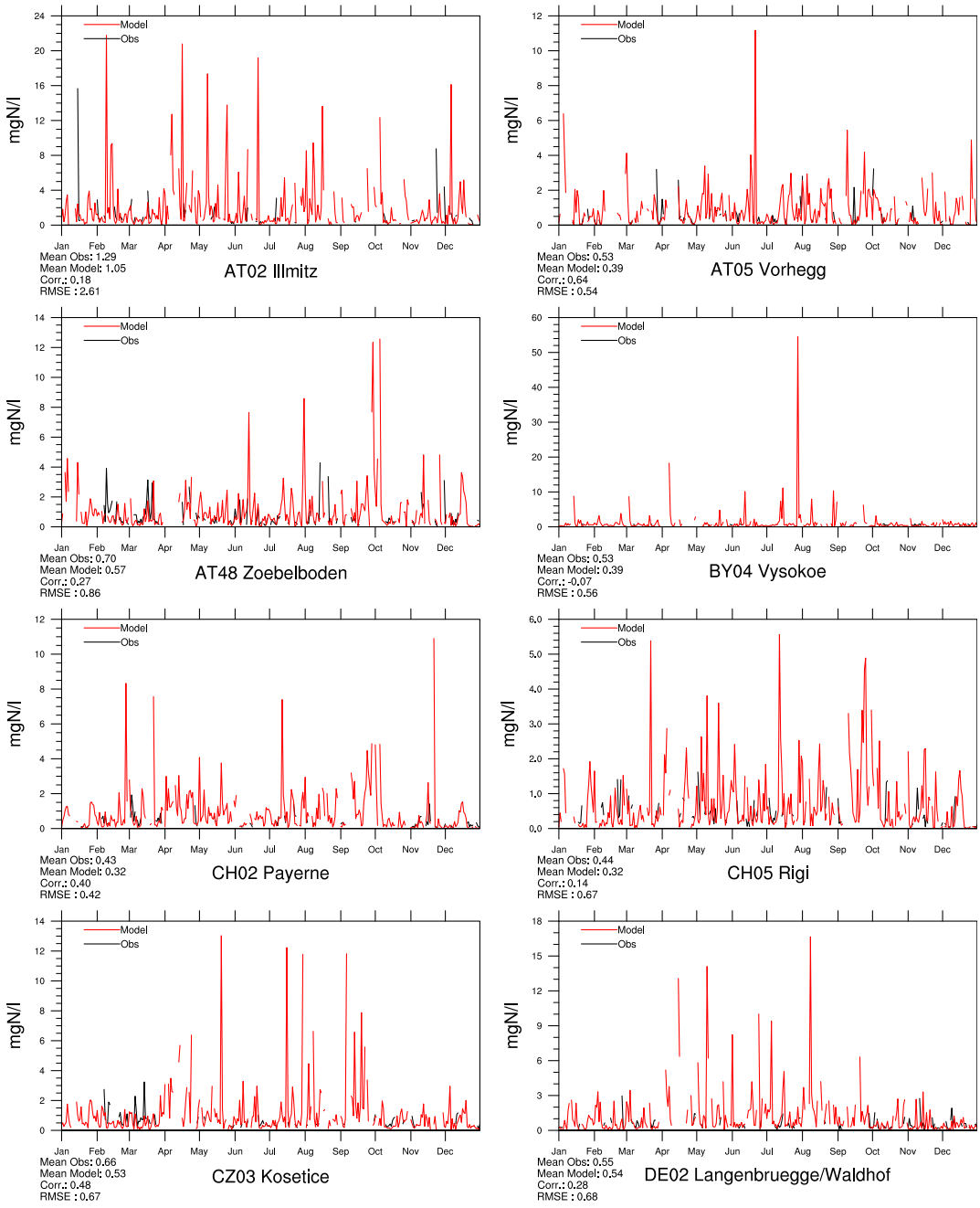

Figure 1.31: Comparison of model results and measurements (daily) for oxidized nitrogen concentrations in precipitation [μg(N)l^{-1}] in 2009.

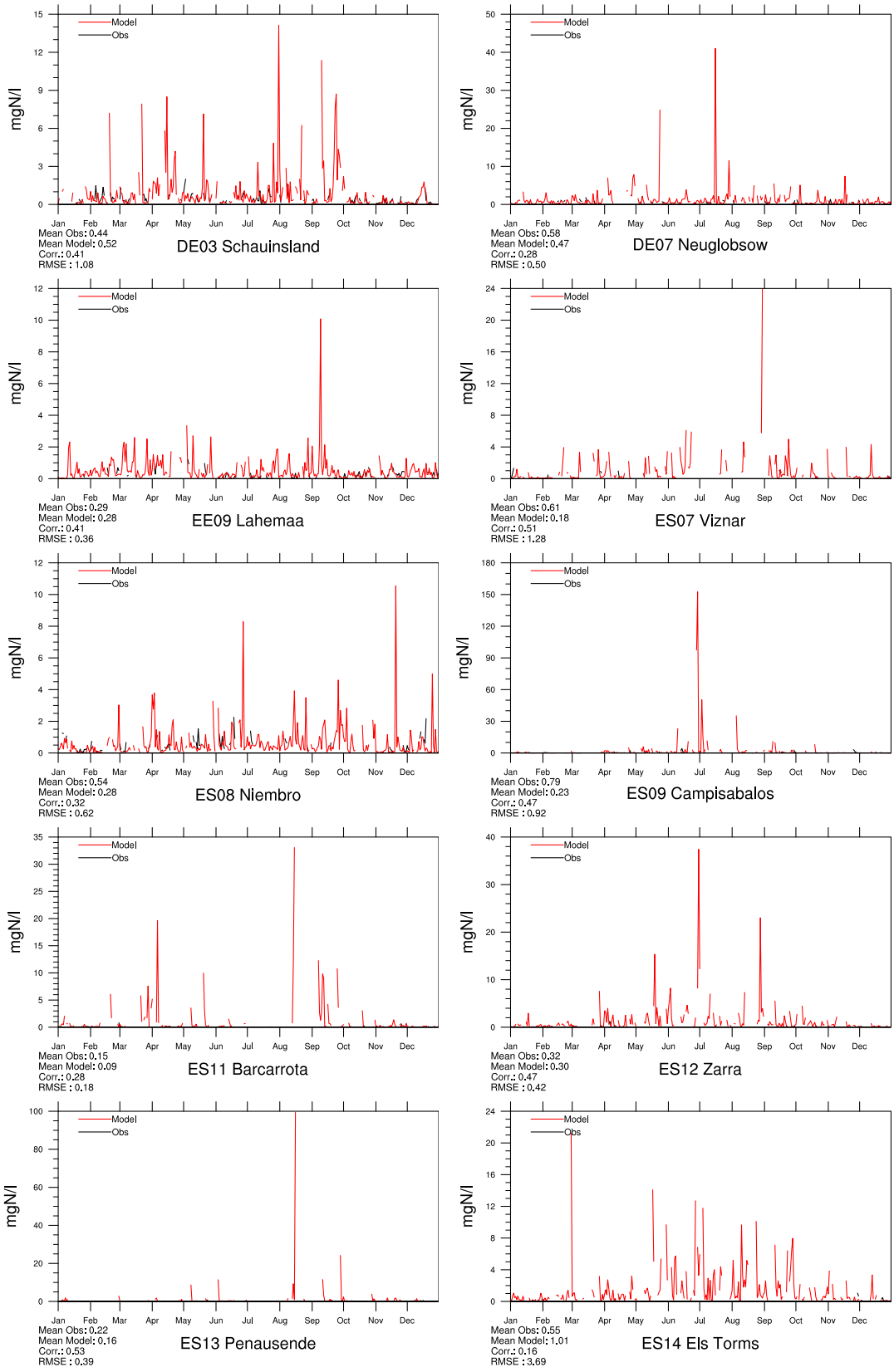

Figure 1.32: Comparison of model results and measurements (daily) for oxidized nitrogen concentrations in precipitation [μg(N)l^{-1}] in 2009.

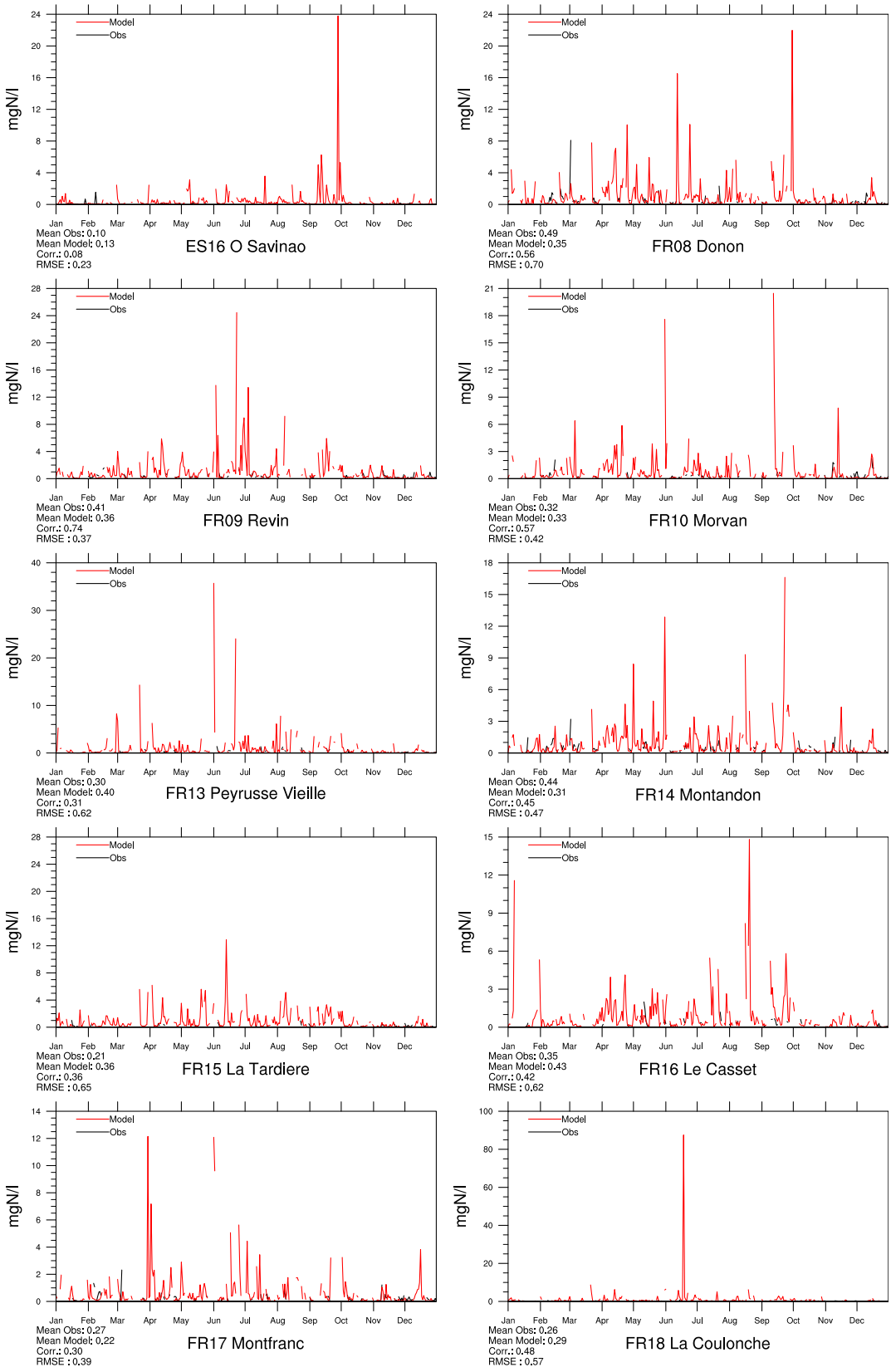

Figure 1.33: Comparison of model results and measurements (daily) for oxidized nitrogen concentrations in precipitation [μg(N)l^{-1}] in 2009.

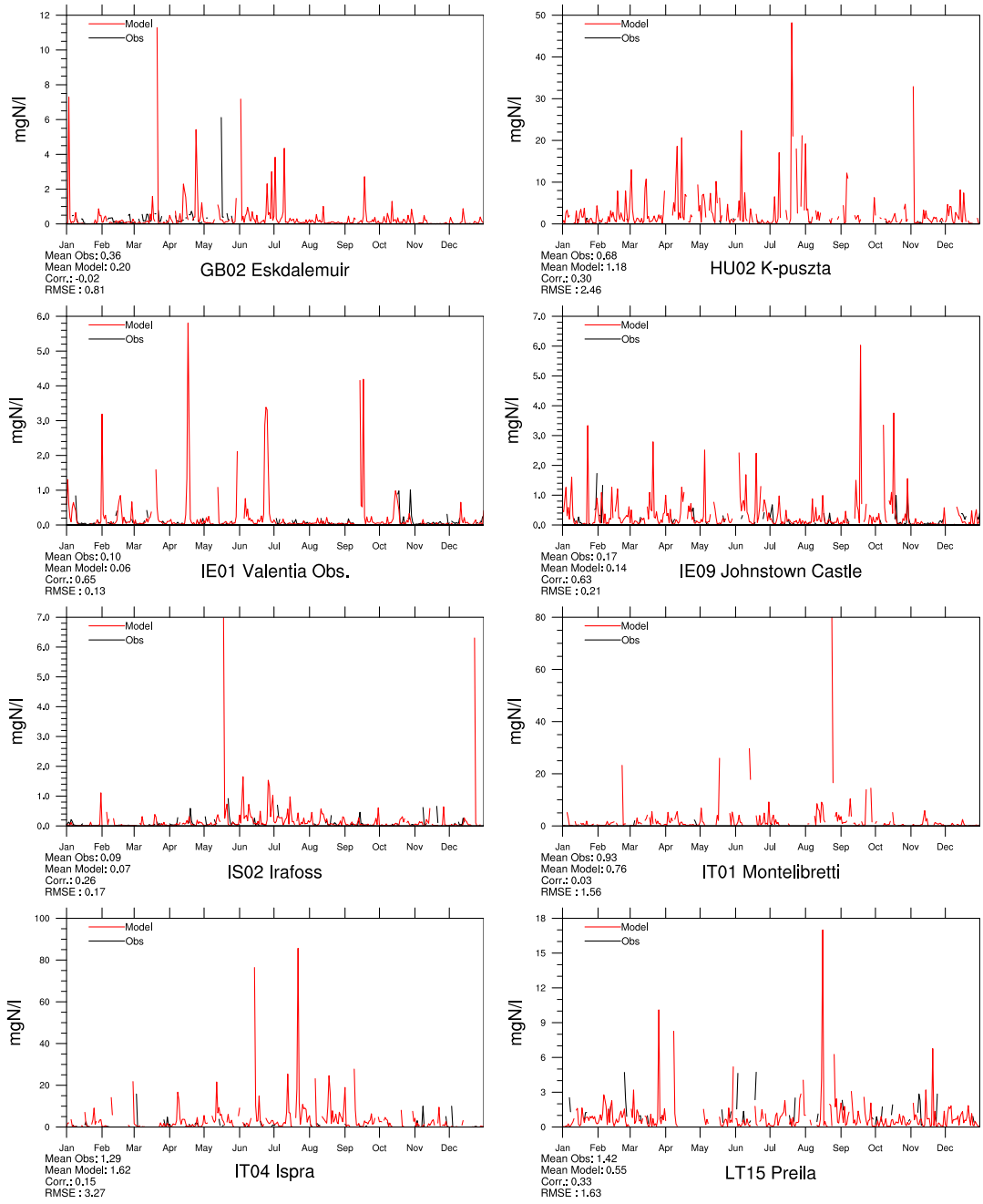

Figure 1.34: Comparison of model results and measurements (daily) for oxidized nitrogen concentrations in precipitation [μg(N)l^{-1}] in 2009.

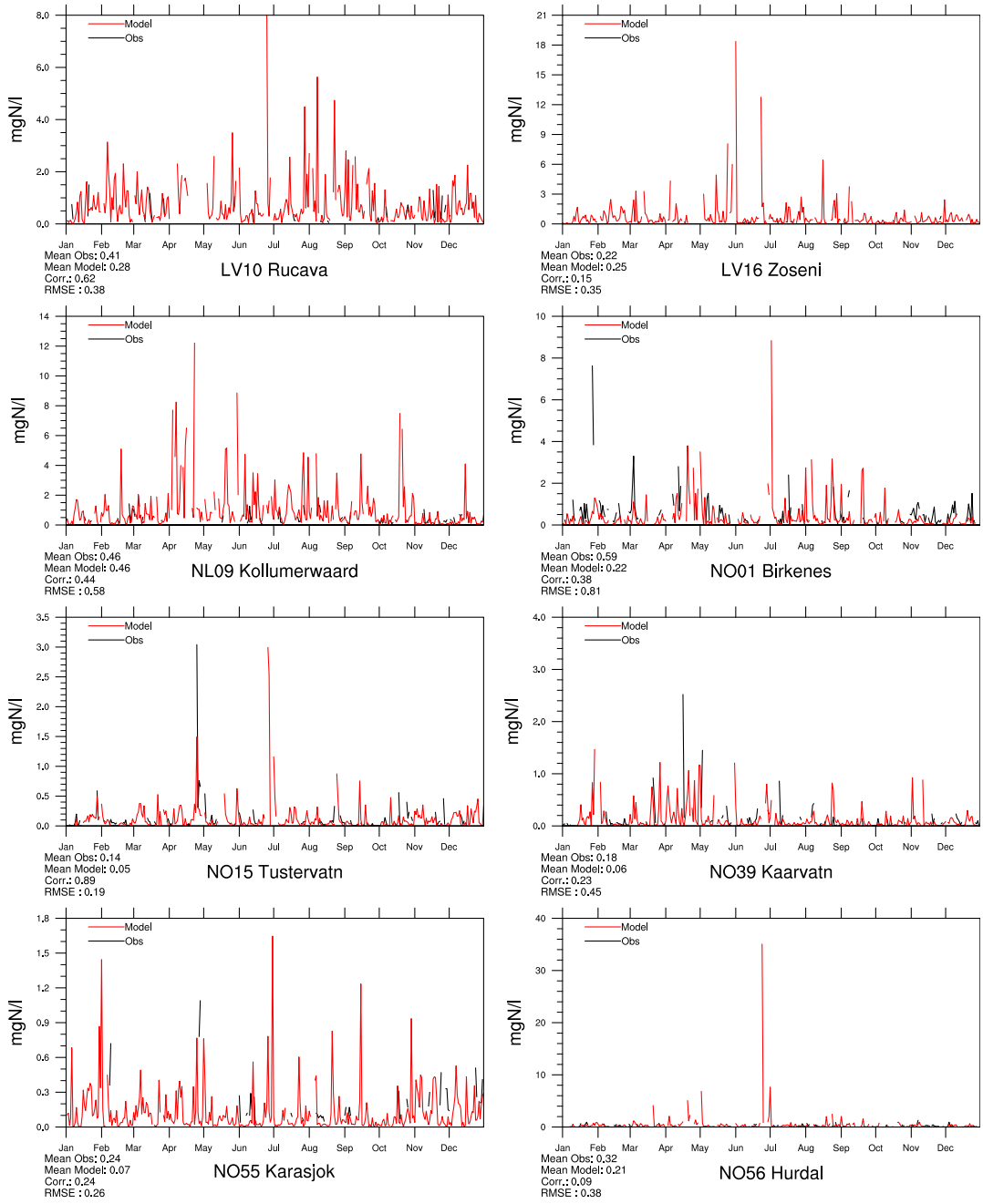

Figure 1.35: Comparison of model results and measurements (daily) for oxidized nitrogen concentrations in precipitation [μg(N)l^{-1}] in 2009.

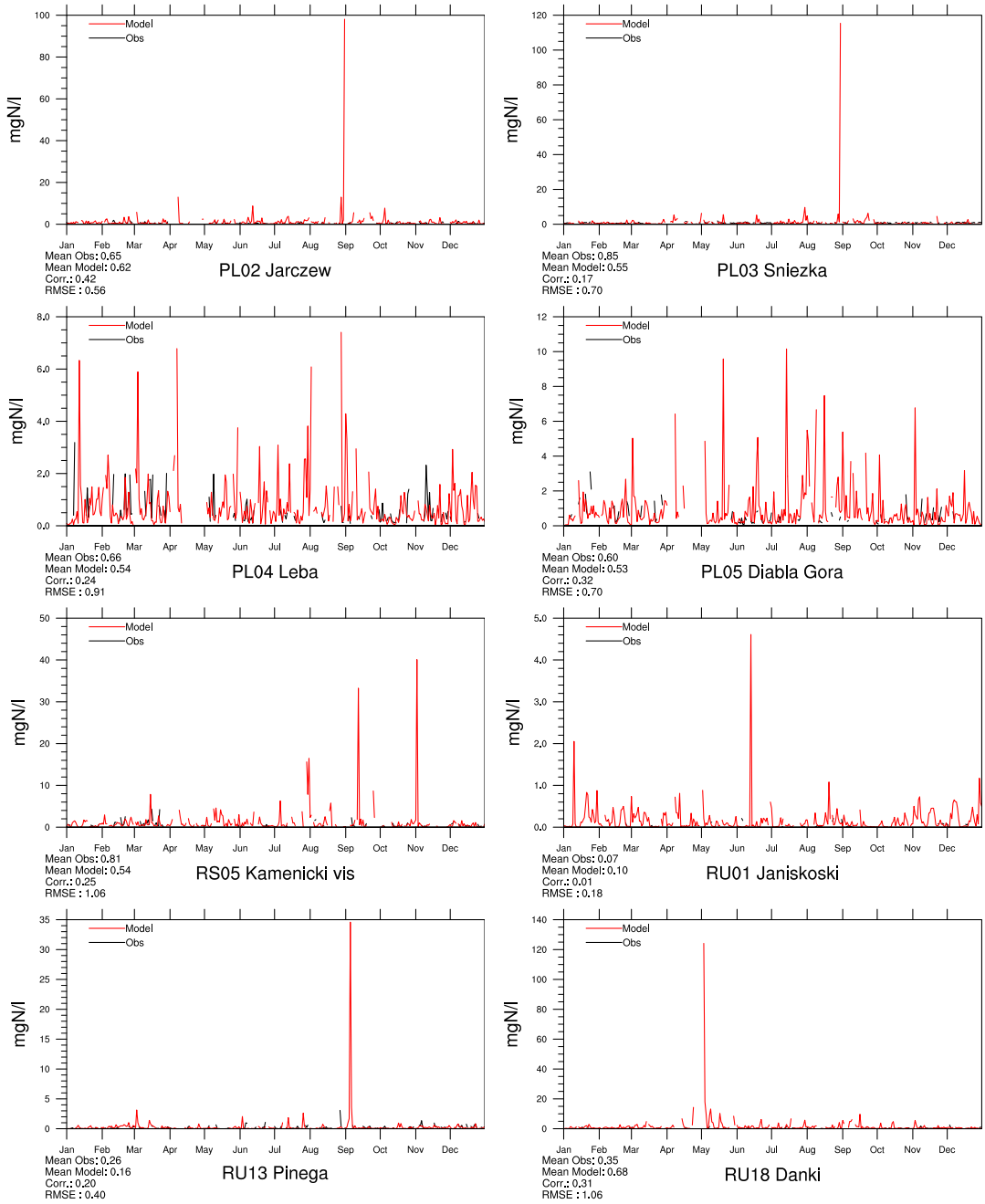

Figure 1.36: Comparison of model results and measurements (daily) for oxidized nitrogen concentrations in precipitation [μg(N)l^{-1}] in 2009.

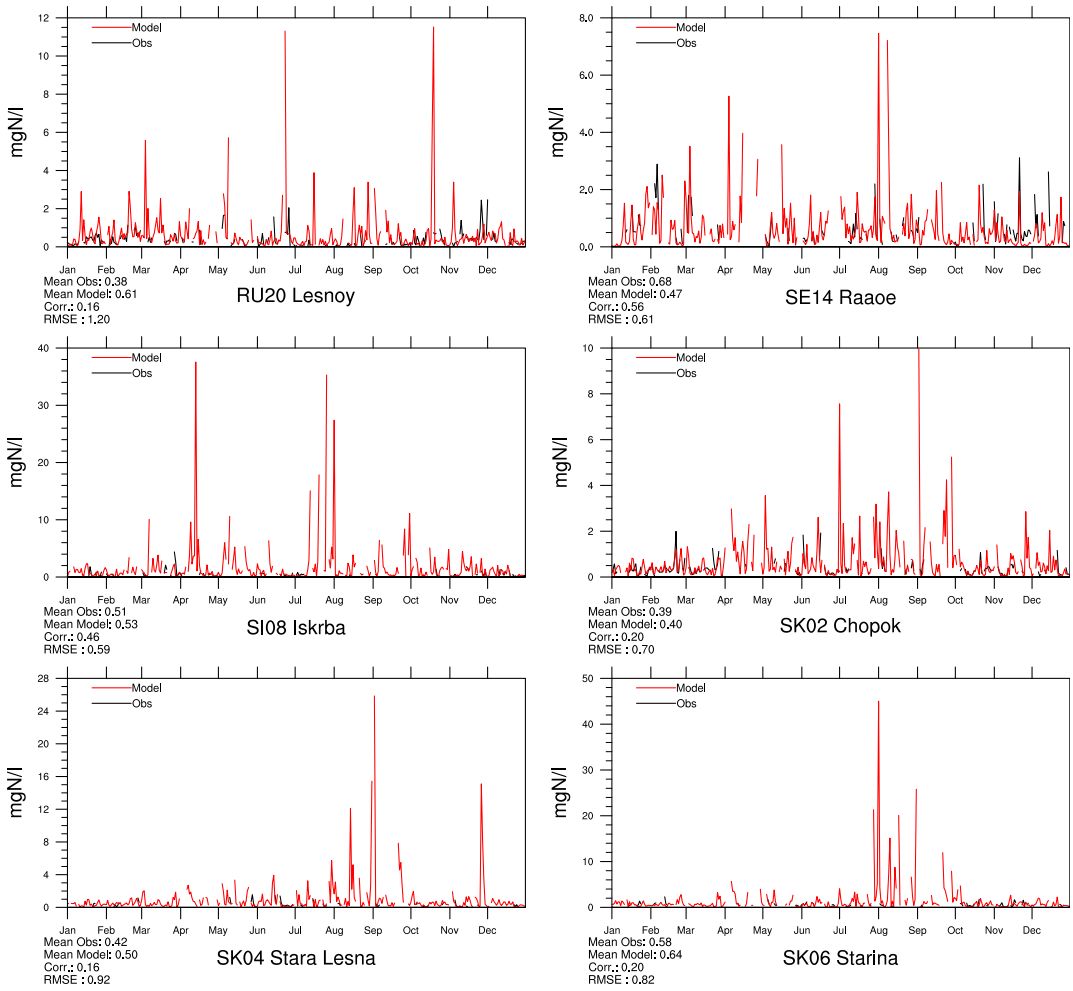

Figure 1.37: Comparison of model results and measurements (daily) for oxidized nitrogen concentrations in precipitation [μg(N)l^{-1}] in 2009.

Reduced nitrogen in precipitation

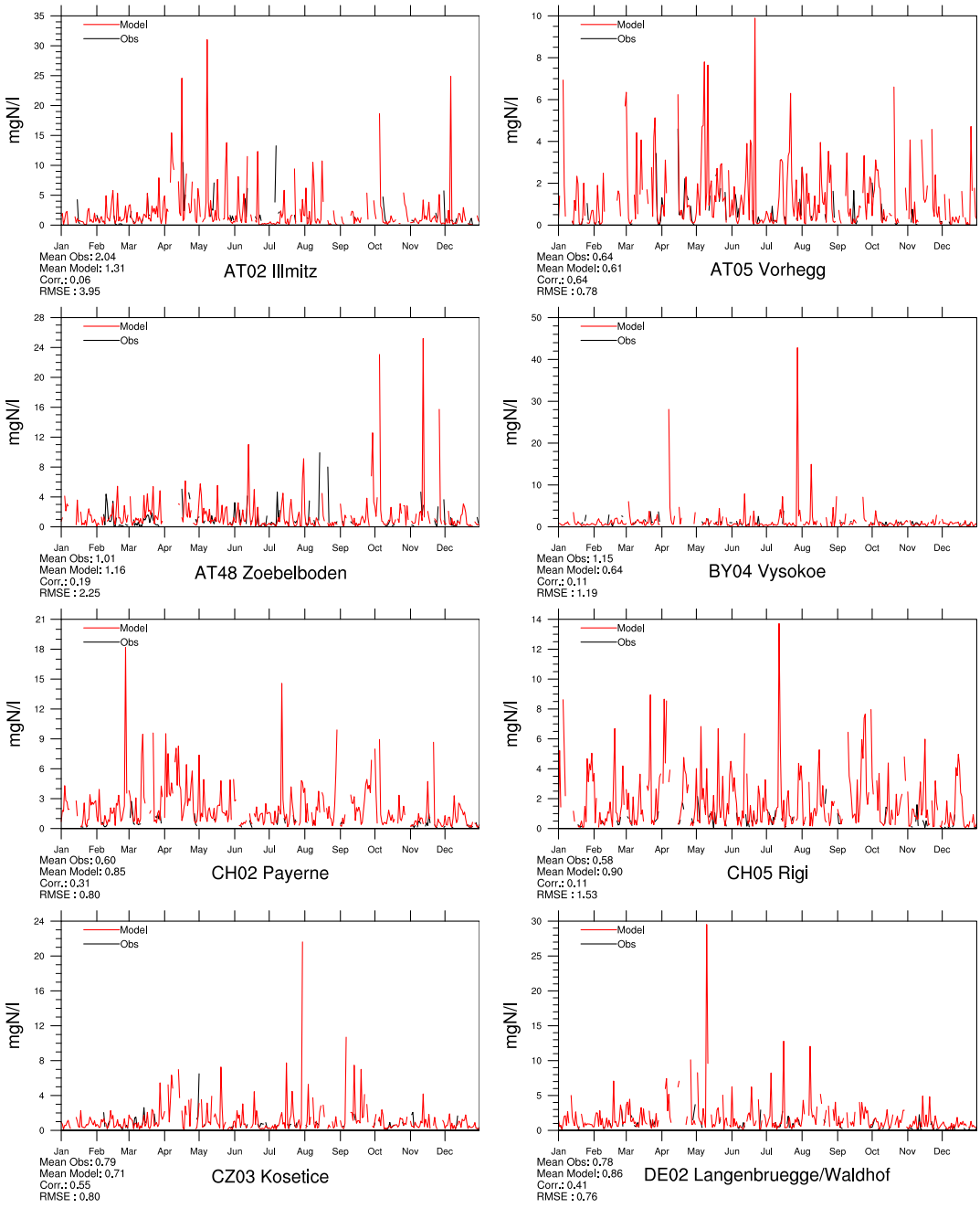

Figure 1.38: Comparison of model results and measurements (daily) for reduced nitrogen concentrations in precipitation [μg(N)l^{-1}] in 2009.

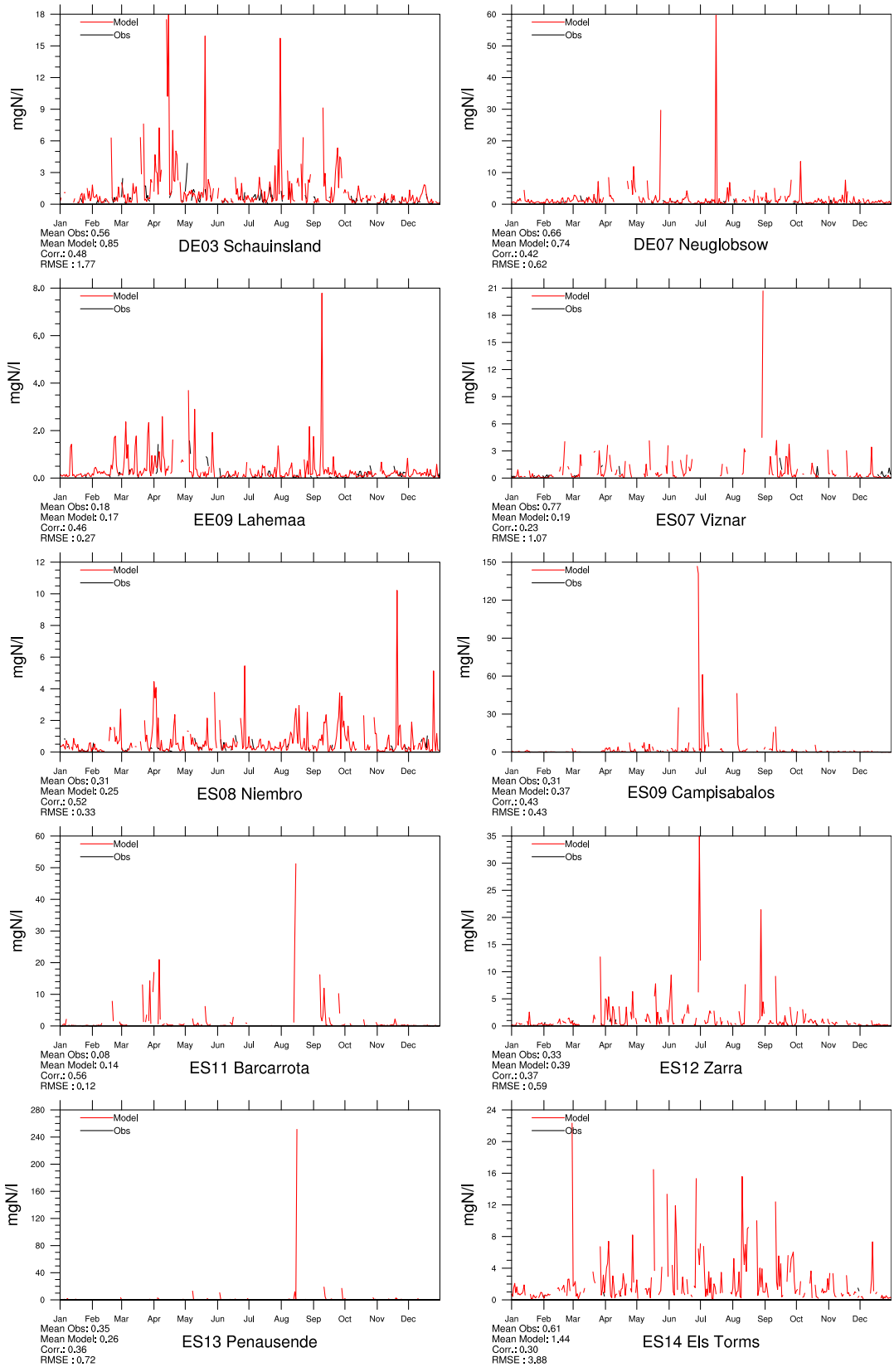

Figure 1.39: Comparison of model results and measurements (daily) for reduced nitrogen concentrations in precipitation [μg(N)l^{-1}] in 2009.

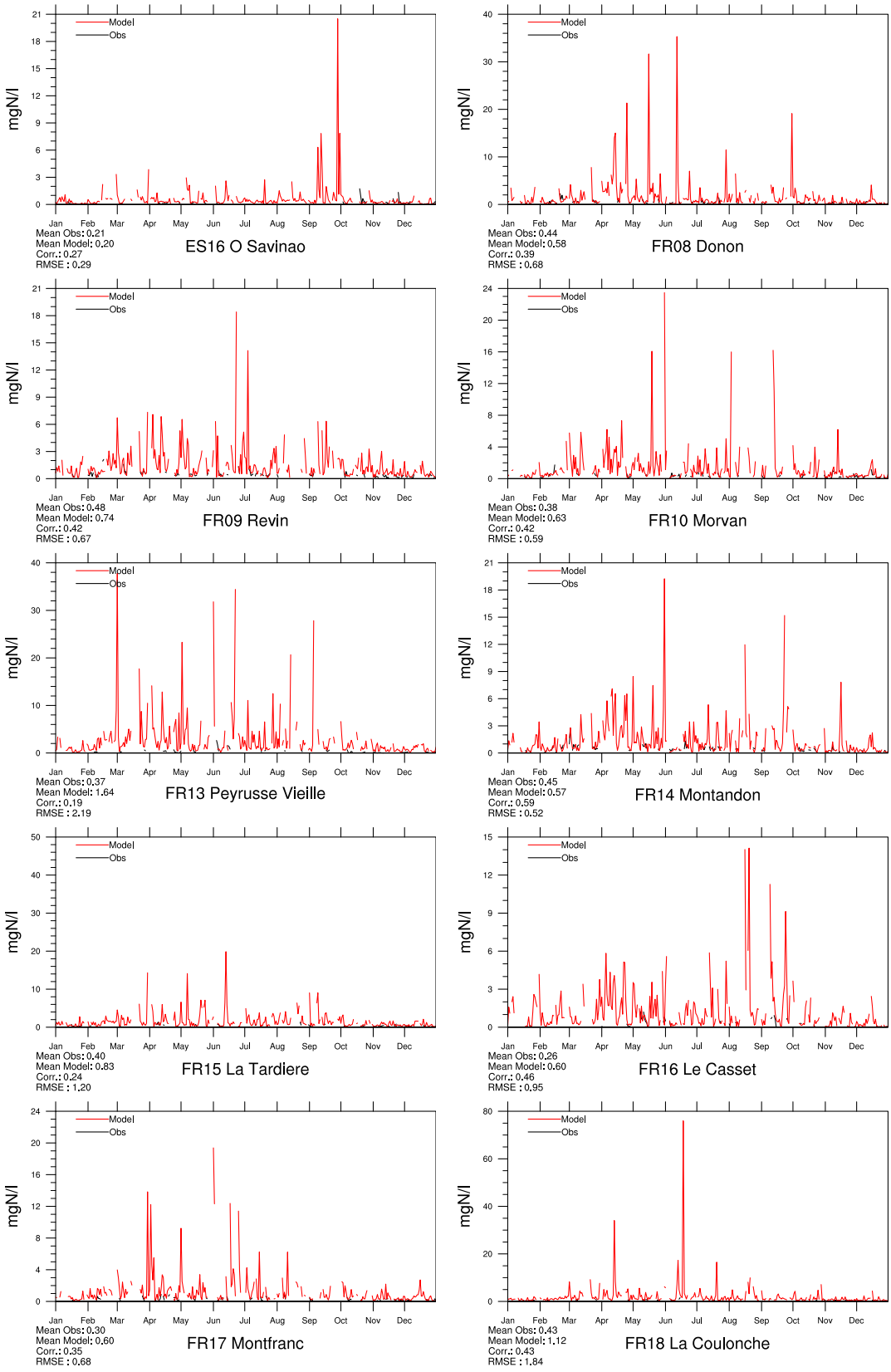

Figure 1.40: Comparison of model results and measurements (daily) for reduced nitrogen concentrations in precipitation [μg(N)l^{-1}] in 2009.

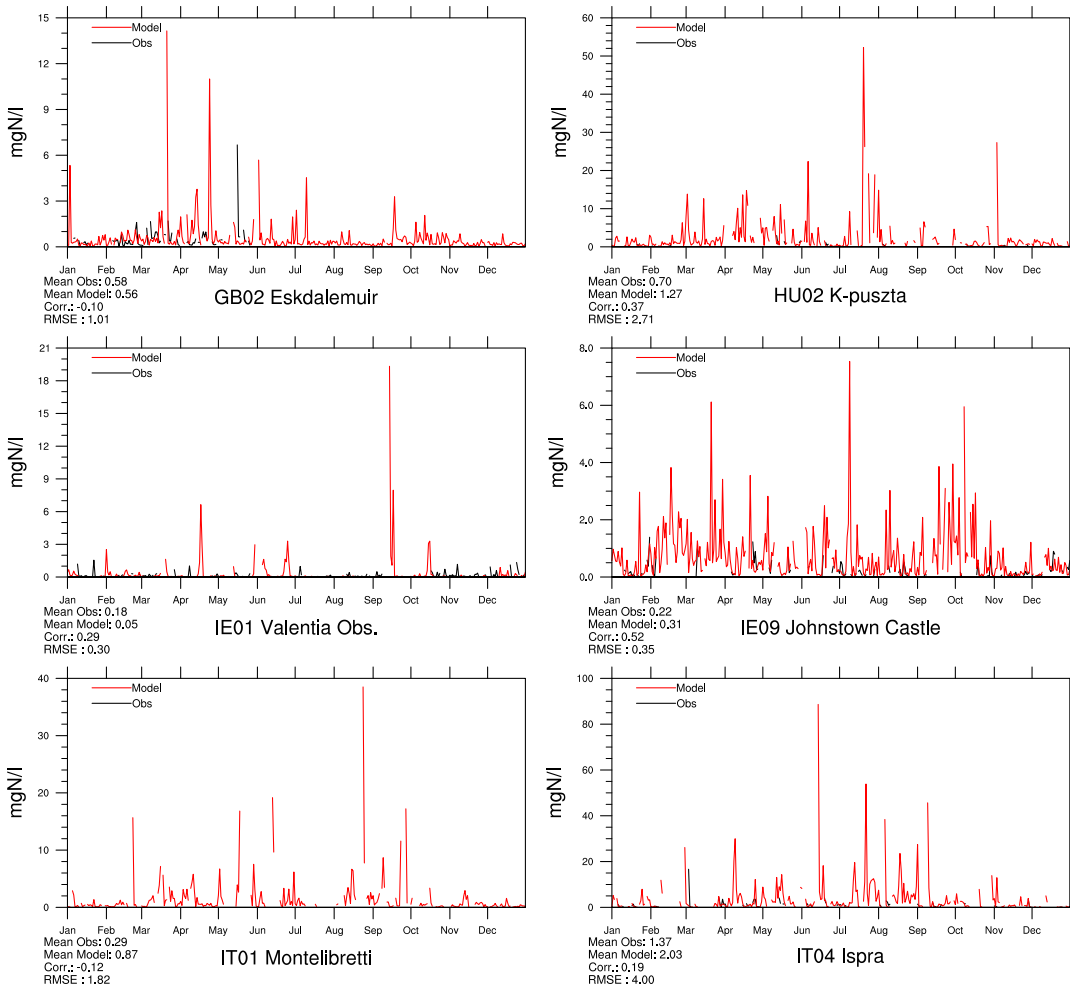

Figure 1.41: Comparison of model results and measurements (daily) for reduced nitrogen concentrations in precipitation [μg(N)l^{-1}] in 2009.

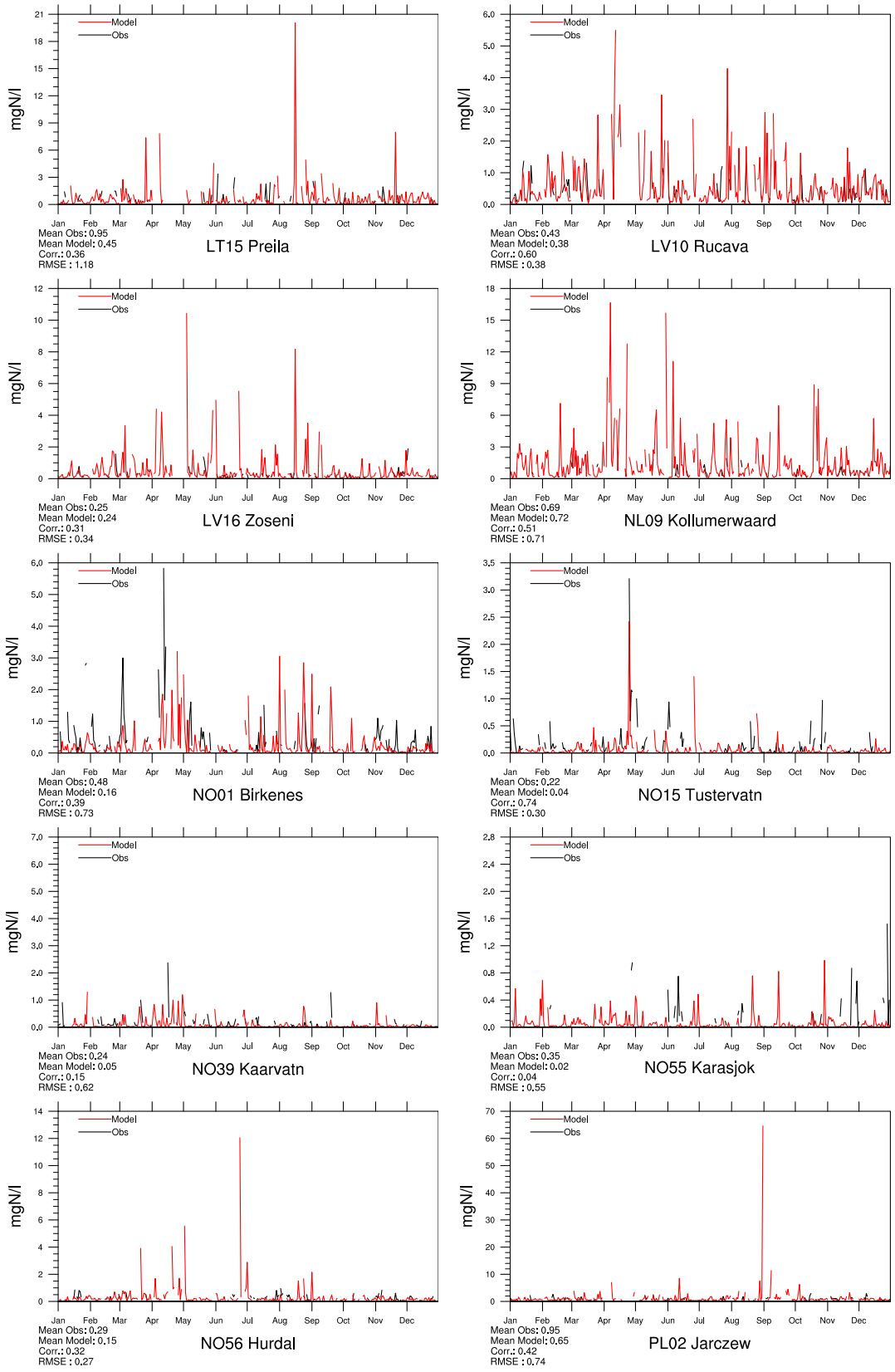

Figure 1.42: Comparison of model results and measurements (daily) for reduced nitrogen concentrations in precipitation [μg(N)l^{-1}] in 2009.

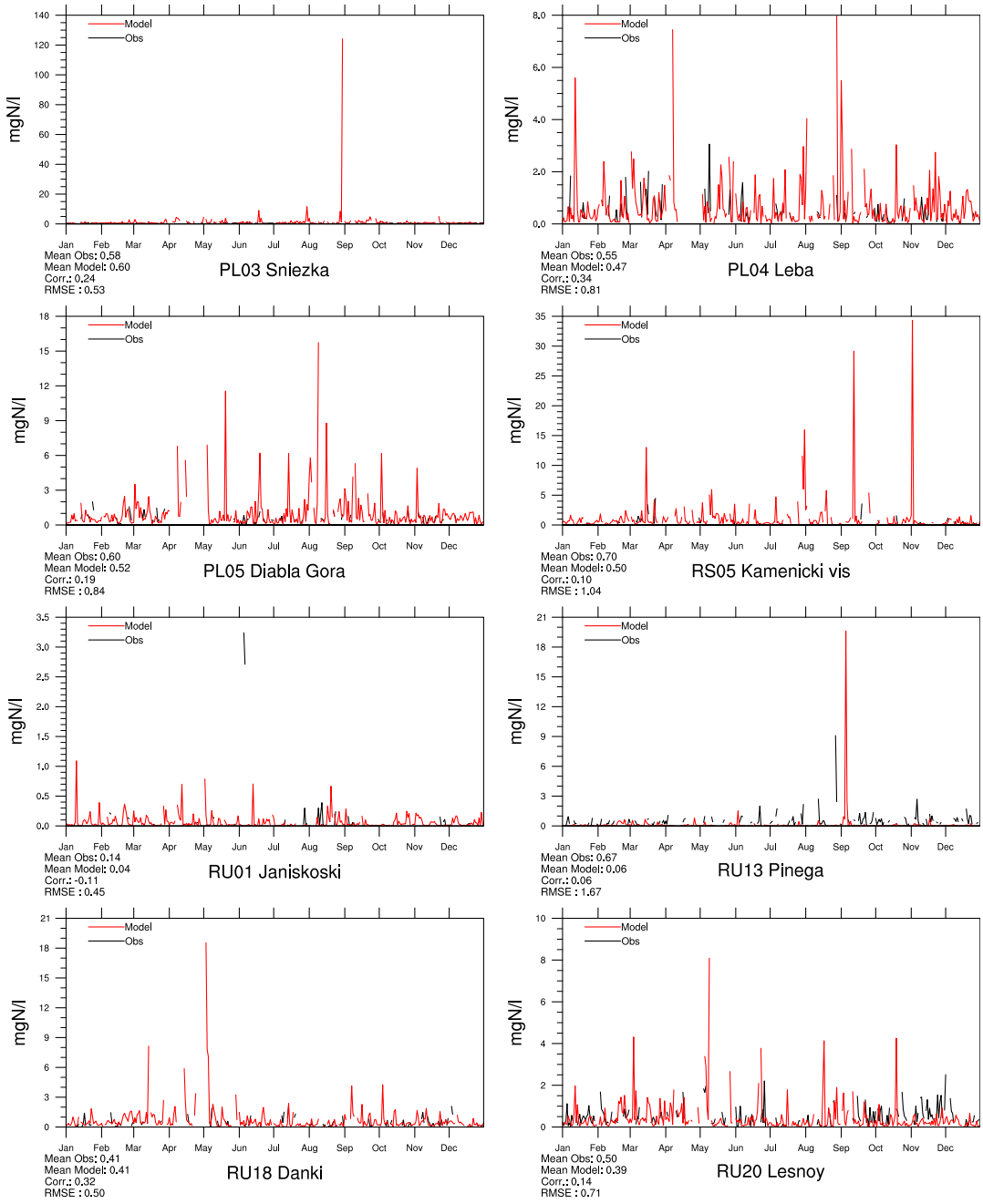

Figure 1.43: Comparison of model results and measurements (daily) for reduced nitrogen concentrations in precipitation [μg(N)l^{-1}] in 2009.

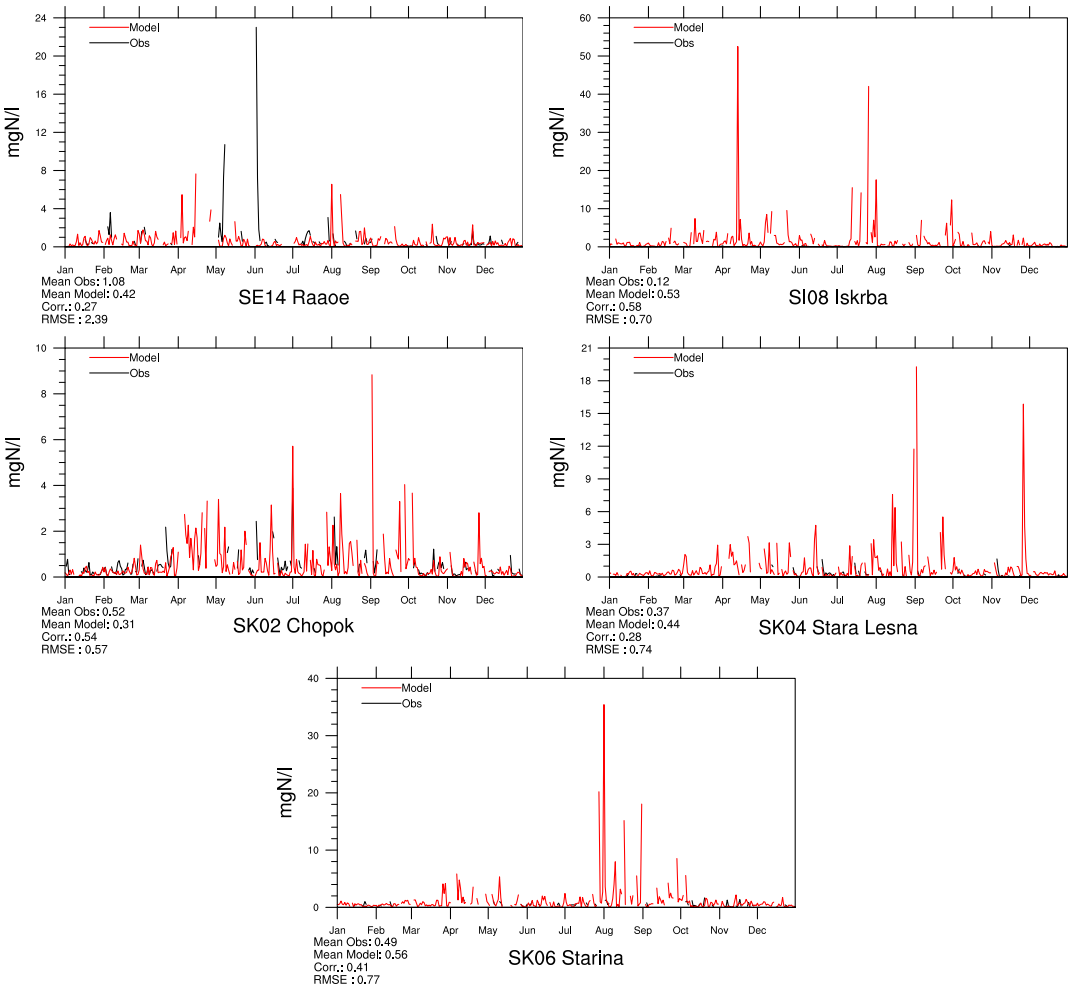

Figure 1.44: Comparison of model results and measurements (daily) for reduced nitrogen concentrations in precipitation [μg(N)l^{-1}] in 2009.

1.3 Combined model results and observations, 2009

In this section, we present the 'best estimates' for air concentrations of SO_2, SO_4^{2-}, NH_3+NH_4^+ and HNO_3+NO_3^- as well as concentrations of oxidized sulphur, oxidized nitrogen and reduced nitrogen in precipitation. The 'best estimates' have been created by using a combination of model results and observations from the EMEP network for 2009. For all measurement points, the difference between the measured value at that point and the modelled value in the corresponding grid cell is calculated. This difference is interpolated spatially using radial basis functions, giving a continuous two-dimensional function describing the difference at any point within the modelled grid. For the interpolated normalized differences (observations-model/(observations+model)), positive values show where the model underpredicts the values, whilst negative values show where the model overpredicts values. The combined maps are derived by adjusting the model results with the interpolated differences, giving large weight to the observed values close to stations, and using the modelled values in areas with no observations. The range of influence of the measured values depends on the component, and has been set to 300 km for NH_3+NH_4^+ and HNO_3+NO_3^- in air, and 500 km for all other components. For each of the components, we present four different figures, visualizing the different steps of the procedure (Figures 1.45 to 1.47).

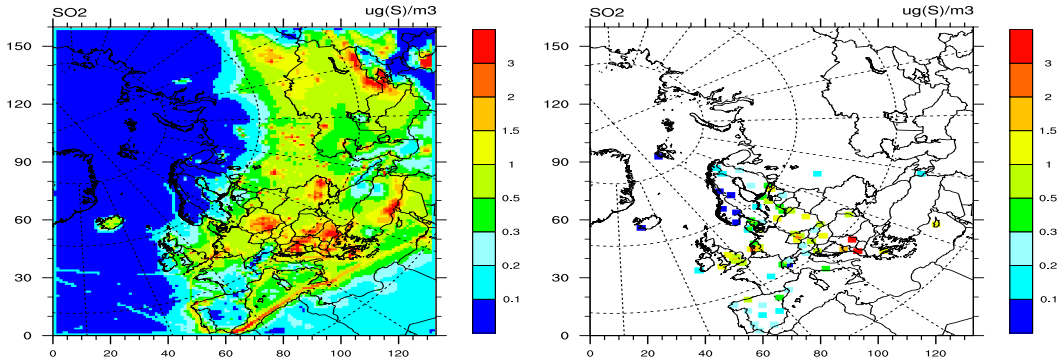

(a) Modelled SO_2 in air

(b) Measured SO_2 in air

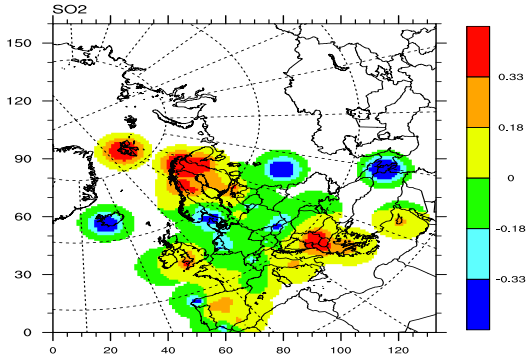

(c) Interpolated normalized differences

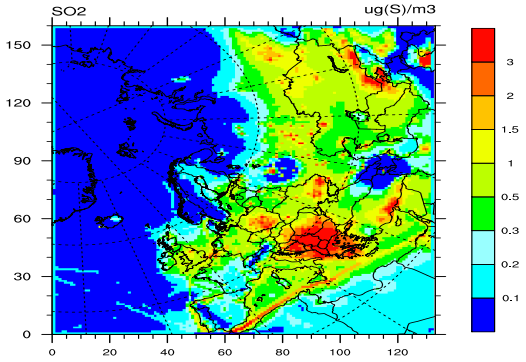

(d) Combined SO_2 in air

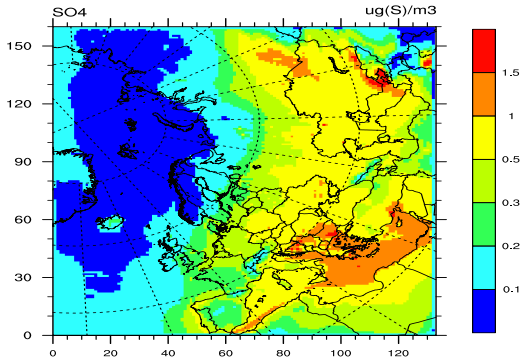

(e) Modelled SO_4^{2-} in air

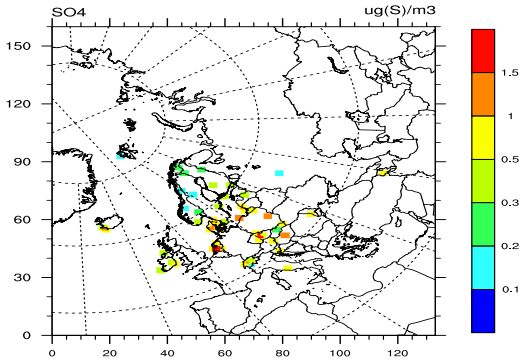

(f) Measured SO_4^{2-} in air

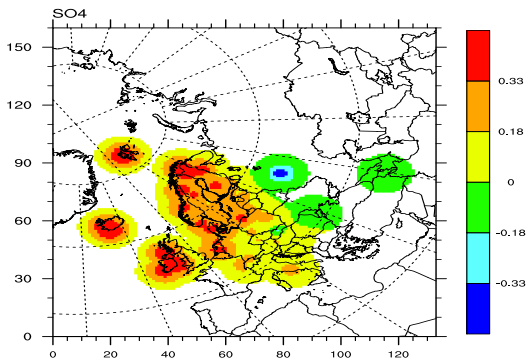

(g) Interpolated normalized differences

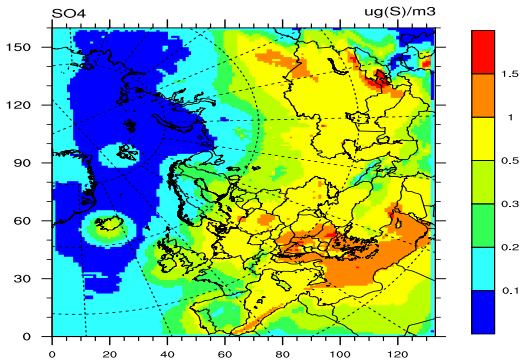

(h) Combined SO_4^{2-} in air

Figure 1.45: Yearly averaged SO_2 (a)-(d) and SO_4^{2-} (e)-(h) concentrations in air [μg(S) m^{-3}] for 2009.

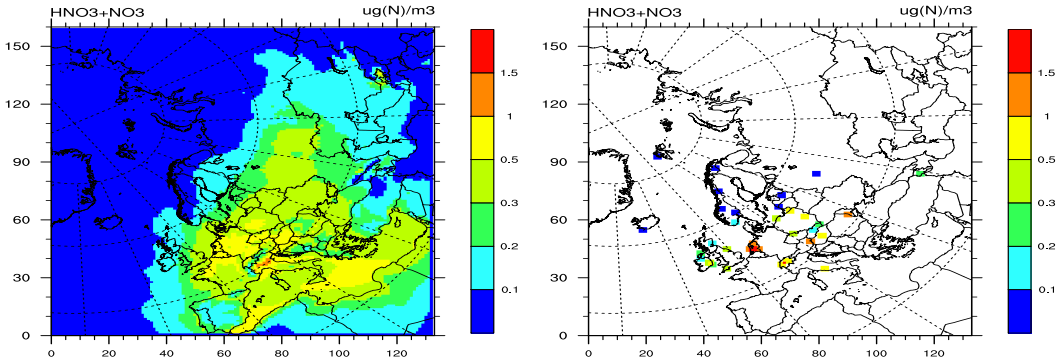

(a) Modelled total nitrate in air

(b) Measured total nitrate in air

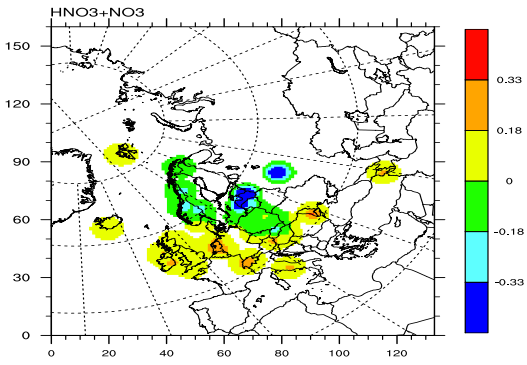

(c) Interpolated normalized differences

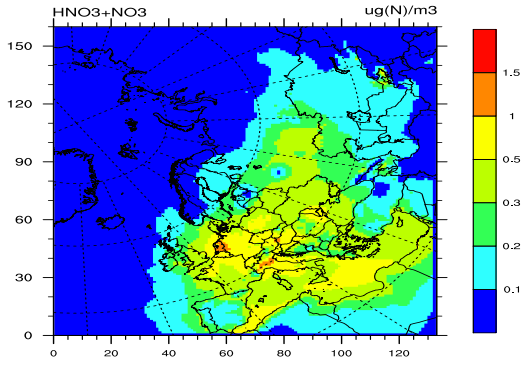

(d) Combined total nitrate in air

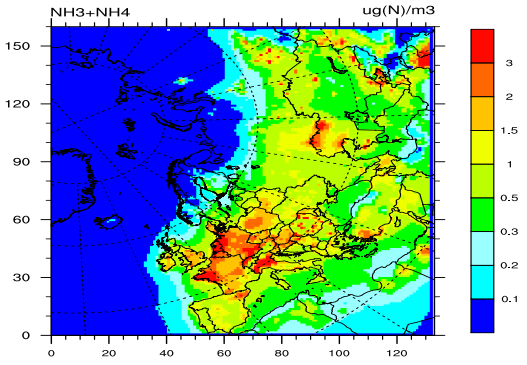

(e) Modelled ammonia+ammonium in air

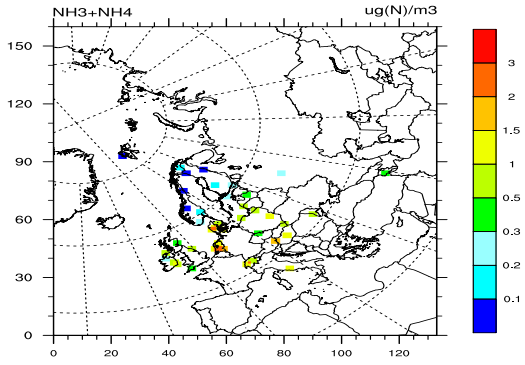

(f) Measured ammonia+ammonium in air

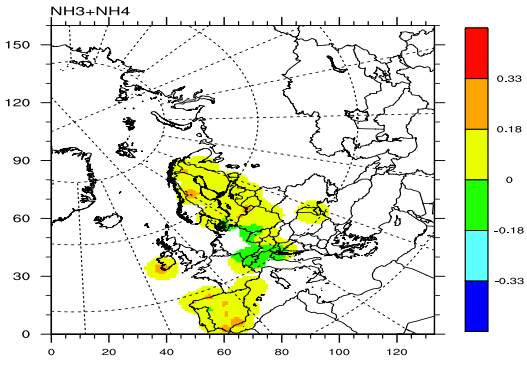

(g) Interpolated normalized differences

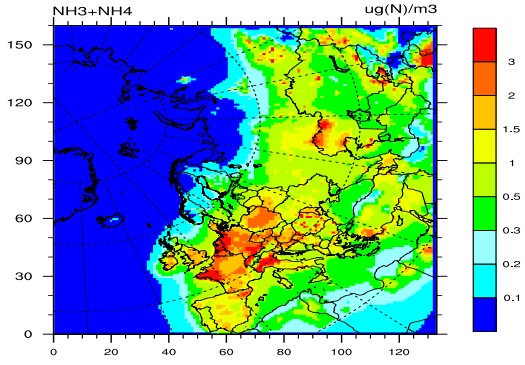

(h) Combined ammonia+ammonium in air

Figure 1.46: Yearly averaged HNO_3+NO_3^- (a)-(d) and NH_3+NH_4^+ (e)-(h) concentrations in air [μg(N) m^{-3}] for 2009.

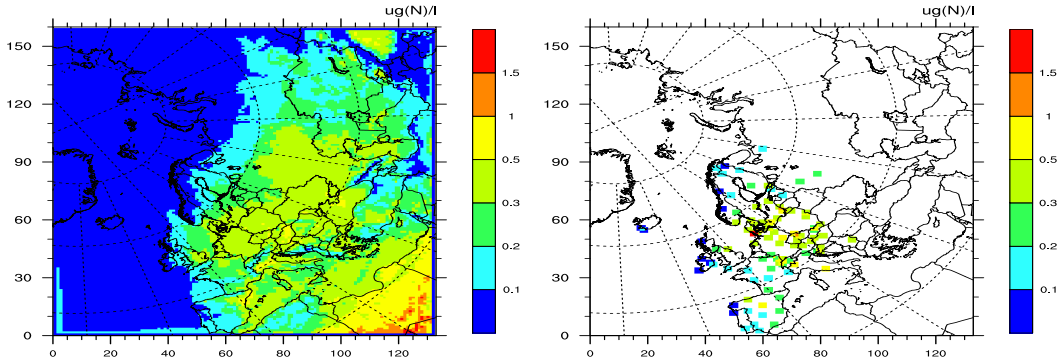

(a) Modelled nitrate in precipitation

(b) Measured nitrate in precipitation

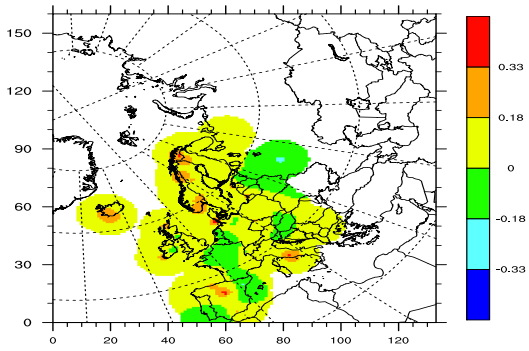

(c) Interpolated normalized differences

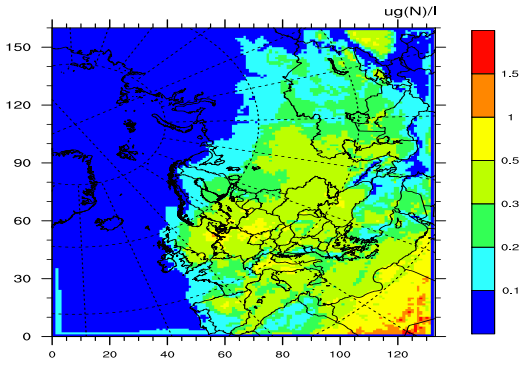

(d) Combined nitrate in precipitation

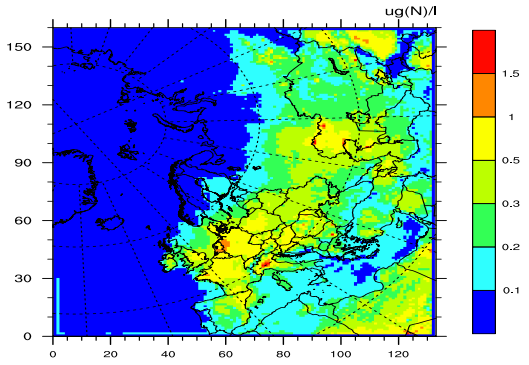

(e) Modelled ammonium in precipitation

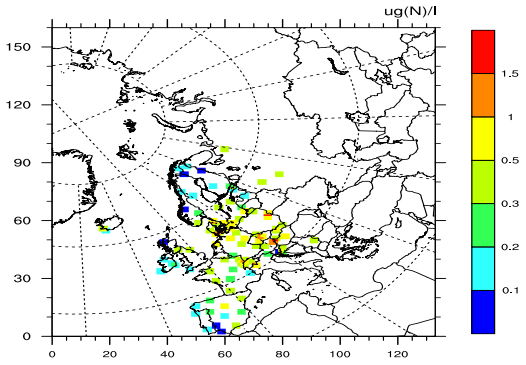

(f) Measured ammonium in precipitation

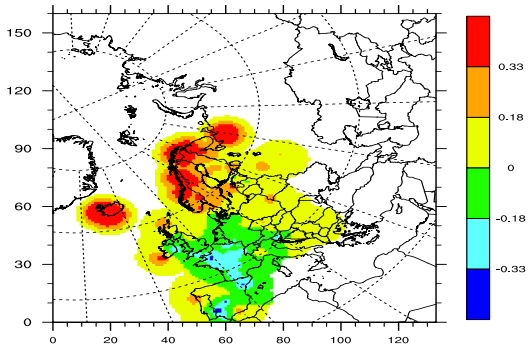

(g) Interpolated normalized differences

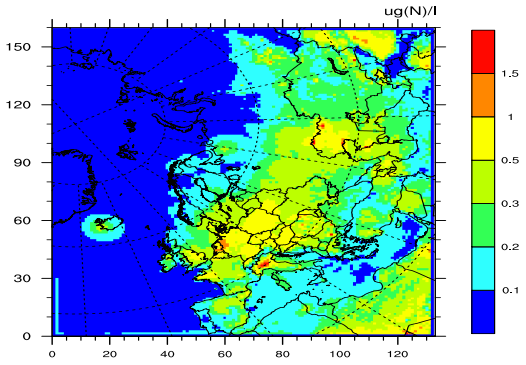

(h) Combined ammonium in precipitation

Figure 1.47: Yearly averaged oxidized nitrogen (a)-(d) and reduced nitrogen (e)-(h) concentrations in precipitation [μg(N)l^{-1}] for 2009.

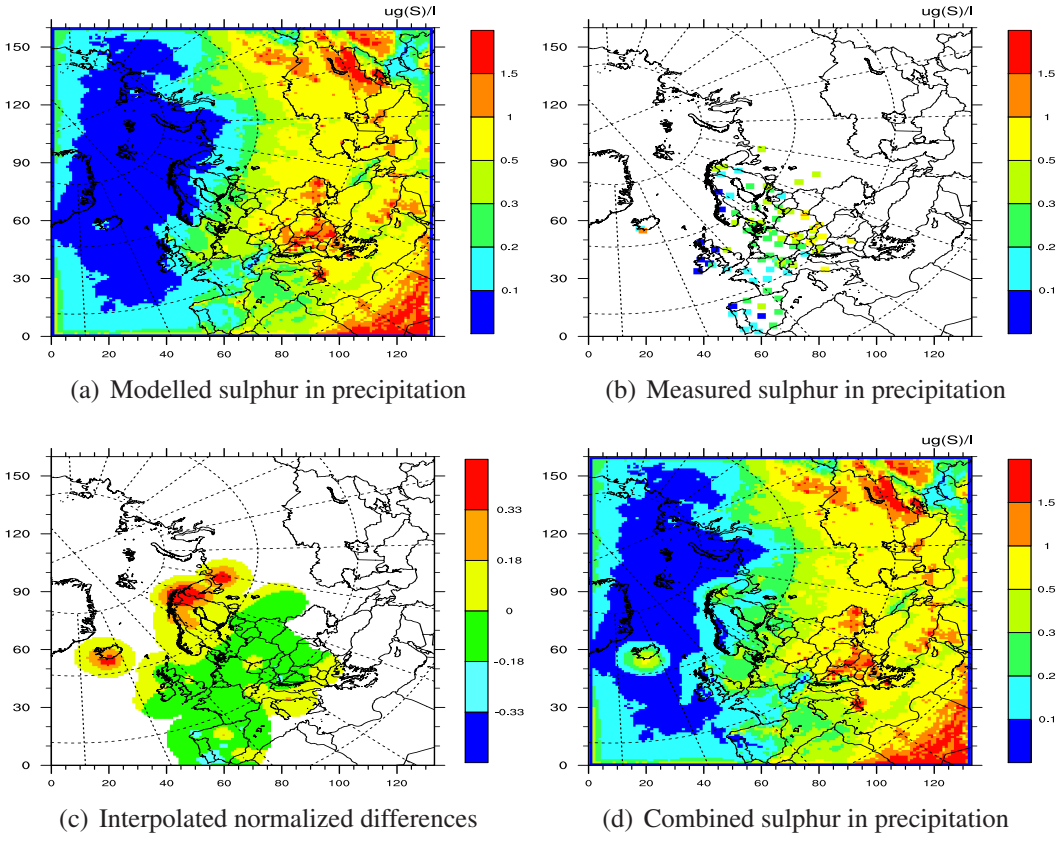

(a) Modelled sulphur in precipitation

(b) Measured sulphur in precipitation

(c) Interpolated normalized differences

(d) Combined sulphur in precipitation

Figure 1.48: Yearly averaged sulphur concentrations in precipitation [μg(S)l^{-1}] for 2009.

References

H. Berge and A.-G. Hjellbrekke. Acidifying and eutrophying components: validation and combined maps. Supplementary material to emep status report 1/2010, available online at `www.emep.int`, The Norwegian Meteorological Institute, Oslo, Norway, 2010.

EMEP MSC-W & CCC . EMEP Unified model performance for acidifying and eutrophying components and photo-oxidants in 2007. Supplementary material to EMEP Status Report 1/09 . Supplementary material to emep status report 1/2009, available online at `www.emep.int`, The Norwegian Meteorological Institute, Oslo, Norway, 2009.

H. Fagerli. Air concentrations and depositions of acidifying and euthrophying components, status 2002. In *Transboundary acidification, eutrophication and ground level ozone in Europe. EMEP Status Report 1/2004*, pages 77–107. The Norwegian Meteorological Institute, Oslo, Norway, 2004.

H. Fagerli. Acidifying and eutrophying components, status in 2003. In *In Transboundary Acidification, Eutrophication and Ground Level Ozone in Europe. EMEP Status Report 1/2005*, pages 9–30. The Norwegian Meteorological Institute, Oslo, Norway, 2005.

H. Fagerli. Air concentrations and depositions of acidifying and euthrophying components, status in 2005. In *Transboundary acidification, eutrophication and ground level ozo ne in Europe in 2005. EMEP Status Report 1/2007*, pages 33–52. The Norwegian Meteorological Institute, Oslo, Norway, 2007.

H. Fagerli and W. Aas. Validation of nitrogen compounds in the emep model. In *Transboundary acidification, eutrophication and ground level ozo ne in Europe in 2005. EMEP Status Report 1/2007*, pages 73–90. The Norwegian Meteorological Institute, Oslo, Norway, 2007.

H. Fagerli and W. Aas. Using the EMEP intensive measurement data to evaluate the performance of the EMEP model for nitrogen compounds. In *In Transboundary Acidification, Eutrophication and Ground Level Ozone in Europe in 2006. EMEP Status Report 1/2008*, pages 109–126. The Norwegian Meteorological Institute, Oslo, Norway, 2008a.

H. Fagerli and A.G. Hjellbrekke. Acidification and eutrophication. In *Transboundary Acidification, Eutrophication and Ground Level Ozone in Europe in 2006. EMEP Status Report 1/2008*, pages 41–56. The Norwegian Meteorological Institute, Oslo, Norway, 2008.

H. Fagerli, D. Simpson, and W. Aas. Model performance for sulphur and nitrogen compounds for the period 1980 to 2000. In L. Tarrasón, editor, *Transboundary*

Acidification, Eutrophication and Ground Level Ozone in Europe. EMEP Status Report 1/2003, Part II Unified EMEP Model Performance, pages 1–66. The Norwegian Meteorological Institute, Oslo, Norway, 2003.

Hilde Fagerli and Wenche Aas. Trends of nitrogen in air and precipitation: Model results and observations at emep sites in europe, 1980-2003. *Environ. Poll.*, 154(3): 448–461, August 2008b.

Agnes Nyíri and A.-G. Hjellbrekke. Acidifying and eutrophying components: validation and combined maps. Supplementary material to emep status report 1/2009, available online at `www.emep.int`, The Norwegian Meteorological Institute, Oslo, Norway, 2009.

D. Simpson, K. Butterbach-Bahl, H. Fagerli, M. Kesik, U. Skiba, and S. Tang. Deposition and emissions of reactive nitrogen over European forests: A modelling study. *Atmos. Environ.*, 40:5712–5726, 2006a. doi: 10.1016/j.atmosenv.2006.04.063.

D. Simpson, H. Fagerli, S. Hellsten, J.C. Knulst, and O. Westling. Comparison of modelled and monitored deposition fluxes of sulphur and nitrogen to ICP-forest sites in Europe. *Biogeosciences*, 3:337–355, 2006b.

David Simpson. Model Updates. In *Transboundary Acidification, Eutrophication and Ground Level Ozone in Europe in 2009. EMEP Status Report 1/2011*. The Norwegian Meteorological Institute, Oslo, Norway, 2011.

CHAPTER 2

Photo-oxidants: evaluation and combined maps

M. Gauss, A. C. Benedictow and A.-G. Hjellbrekke

In this chapter the EMEP/MSC-W model is evaluated with respect to surface ozone and NO_2. In section 2.1 we present time-series plots for selected stations to illustrate the performance of the EMEP/MSC-W model for the year 2009. In section 2.2 we present 'best estimate' maps of ozone and NO_2 for 2009, created by combining measurements and model results.

2.1 Evaluation

Modelled daily maximum ozone values have been evaluated against measurements from all stations that supply data to EMEP CCC. Table 2.1 summarises these comparisons, and Figures 2.1–2.17 show time-series plots for selected stations representing the different regions of Europe. To judge model performance Table 2.1 shows root mean square error (RMSE) and the *index of agreement* (IOA). IOA varies between 0 and 1. A value of 1 corresponds to perfect agreement between model and observations and 0 is the theoretical minimum. It is worth noting that the index of agreement has improved compared to last year's evaluation report at most of the stations, especially in Northern and Central Europe. In the following sections the model performances in different regions within Europe are discussed separately.

Table 2.1: Comparison of modelled versus observed ozone for year 2009. Concentrations are given as means of daily maximum ozone values [ppb]. Correlation coefficients (r), root mean square error (RMSE), and index of agreement (IOA) are included to judge the agreement between model and observations (for details see beginning of this section).

Code	Station	Obs. [ppb]	Mod. [ppb]	r	RMSE	IOA
		Nordic countries				
DK05	Keldsnor	39.79	38.74	0.73	8.18	0.85
DK31	Ulborg	39.79	40.10	0.86	5.97	0.92
DK41	Lille Valby	38.22	38.07	0.88	5.41	0.94
FI09	Utoe	35.38	40.52	0.83	7.32	0.83
FI17	Virolahti II	31.62	36.09	0.81	7.47	0.85
FI22	Oulanka	30.06	34.15	0.76	7.85	0.83
FI37	Aehtaeri II	32.59	34.84	0.82	6.08	0.89
FI96	Pallas	36.98	33.34	0.80	6.53	0.85
NO01	Birkenes	31.75	38.84	0.77	9.30	0.76
NO15	Tustervatn	37.75	37.06	0.83	4.92	0.91
NO39	Kaarvatn	37.86	41.07	0.68	7.26	0.78
NO42	Spitzbergen, Zeppelin	36.37	37.31	0.67	5.61	0.80
NO43	Prestebakke	35.43	38.08	0.81	6.60	0.88
NO52	Sandve	38.43	40.33	0.74	6.05	0.85
NO55	Karasjok	35.60	34.03	0.79	5.70	0.88
NO56	Hurdal	34.00	36.48	0.78	6.67	0.86
SE05	Bredkaelen	33.39	35.21	0.79	6.08	0.88
SE11	Vavihill	35.83	38.59	0.78	7.26	0.86
SE12	Aspvreten	35.46	37.75	0.85	5.77	0.91
SE13	Esrange	36.68	34.45	0.80	5.92	0.87
SE14	Raaoe	36.93	37.07	0.73	7.27	0.85
SE32	Norra-Kvill	36.80	38.03	0.86	5.28	0.92
SE35	Vindeln	34.63	34.85	0.81	5.68	0.90
SE39	Grimsoe	32.86	36.28	0.83	6.39	0.88
		Eastern European Countries				
BG53	Rojen peak	46.92	48.60	0.64	8.49	0.76
CZ01	Svratouch	31.06	42.18	0.77	13.83	0.74
CZ03	Kosetice	40.32	43.00	0.85	7.41	0.91
EE09	Lahemaa	34.97	36.38	0.83	6.00	0.90
EE11	Vilsandy	38.54	39.95	0.84	5.71	0.90
HU02	K-puszta	43.88	44.15	0.87	8.96	0.91
LT15	Preila	37.71	42.33	0.86	7.88	0.89
LV10	Rucava	33.74	38.13	0.68	8.93	0.79
LV16	Zoseni	35.80	36.38	0.79	6.70	0.88
PL02	Jarczew	37.95	39.93	0.81	8.35	0.89

continued on next page

Code	Station	Obs.	Mod.	r	RMSE	IOA
PL03	Sniezka	47.17	41.76	0.74	9.53	0.80
PL04	Leba	39.35	41.77	0.81	7.39	0.88
PL05	Diabla Gora	35.54	37.81	0.84	6.92	0.90
SK02	Chopok	51.67	44.74	0.72	10.13	0.75
SK04	Stara Lesna	41.94	44.09	0.75	8.21	0.85
SK06	Starina	43.80	41.84	0.72	11.60	0.78
SK07	Topolniky	37.53	34.99	0.68	7.85	0.80
	Central and NW European Countries					
AT02	Illmitz	42.09	44.09	0.88	7.96	0.93
AT05	Vorhegg	45.17	46.47	0.75	8.71	0.85
AT30	Pillersdorf	40.46	43.21	0.89	8.07	0.92
AT32	Sulzberg	47.02	46.19	0.78	7.42	0.88
AT34	Sonnblick	54.06	50.05	0.68	7.72	0.78
AT37	Zillertalen Alpen	51.15	52.26	0.72	7.02	0.84
AT38	Gerlitzen	51.54	46.68	0.78	8.63	0.83
AT40	Masenberg	46.76	44.03	0.79	8.01	0.87
AT41	Haunsberg	43.68	43.81	0.81	7.81	0.89
AT42	Heidenreichstein	38.87	43.72	0.86	8.26	0.89
AT43	Forsthof	42.10	43.42	0.86	7.79	0.92
AT44	Graz Platte	46.03	43.88	0.85	8.08	0.91
AT45	Dunkelsteinerwald	39.86	42.70	0.87	8.53	0.91
AT46	Gaenserndorf	40.82	42.72	0.90	7.58	0.94
AT47	Stixneusiedl	42.79	44.13	0.89	7.44	0.94
AT48	Zoebelboden	43.99	43.69	0.75	8.85	0.86
AT49	Grebenzen	48.70	44.46	0.69	9.26	0.78
BE01	Offagne	38.57	42.69	0.83	7.89	0.87
BE32	Eupen	37.40	40.58	0.80	8.80	0.87
BE35	Vezin	36.45	40.91	0.83	9.05	0.88
CH01	Jungfraujoch	41.70	51.13	0.58	11.93	0.56
CH02	Payerne	42.46	46.00	0.80	9.86	0.86
CH03	Taenikon	41.50	45.90	0.74	11.64	0.82
CH04	Chaumont	47.41	46.00	0.77	7.93	0.87
CH05	Rigi	47.53	46.46	0.77	8.40	0.87
DE01	Westerland/Wenningsted	39.84	40.72	0.83	6.52	0.90
DE02	Langenbruegge/Waldhof	35.53	38.58	0.89	7.11	0.93
DE03	Schauinsland	50.37	45.47	0.80	8.54	0.84
DE07	Neuglobsow	37.79	38.61	0.89	6.88	0.93
DE08	Schmuecke	40.90	41.69	0.81	7.41	0.89
DE09	Zingst	36.22	39.56	0.84	7.37	0.89
FR08	Donon	41.77	43.73	0.83	6.84	0.90
FR09	Revin	38.03	42.22	0.82	8.21	0.87
FR10	Morvan	42.54	43.54	0.78	6.56	0.88

continued on next page

Code	Station	Obs.	Mod.	r	RMSE	IOA
FR13	Peyrusse Vieille	40.64	42.06	0.58	8.97	0.75
FR14	Montandon	39.09	45.11	0.74	10.06	0.80
FR15	La Tardiere	41.07	41.56	0.70	8.33	0.83
FR16	Le Casset	52.29	45.97	0.65	10.16	0.70
FR17	Montfranc	44.75	43.91	0.76	6.07	0.86
FR18	La Coulonche	39.10	40.85	0.79	5.92	0.87
FR30	Puy de Dome	47.33	45.14	0.71	6.65	0.82
GB02	Eskdalemuir	36.83	40.54	0.75	7.24	0.81
GB06	Lough Navar	32.26	40.02	0.64	9.61	0.61
GB13	Yarner Wood	39.32	42.06	0.78	6.43	0.85
GB14	High Muffles	42.49	42.60	0.76	9.64	0.79
GB15	Strath Vaich Dam	39.34	39.40	0.81	4.38	0.90
GB31	Aston Hill	39.00	40.92	0.75	6.48	0.84
GB33	Bush	35.70	39.33	0.79	6.09	0.84
GB35	Great Dun Fell	33.04	39.88	0.68	8.98	0.69
GB36	Harwell	34.74	39.64	0.76	8.09	0.81
GB37	Ladybower	34.79	38.66	0.75	7.02	0.82
GB38	Lullington Heath	38.62	41.59	0.64	7.67	0.77
GB39	Sibton	36.50	39.45	0.64	8.61	0.77
GB43	Narberth	37.23	41.56	0.77	7.50	0.81
GB45	Wicken Fen	37.25	39.29	0.78	7.12	0.86
GB48	Auchencorth Moss	34.72	39.17	0.75	7.11	0.80
GB49	Weybourne	42.31	40.37	0.73	7.41	0.83
GB50	St. Osyth	37.13	38.85	0.64	8.92	0.77
GB51	Market Harborough	36.47	39.13	0.79	7.24	0.86
GB52	Lerwick	40.30	41.88	0.75	5.58	0.85
GB53	Charlton Mackrell	37.36	40.28	0.79	6.51	0.86
IE31	Mace Head	42.21	42.28	0.79	4.66	0.88
NL07	Eibergen	32.84	38.28	0.87	8.97	0.89
NL09	Kollumerwaard	33.86	39.11	0.84	8.37	0.86
NL10	Vreedepeel	31.43	37.48	0.88	8.95	0.89
NL11	Cabauw	30.98	36.43	0.80	9.73	0.84
NL91	De Zilk	34.21	40.52	0.80	9.99	0.83
	Mediterranean Countries and Portugal					
CY02	Ayia Marina	55.11	48.30	0.44	11.11	0.59
ES01	Toledo	49.88	47.69	0.78	6.30	0.86
ES07	Viznar	48.35	47.65	0.68	6.62	0.80
ES08	Niembro	41.85	46.13	0.75	7.22	0.81
ES09	Campisabalos	48.66	47.83	0.83	5.91	0.89
ES10	Cabo de Creus	46.76	48.13	0.63	10.03	0.78
ES11	Barcarrota	40.56	47.01	0.60	9.71	0.67
ES12	Zarra	49.37	47.93	0.86	5.85	0.91

continued on next page

Code	Station	Obs.	Mod.	r	RMSE	IOA
ES13	Penausende	44.76	46.42	0.83	5.80	0.88
ES14	Els Torms	51.12	47.70	0.81	9.42	0.86
ES16	O Savinao	40.27	45.39	0.81	8.26	0.82
ES17	Donana	41.54	50.09	0.60	12.40	0.67
GR02	Finokalia	50.67	52.08	0.65	7.35	0.77
IT01	Montelibretti	51.45	49.59	0.81	12.49	0.83
PT04	Monte Velho	45.23	49.69	0.64	10.25	0.75
SI08	Iskrba	45.44	45.17	0.83	8.10	0.89
SI31	Zarodnje	45.05	46.20	0.85	7.43	0.90
SI32	Krvavec	54.69	46.66	0.77	11.21	0.77
SI33	Kovk	42.84	45.63	0.80	8.89	0.87

Nordic sites

In addition to the statistics for the Nordic sites listed in Table 2.1, measured and modelled ozone levels are compared for Nordic sites in Figures 2.1–2.3. At most Nordic sites the IOA is between 0.85 and 0.95, which is a very good result. In particular, the model performance has improved at 20 of the 24 sites since last year's report (Berge et al. 2010). Nevertheless, there are stations where the correlation and root mean square error indicate problems. E.g. Spitzbergen (NO42), which is far away from the major emission sources, the model has problems capturing the sudden drops in ozone observed during spring, similar to previous years. The correlation at this station is among the lowest in the Nordic area (0.67), although the performance has improved since last year (0.61). Other stations where the correlation with model data is relatively low ($<$0.75) are Keldsnor (DK05), Kaarvatn (NO39), Sandve (NO52), and Raaoe (SE14). Birkenes (NO01) and Kaarvatn (NO39) are the only stations with an index of agreement below 0.8. The biases, as indicated by the difference between modelled and observed means, are rather low, but it is noteworthy that ozone is slightly overestimated at about three quarters of the measurement sites.

Eastern European sites

Measured and modelled maximum ozone levels for sites in the Eastern European region are shown in Figures 2.4 to 2.6. These sites are mostly typical continental sites with a clear summer maximum, reflecting local/regional ozone production in summer, and a winter minimum. In general the model performance is rather good, and in line with the performance in previous years (Simpson 2006, Jonson et al. 2007, Simpson and Hjellbrekke 2008, Gauss and Hjellbrekke 2009, Berge et al. 2010).

However this year the model has higher concentration than observed at all Eastern European stations except Chopok (SK02) and Sniezka (PL03), Starina (SK06) and

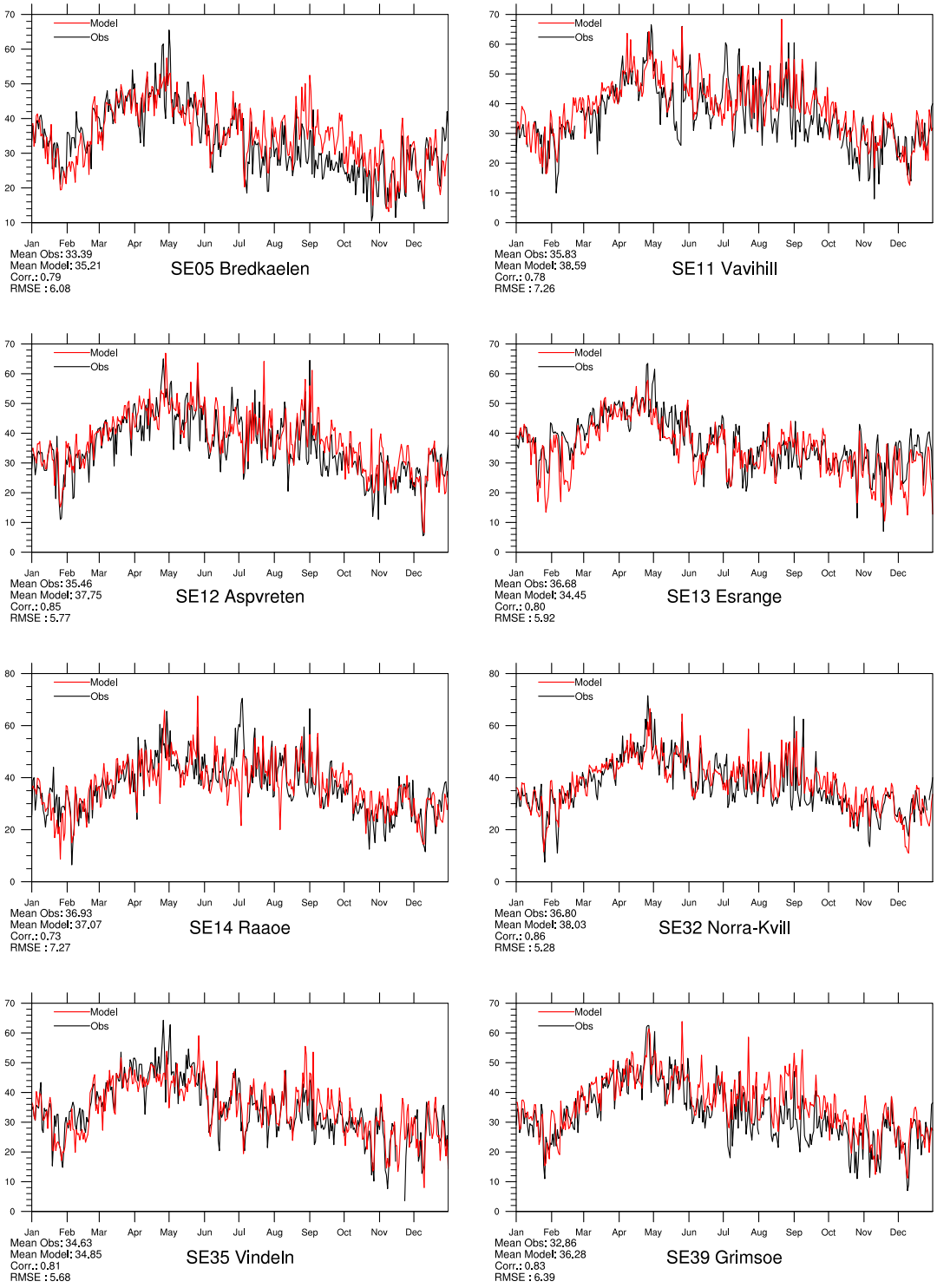

Figure 2.1: Modelled versus Observed Daily Maximum Ozone [ppb] at Swedish sites for 2009. *Note that in some plots the vertical axis does not start at zero.*

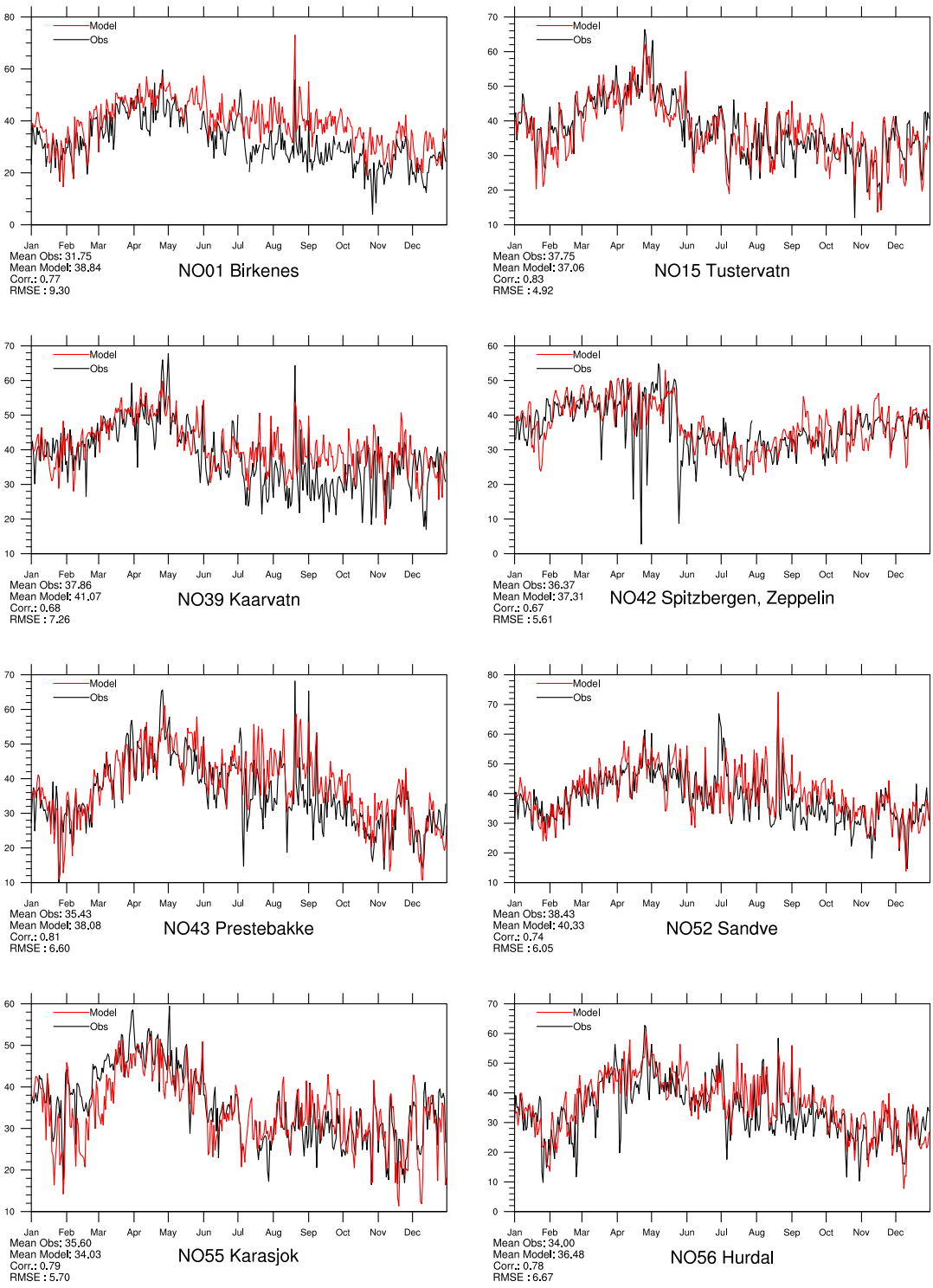

Figure 2.2: Modelled versus Observed Daily Maximum Ozone [ppb] at Norwegian sites for 2009. *Note that in some plots the vertical axis does not start at zero.*

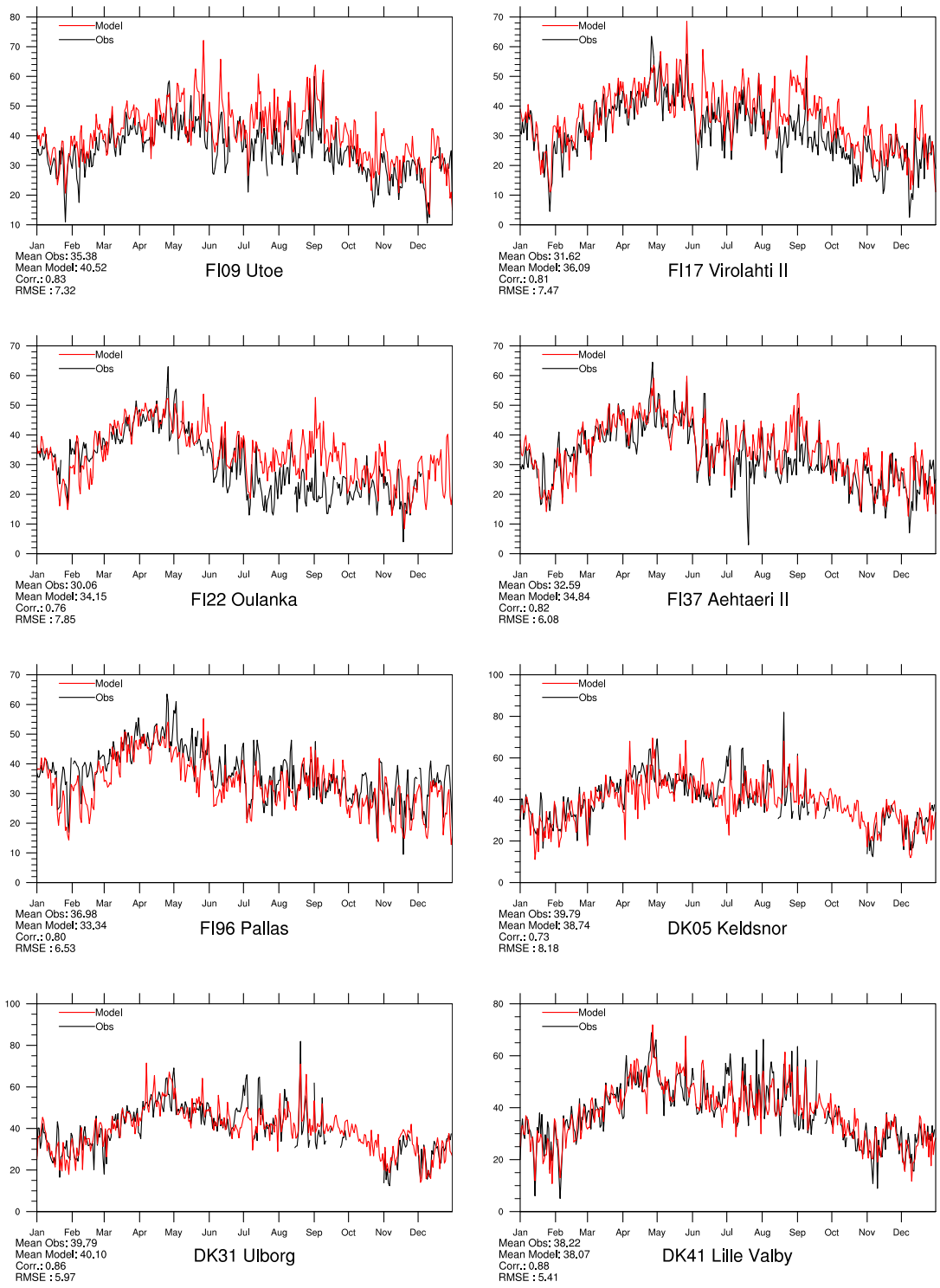

Figure 2.3: Modelled versus Observed Daily Maximum Ozone [ppb] at Finnish and Danish sites for 2009. *Note that in some plots the vertical axis does not start at zero.*

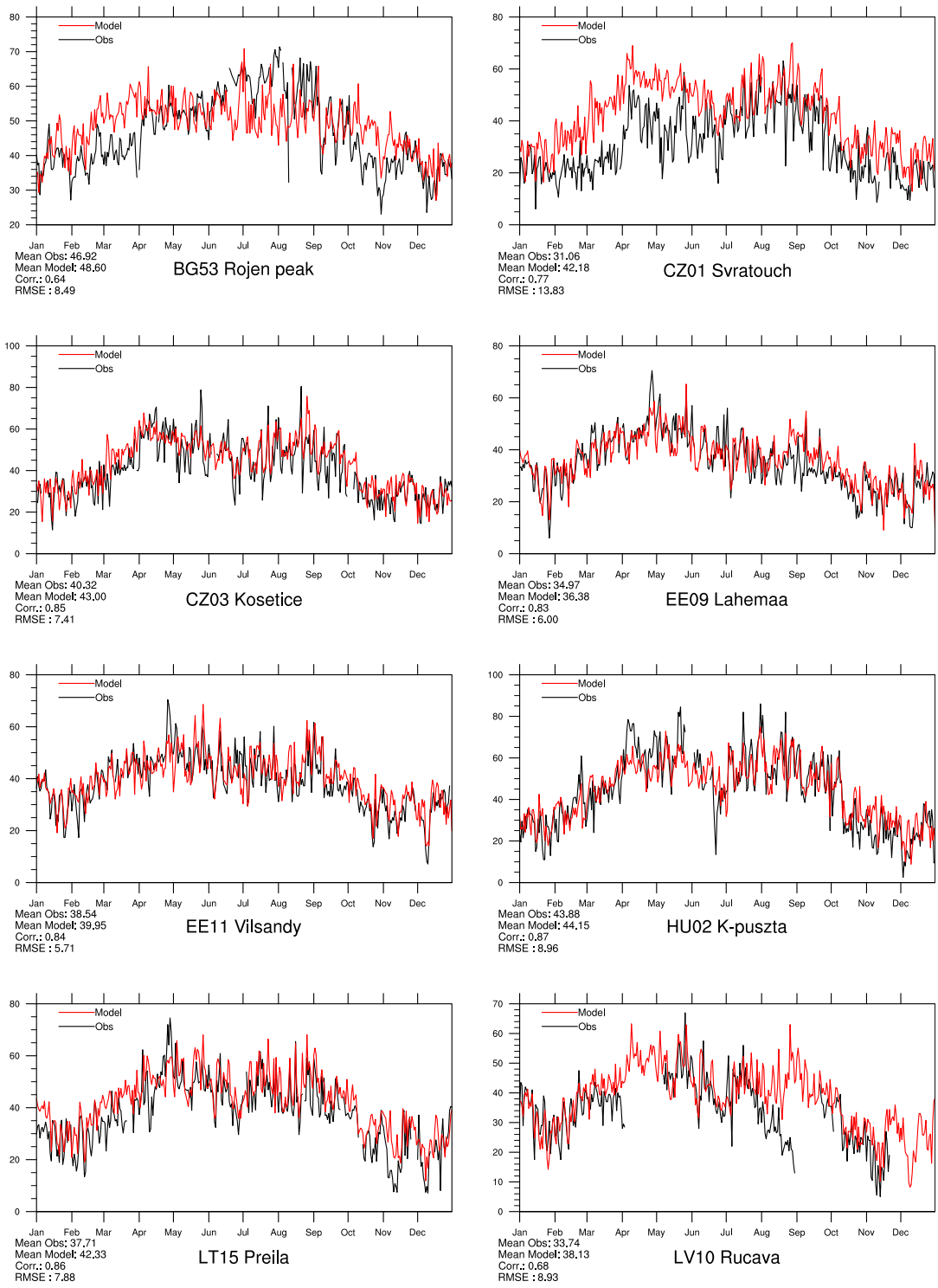

Figure 2.4: Modelled versus Observed Daily Maximum Ozone [ppb] at Eastern European sites for 2009. *Note that in some plots the vertical axis does not start at zero.*

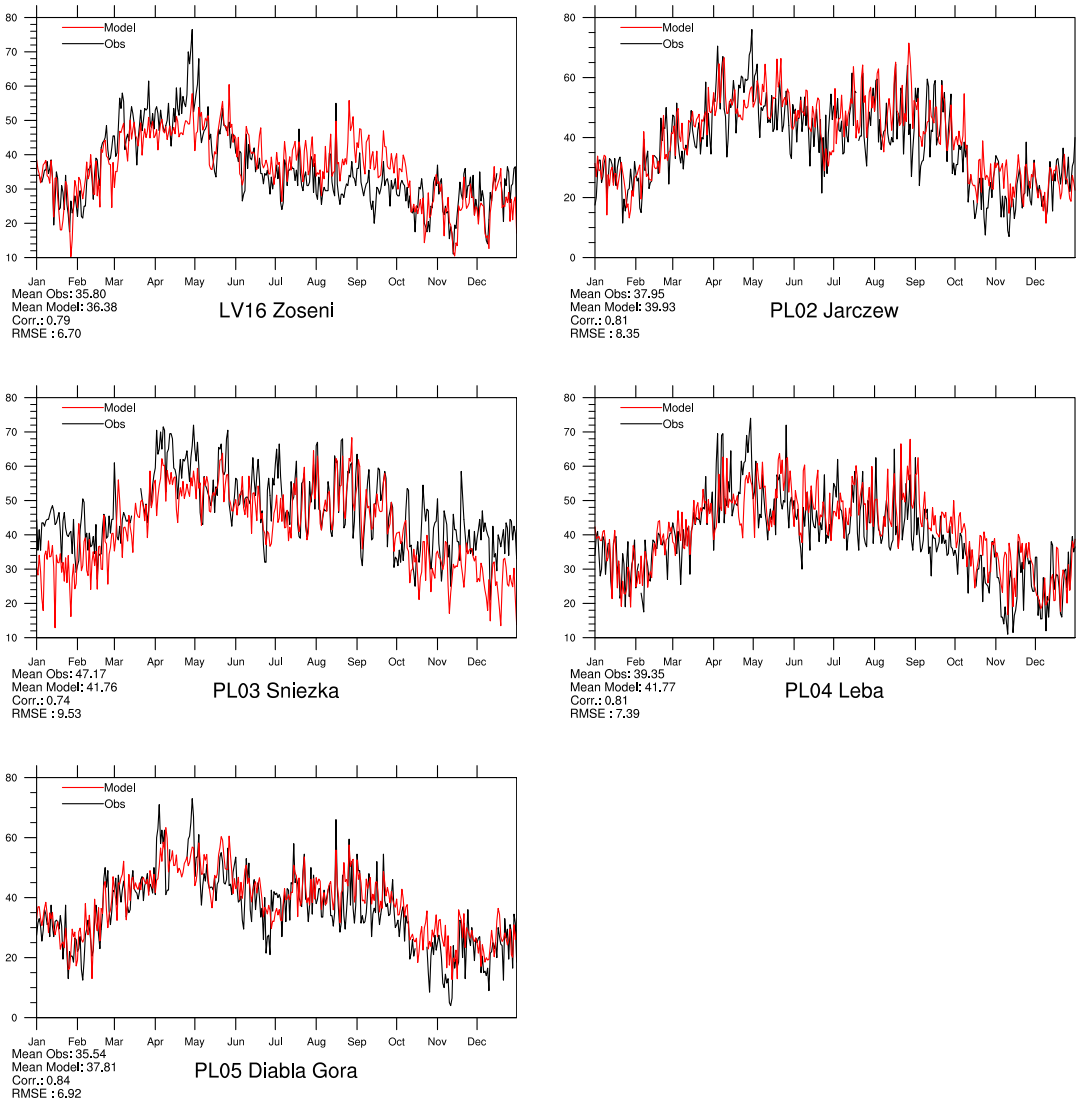

Figure 2.5: Modelled versus Observed Daily Maximum Ozone [ppb] at Eastern European sites for 2009. *Note that in some plots the vertical axis does not start at zero.*

Topolniki (SK07). The overestimation of ozone is highest during autumn. A relatively high bias is found at Preila (LT15), as was the case also last year, with the model overestimating ozone. The index of agreement (IOA) is below 0.8 at 5 of the 17 stations, but has improved since last year at 10 stations. K-Puszta is the station where both correlation and IO are the highest among the Eastern European sites.

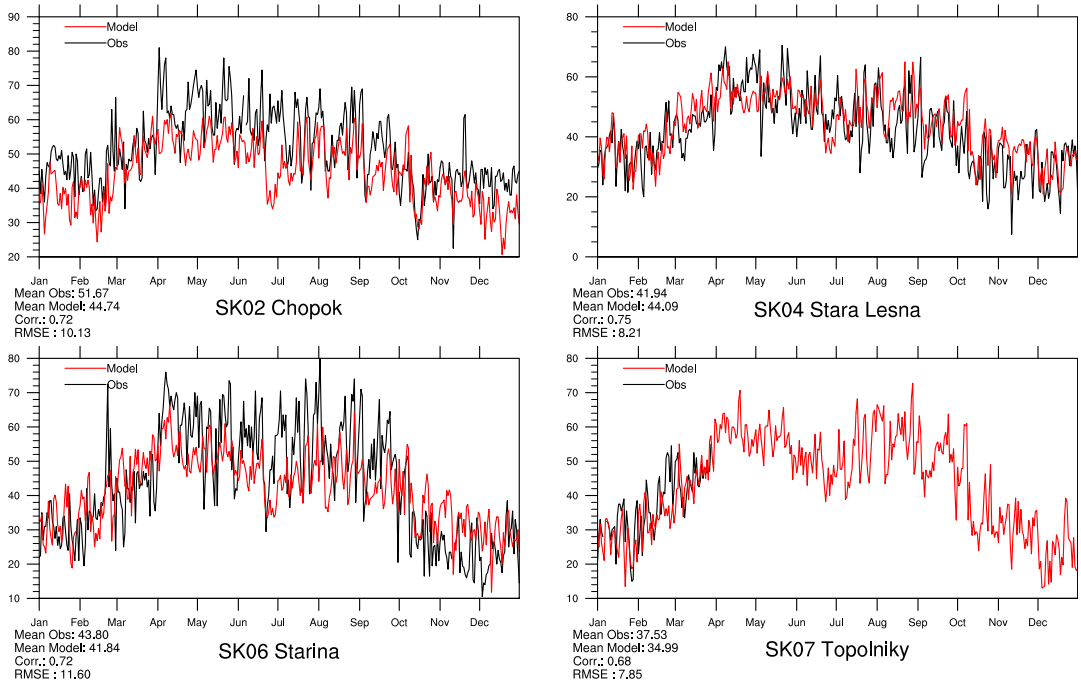

Figure 2.6: Modelled versus Observed Daily Maximum Ozone [ppb] at Eastern European sites for 2009. *Note that in some plots the vertical axis does not start at zero.*

Central and Northwestern European sites

Measured and modelled maximum ozone levels for selected sites in Central and Northwestern Europe are shown in Figures 2.7–2.15. These sites are mainly typical continental sites with a clear summer maximum, reflecting local/regional ozone production in summer, and a winter minimum. Concentrations at the site Mace Head in Ireland (IE31) are partly used to specify background conditions for the EMEP model, so good performance for the seasonal cycle is guaranteed.

The overall model performance is very good in this area with many correlations better than 0.8 and small biases. At about two thirds of the stations the model has improved IOA compared to last year's report. Most of the stations where IOA has become slightly worse are in Great Britain.

Relatively low correlations (below 0.6) are seen at Jungfraujoch (CH01) and Peyrusse Vieille (FR13). At Jungfraujoch the index of agreement is low and bias is high, which might be explained by the fact that this is a mountain site (3578 m.a.s). Because of its high elevation, for a long-term run, this site will often be above the boundary layer, especially in the winter. With the coarse topography in the regional scale model, this cannot be well captured by the model.

However, it is reassuring to see that the IOA is high (between 0.85 and 0.95) at more than half of the stations.

Mediterranean sites

Measured and modelled ozone levels for selected sites in the Mediterranean region are shown in Figures 2.16–2.18. The meteorological situation in and around the Mediterranean basin differs considerably from the rest of Europe. This region also receives more solar radiation resulting in conditions favourable for ozone production. Hence these sites have some of the highest ozone levels in Europe.

This year, CY02, ES01, ES17 and PT04 are included. The model shows lowest IOA at CY02 and ES17. At CY02 ozone is clearly underestimated, while at ES17 it is overestimated. A relatively low IOA (< 0.7) is also seen at Barcarrota (ES11), with a large overestimation of ozone.

However, in general the model performance is good for most sites also in this region.

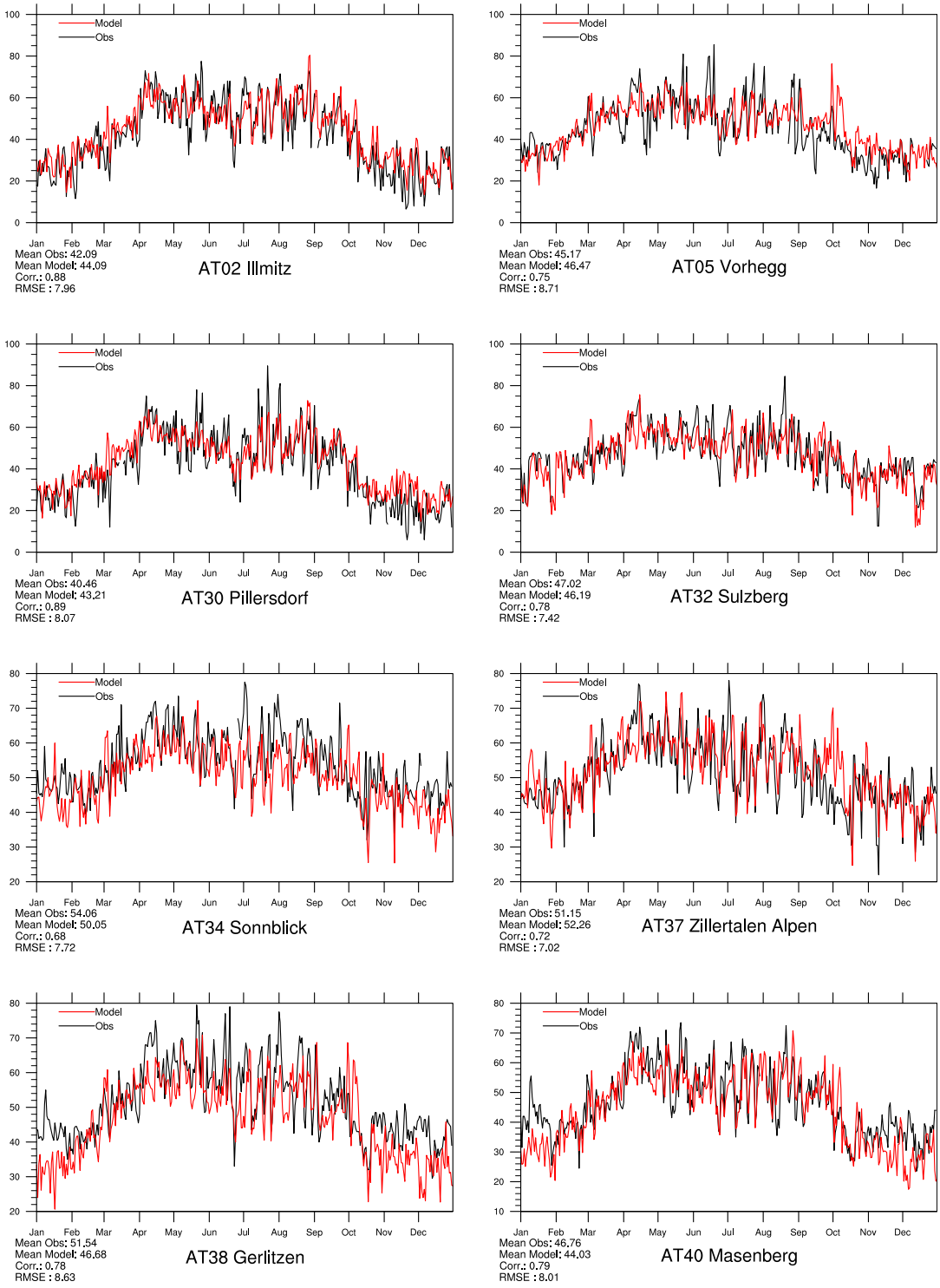

Figure 2.7: Modelled versus Observed Daily Maximum Ozone [ppb] at Austrian sites for 2009. *Note that in some plots the vertical axis does not start at zero.*

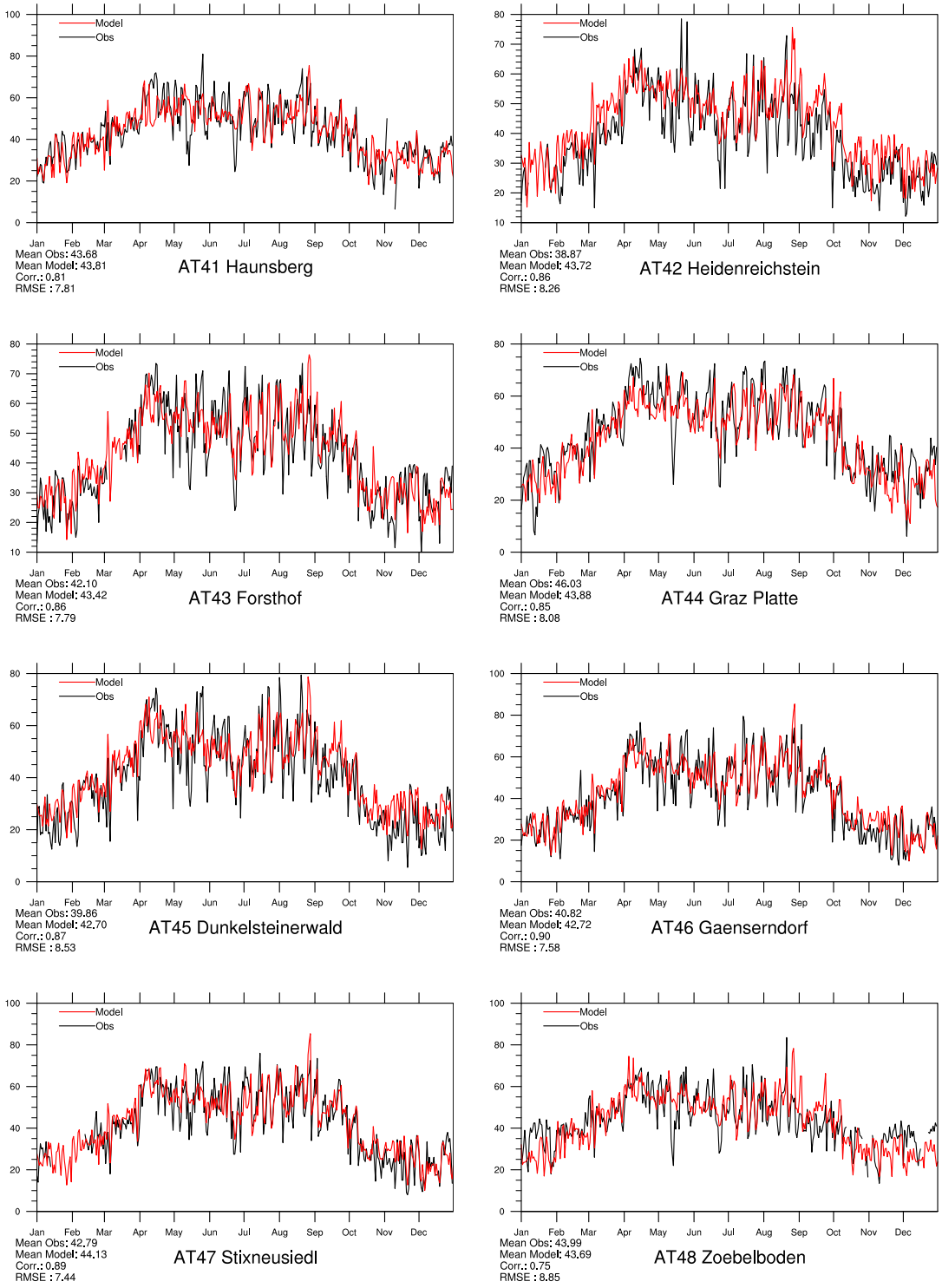

Figure 2.8: Modelled versus Observed Daily Maximum Ozone [ppb] at Austrian sites for 2009. *Note that in some plots the vertical axis does not start at zero.*

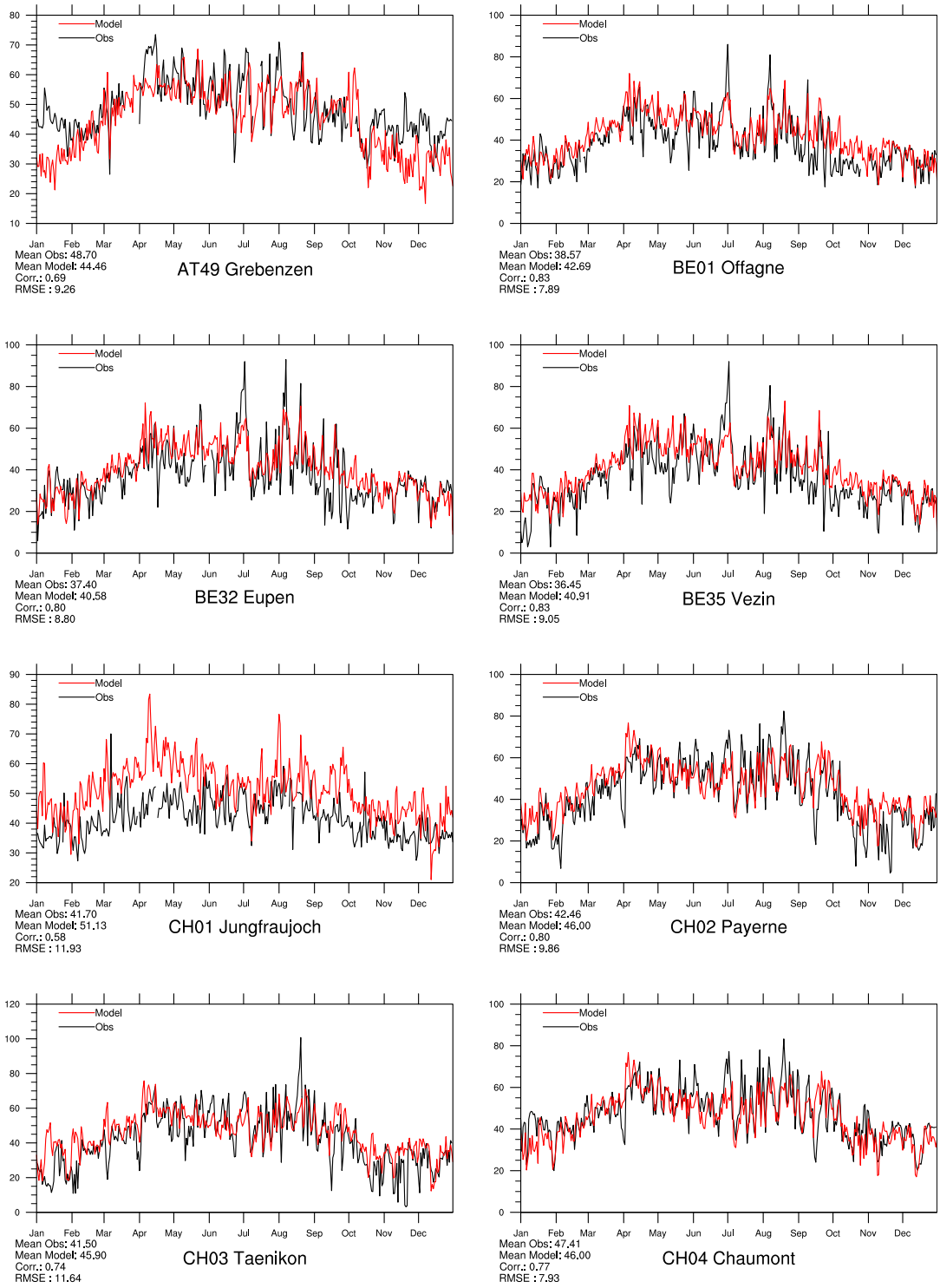

Figure 2.9: Modelled versus Observed Daily Maximum Ozone [ppb] at sites in Austria, Belgium, and Switzerland for 2009. *Note that in some plots the vertical axis does not start at zero.*

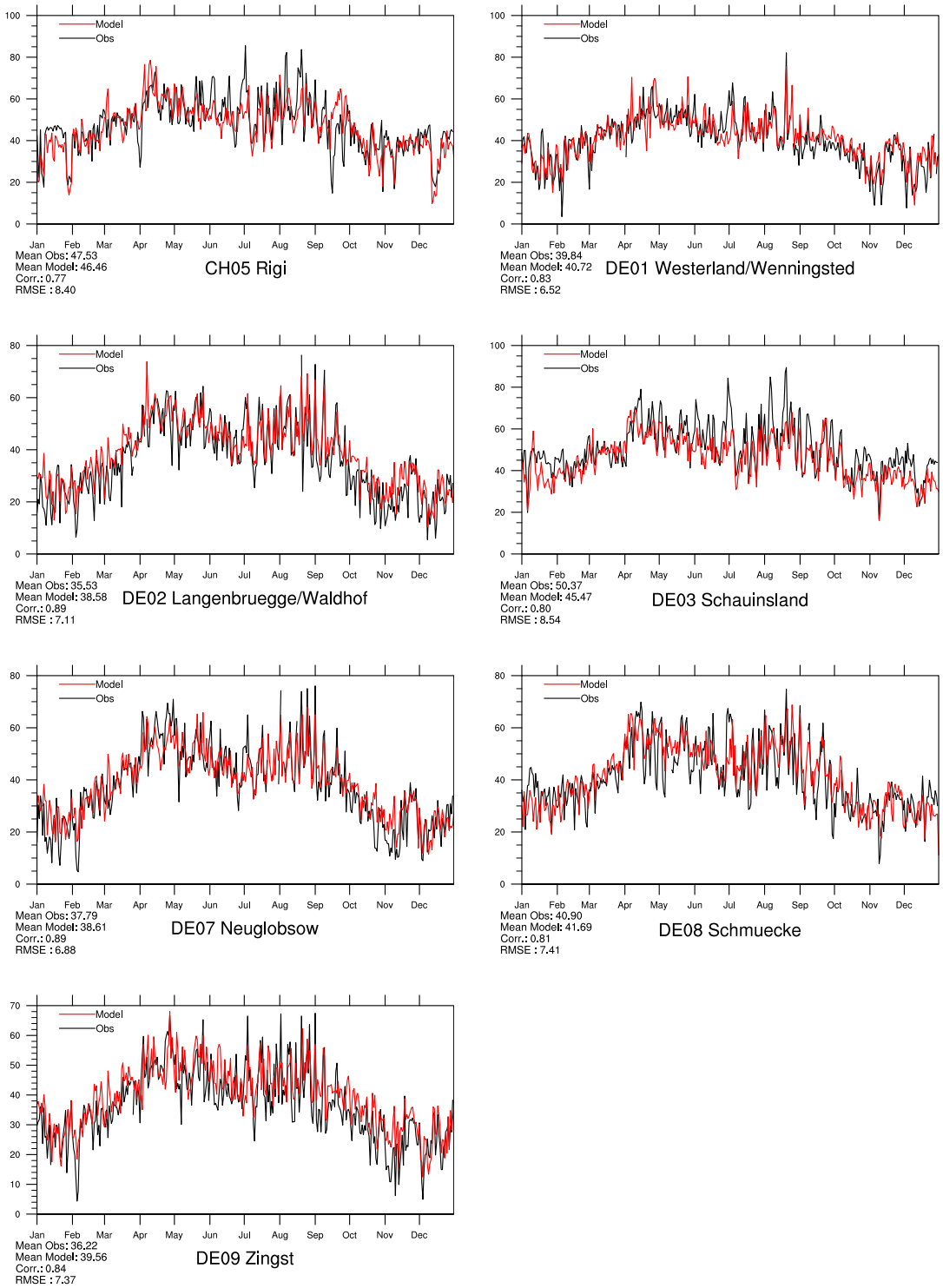

Figure 2.10: Modelled versus Observed Daily Maximum Ozone [ppb] at sites in Switzerland and Germany for 2009. *Note that in some plots the vertical axis does not start at zero.*

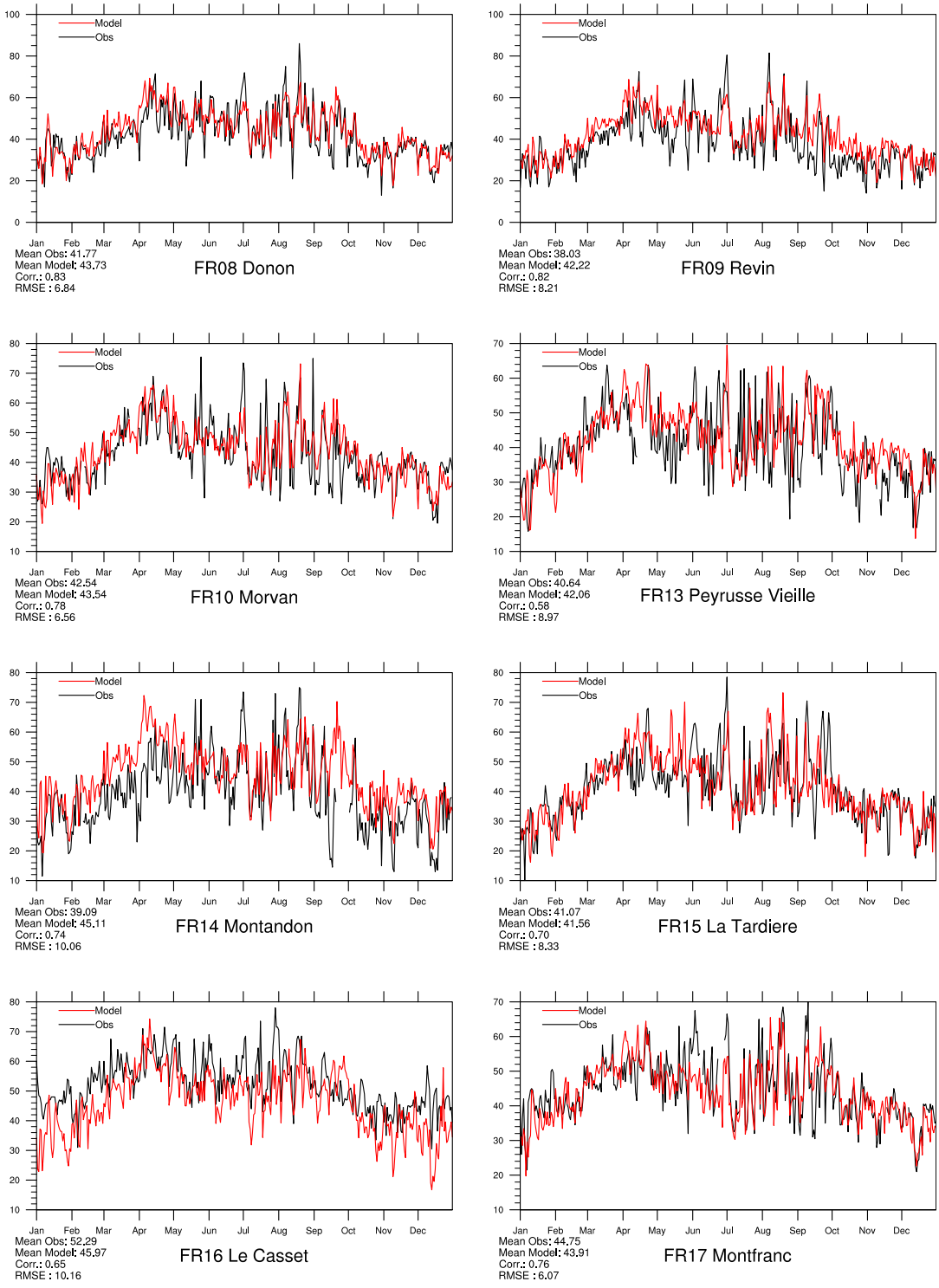

Figure 2.11: Modelled versus Observed Daily Maximum Ozone [ppb] at French sites for 2009. *Note that in some plots the vertical axis does not start at zero.*

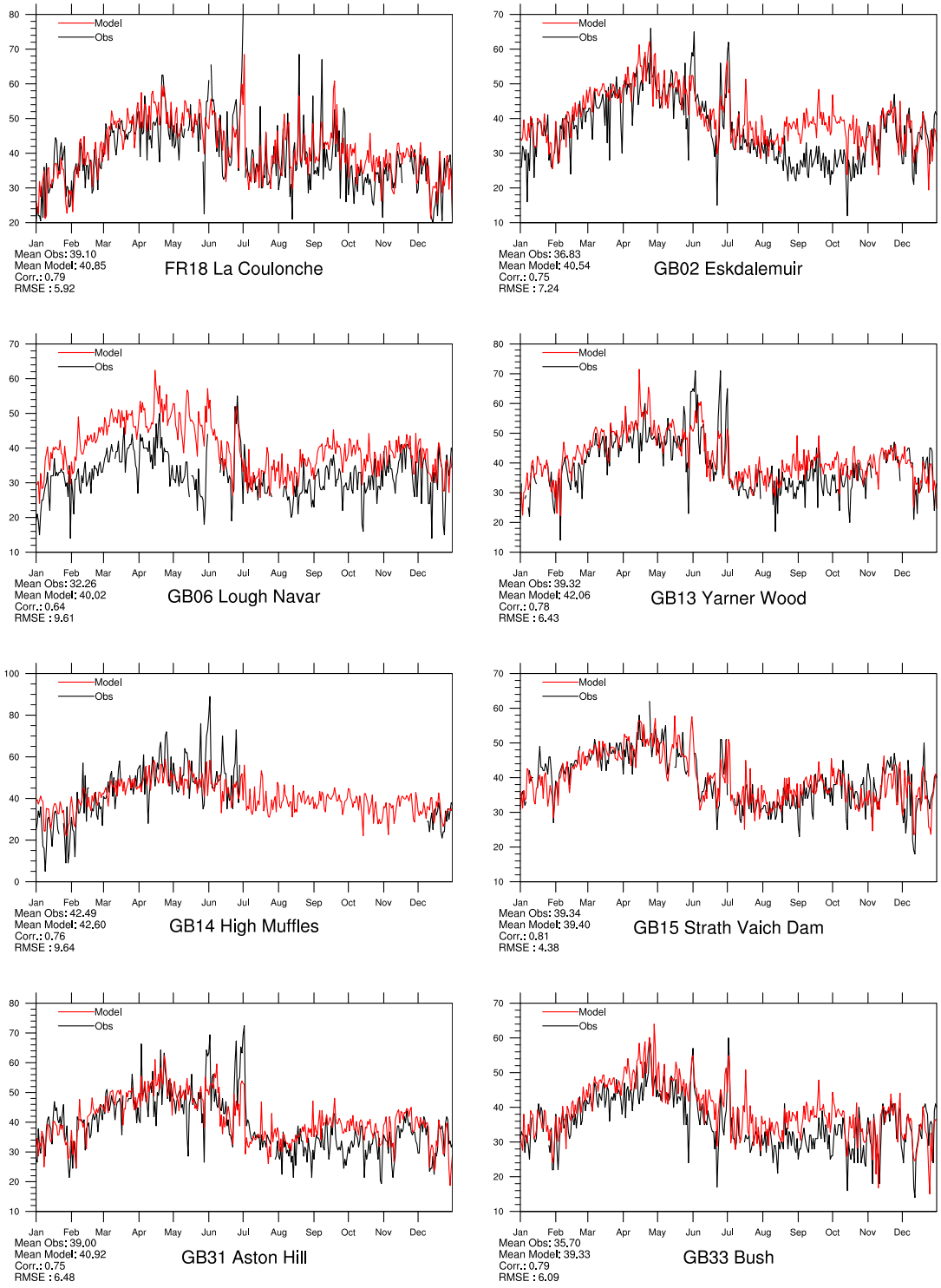

Figure 2.12: Modelled versus Observed Daily Maximum Ozone [ppb] at French and British sites for 2009. *Note that in some plots the vertical axis does not start at zero.*

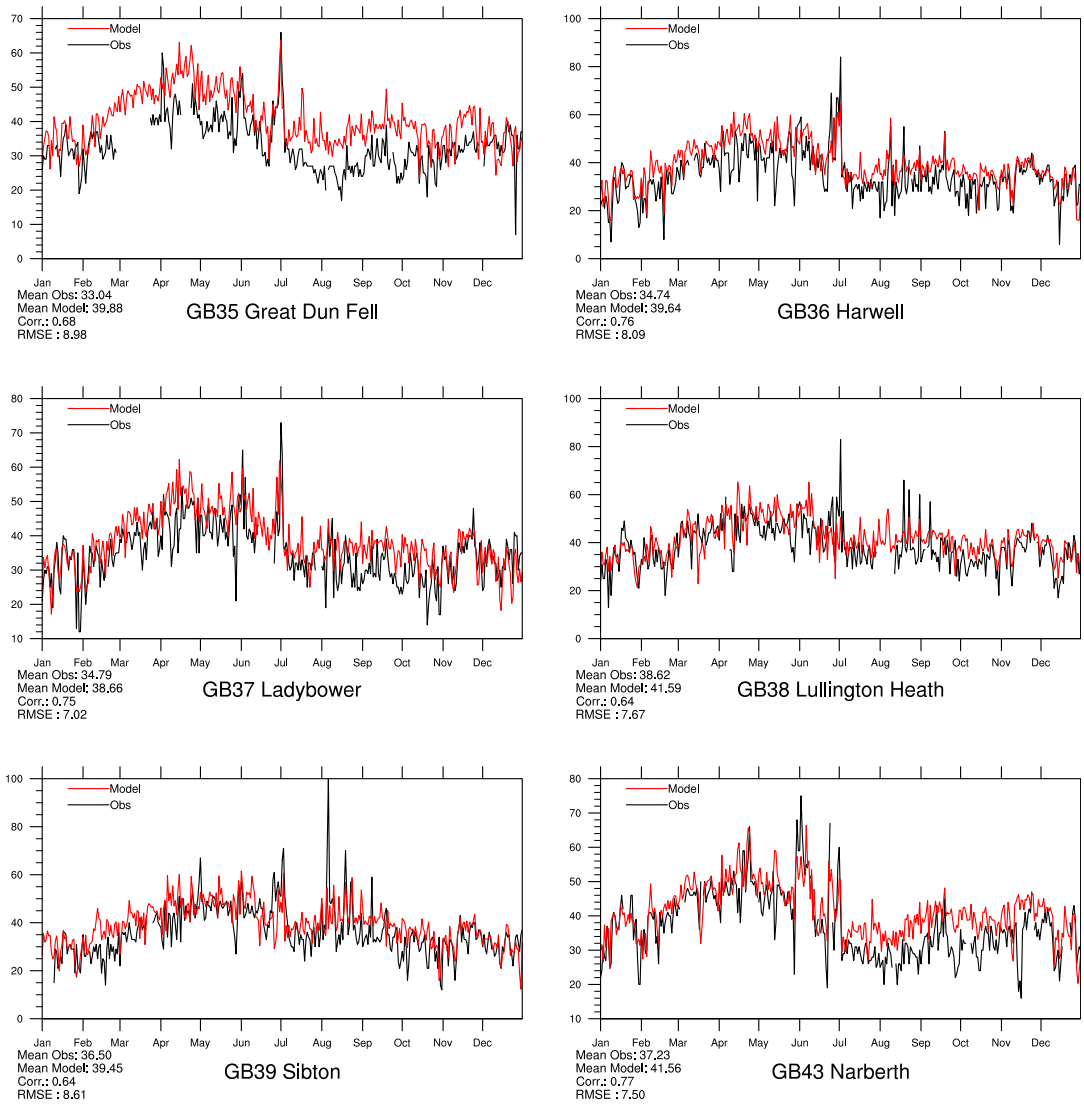

Figure 2.13: Modelled versus Observed Daily Maximum Ozone [ppb] at British sites for 2009. *Note that in some plots the vertical axis does not start at zero.*

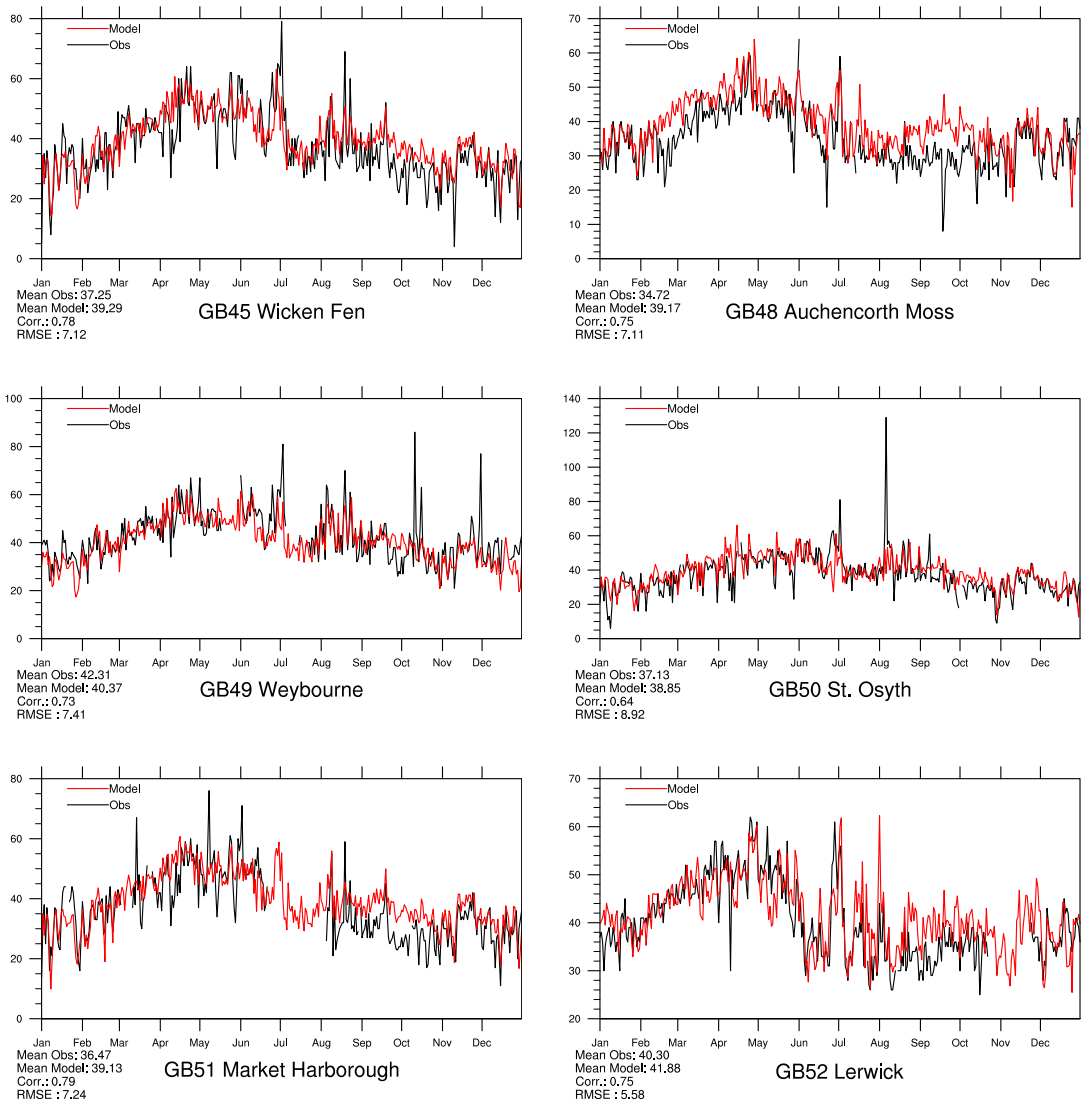

Figure 2.14: Modelled versus Observed Daily Maximum Ozone [ppb] at British sites for 2009. *Note that in some plots the vertical axis does not start at zero.*

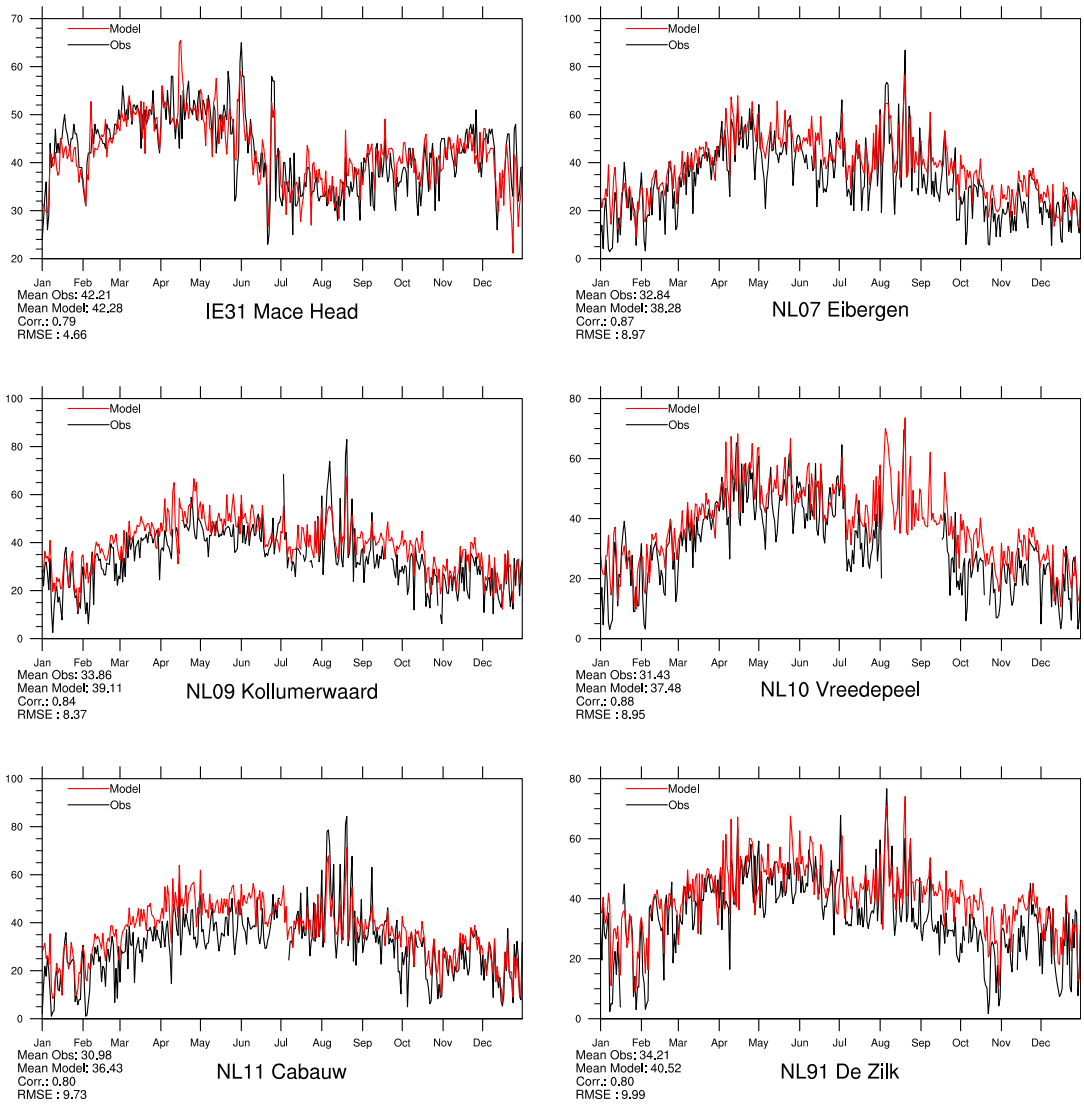

Figure 2.15: Modelled versus Observed Daily Maximum Ozone [ppb] at sites in Ireland and the Netherlands for 2009. *Note that in some plots the vertical axis does not start at zero.*

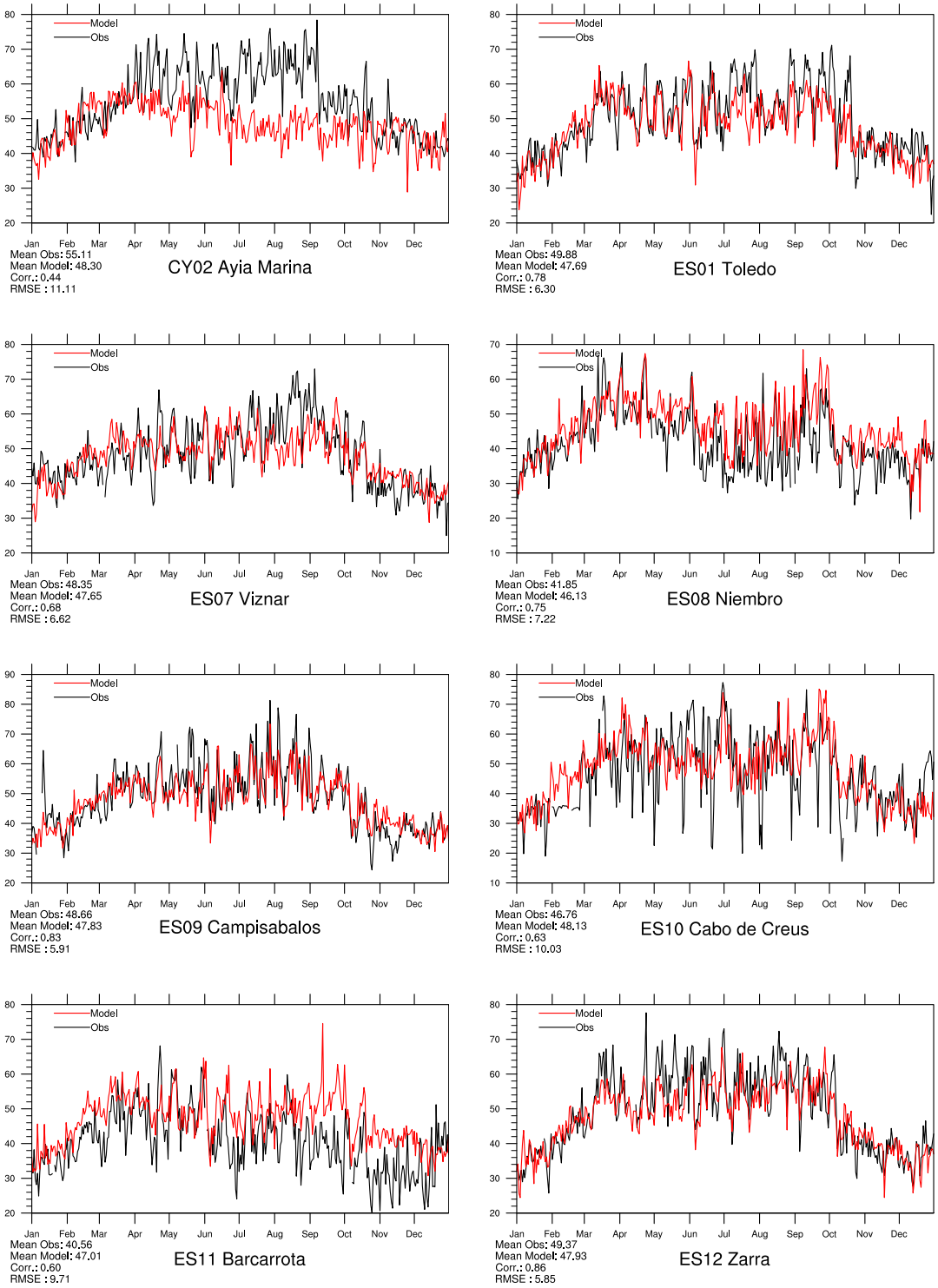

Figure 2.16: Modelled versus Observed Daily Maximum Ozone [ppb] at Mediterranean sites for 2009. *Note that in some plots the vertical axis does not start at zero.*

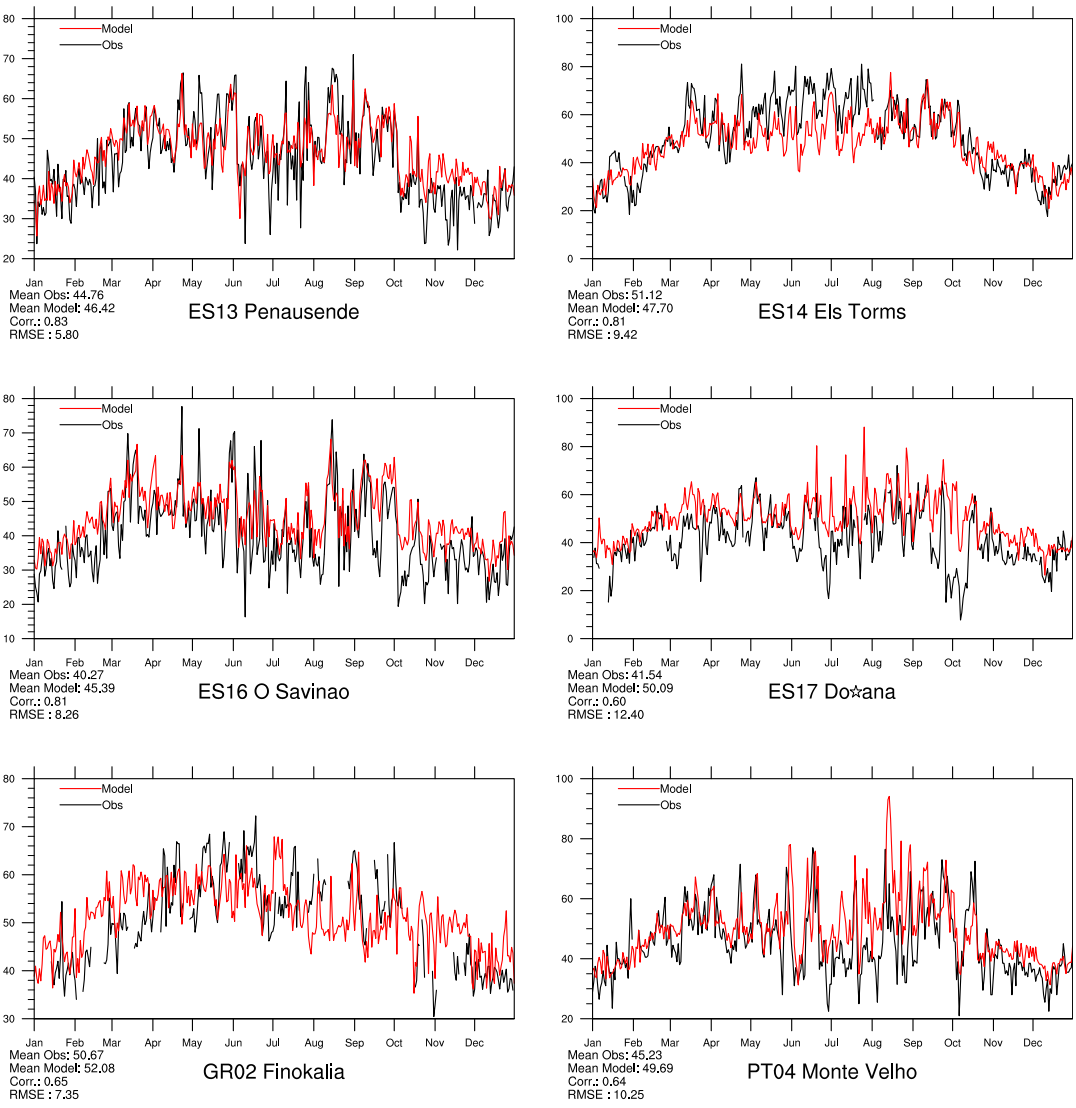

Figure 2.17: Modelled versus Observed Daily Maximum Ozone [ppb] at Mediterranean Sites for 2009. *Note that in some plots the vertical axis does not start at zero.*

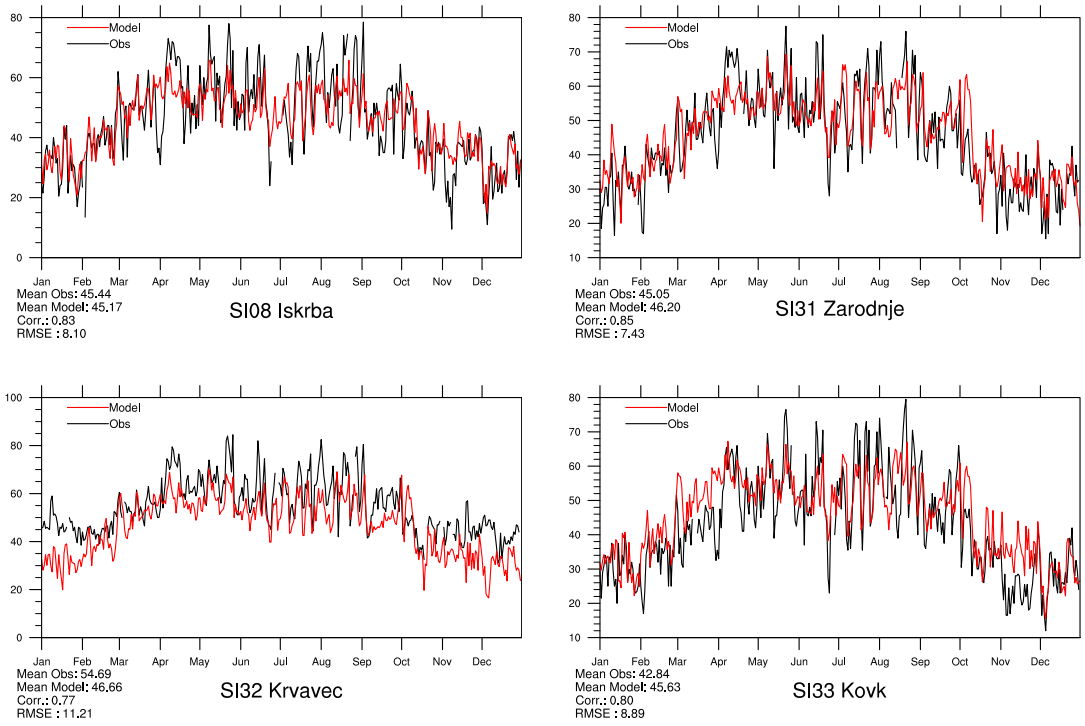

Figure 2.18: Modelled versus Observed Daily Maximum Ozone [ppb] at Mediterranean Sites for 2009. *Note that in some plots the vertical axis does not start at zero.*

2.2 Combined model results and observations, 2009

In this section we present 'best estimates' for concentrations of ozone and NO_2. The 'best estimates' have been created by using a combination of model results and observations from the EMEP network for 2009 and are shown in Figures 2.20–2.21.

2.2.1 Method

For all measurement points, the difference between the measured value at that point and the modelled value in the corresponding grid cell is calculated. This difference is interpolated spatially using radial basis functions, giving a continuous two-dimensional function describing the difference at any point within the modelled grid. The combined maps are derived adjusting the model calculations with the interpolated differences, giving large weight to the observed values close to stations, and using the modelled values in areas with no observations. The range of influence of the measured values depends on the component, but has been set to 500 km for ozone and NO_2.

2.2.2 Ozone

Figure 2.19 shows maps of modelled and combined model-obs daily maximum ozone levels, as annual averages. The normalised error is also shown. In general the normalised errors are relatively small, within 5% almost everywhere Europe. Errors above 5% (but still below 10%) are seen only in confined regions in BeNeLux, Great Britain, the southern tip of Portugal, Spain, and Norway. These are connected with the model performance at stations that were already identified in section 2.1. The only occurrence of a normalized error above 10% is in Cyprus.

2.2.3 NO_2

Figure 2.21 shows maps of model calculated and combined model-observed annually averaged daily mean NO_2 concentrations, along with the normalised error. NO_2 is a difficult compound, in that it has a short lifetime in the atmosphere, and the variability within the 50×50 km^2 grid is large. Normalised errors are larger than for ozone, but still most areas of Europe show normalised errors within the $\pm18\%$ band shown in Figure 2.21(c). The influence of a few sites is very evident though, e.g. in southern Greece or Turkey where the model significantly under-predicts the observed NO_2 concentrations.

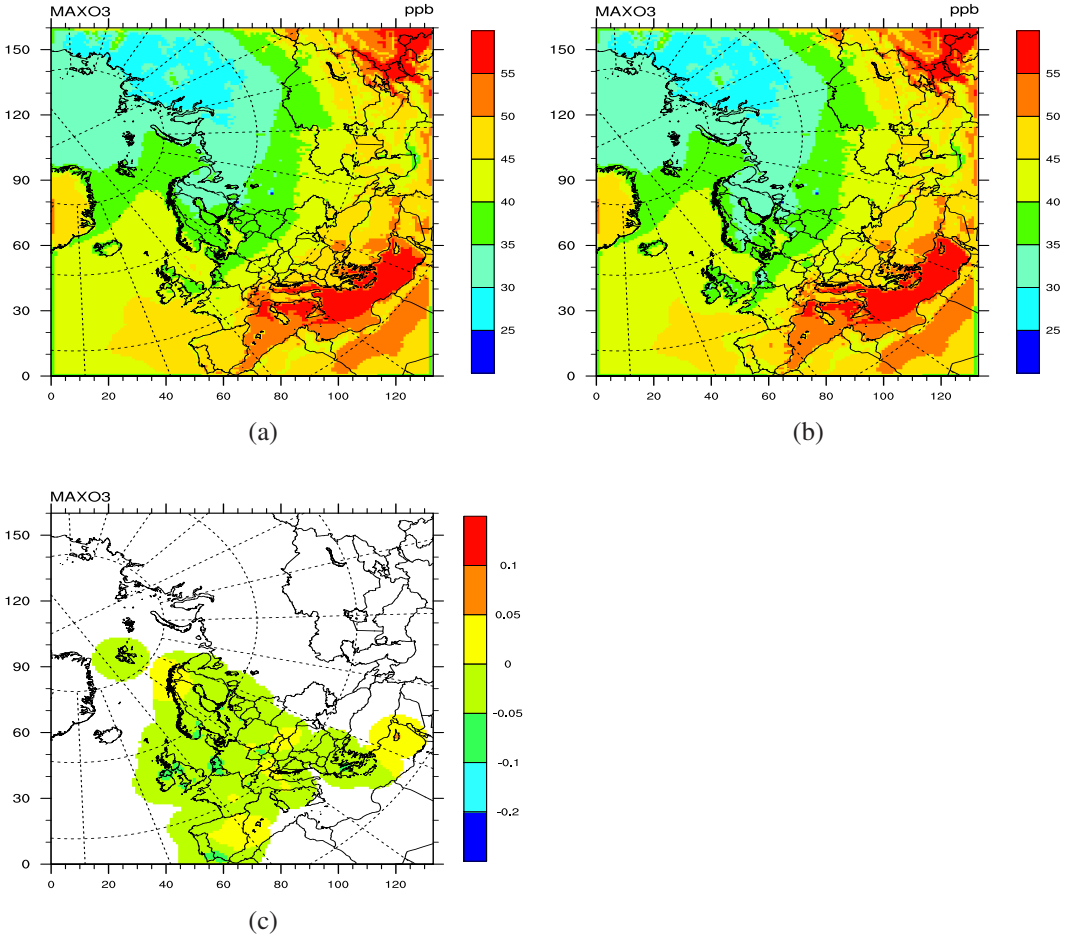

Figure 2.19: Average of daily maximum ozone in 2009. a: modelled concentrations, b: 'combined' (model+obs.) concentrations, and c: normalised errors. Concentration maps have units of ppb. For the maps of normalised error, positive values denote model under-prediction, and negative values model over-prediction.

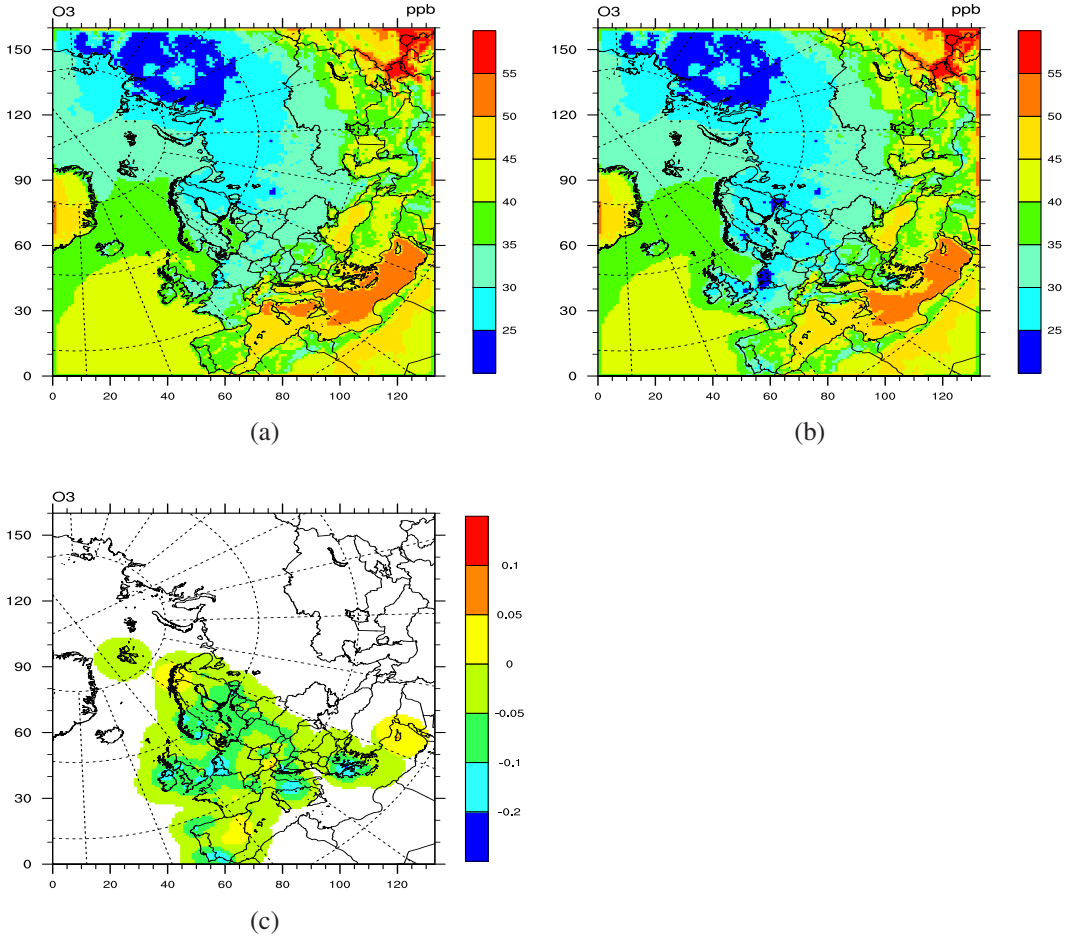

Figure 2.20: Daily mean ozone in 2009. a: modelled concentrations, b: 'combined' (model+obs.) concentrations, and c: normalised errors. Concentration maps have units of ppb. For the maps of normalised error, positive values denote model under-prediction, and negative values model over-prediction.

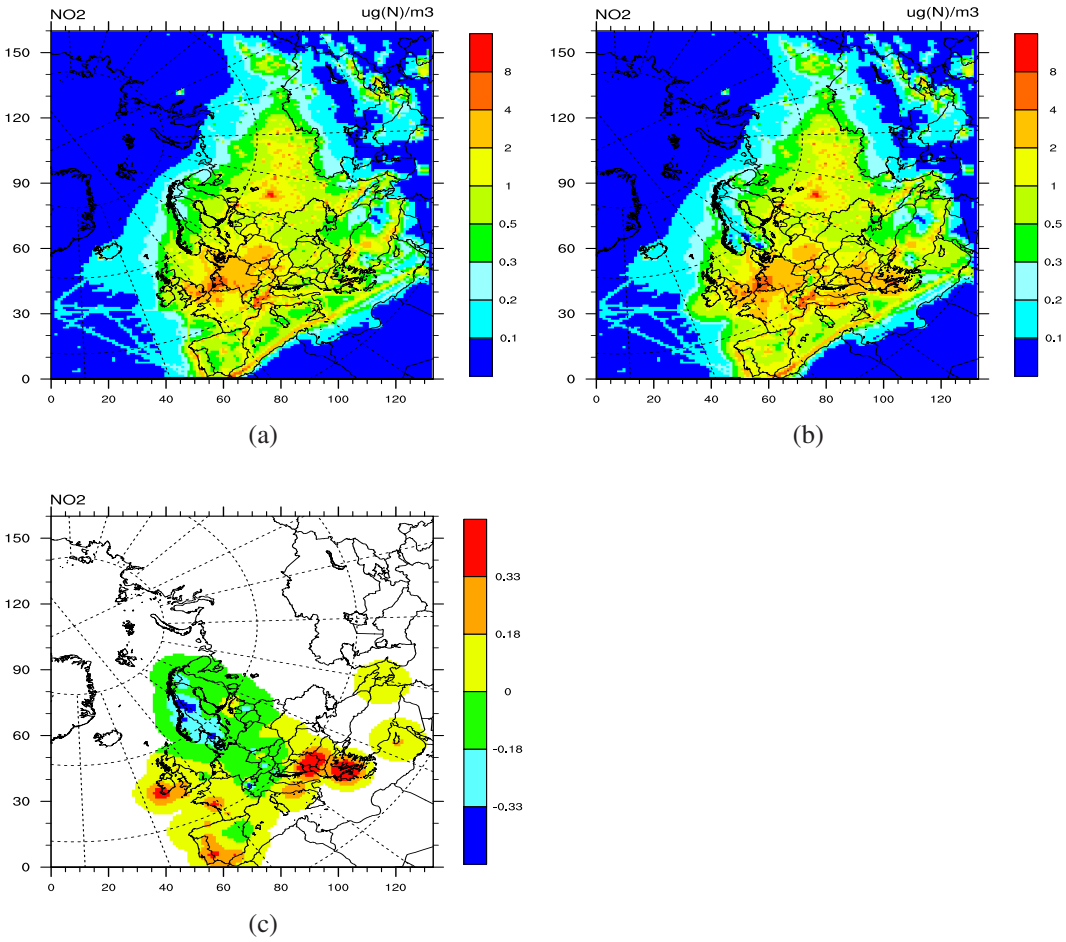

Figure 2.21: NO_2 in 2009. a: modelled concentrations, b: 'combined' (model+obs.) concentrations, and c: normalised errors. Concentration maps have units of μg(N) m^{-3}. For the maps of normalised error, positive values denote model under-prediction, and negative values model over-prediction.

References

H. Berge, M. Gauss, and A.-G. Hjellbrekke. Photo-oxidants: validation and combined maps. Supplementary material to emep status report 1/2010, available online at `www.emep.int`, The Norwegian Meteorological Institute, Oslo, Norway, 2010.

M. Gauss and A.-G. Hjellbrekke. Photo-oxidants: validation and combined maps. Supplementary material to emep status report 1/2009, available online at `www.emep.int`, The Norwegian Meteorological Institute, Oslo, Norway, 2009.

J.E. Jonson, L. Tarrasón, A. Benedictow, and A.G. Hjeĺbrekke. Photo-oxidants, status in 2005. In *In Transboundary Acidification, Eutrophication and Ground Level Ozone in Europe. EMEP Status Report 1/2007*, pages 53–69. The Norwegian Meteorological Institute, Oslo, Norway, 2007.

D. Simpson and A.G. Hjellbrekke. Photo-oxidants: validation and combined maps. In *In Transboundary Acidification, Eutrophication and Ground Level Ozone in Europe in 2006. EMEP Status Report 1/2008*, pages 53–66. The Norwegian Meteorological Institute, Oslo, Norway, 2008.

David Simpson. Ozone. In *Transboundary Acidification, Eutrophication and Ground Level Ozone in Europe since 1990 to 2004, EMEP Status Report 1/2006*, pages 53–62. The Norwegian Meteorological Institute, Oslo, Norway, 2006.